

THESIS FOR THE DEGREE OF DOCTOR OF PHILOSOPHY (PhD)

**ROLE OF IRON-FERRITIN/FERROXIDASE AND HYDROGEN SULFIDE IN
THE DEVELOPMENT OF THE VALVULAR MINERALIZATION:
IMPLICATIONS FOR CALCIFIC AORTIC VALVE DISEASE**

Katalin Éva Sikura

Supervisor: József Balla MD, PhD, DSc



UNIVERSITY OF DEBRECEN
KÁLMÁN LAKI DOCTORAL SCHOOL
DEBRECEN, 2019

TABLE OF CONTENTS

Table of contents	2
Abbreviations	5
1. Introduction	7
1.1. Vascular and valvular calcification; CAVD	7
1.2. Ferritin/Ferroxidase system	8
1.3. Role of H ₂ S	9
2. Aim of the study	10
3. Materials and Methods	11
3.1. Materials	11
3.2. Human Tissue samples and cell isolation	11
3.3. Flow cytometry	11
3.4. Animals	11
3.5. Induction of calcification, calcium measurement, Alizarin Red S staining	12
3.6. Quantification of osteocalcin	12
3.7. Alkaline phosphatase staining	12
3.8. Cell viability assay	12
3.9. Immunofluorescence staining, STED Nanoscopy.....	12
3.10. Nuclear and cytoplasmic protein extraction.....	13
3.11. Western blot	13
3.12. Quantitative Real-Time PCR (qRT-PCR)	14
3.13. Intracellular phosphate uptake measurement	14
3.14. Pyrophosphate assay	14
3.15. Isolation of lysosomes	14
3.16. Determination of sulfide level from AS and AI valve tissue with zinc precipitation assay	15
3.17. H-ferritin, Cystathionine - γ -lyase and cystathionine- β -synthase double gene silencing	15
3.18. Pharmacological inhibition of CSE and CBS and 3MST	15
3.19. Immunohistochemistry	15
3.20. Immunohistochemistry from mouse heart valves	16

3.21. LDH cytotoxicity assay	16
3.22. Statistical analysis	16
4. Results	18
Part 1	
4.1. Role of iron, D3T, and apo-ferritin (AF) in mitigating VIC calcification process ...	18
4.2. Calcification potential of VIC derived from isolated insufficient aortic valve and stenotic aortic heart valves	20
4.3. Effect of iron, apo-ferritin and D3T in localization of RUNX2 under calcific condition of VIC	20
4.4. Sox9 in valvular mineralization	22
4.5. Regulation of VIC phosphate uptake by iron, apo-ferritin, D3T and H-ferritin	23
4.6. H-ferritin and inorganic phosphate association in the lysosome under calcific conditions	25
4.7. Role of extracellular pyrophosphate in the inhibition of valvular calcification.....	27
4.8. H-ferritin and ALP expression in stenotic aortic valve	29
4.9. Association between increased level of H-ferritin and inflammation in AS valves	31
4.10. Function of H-ferritin in the development of inflammation of heart valve.....	33
Part 2	
4.11. H ₂ S function in the calcification of valvular interstitial cells <i>in vitro</i>	34
4.12. Association of AP72 source and RUNX2 localization under calcification of VIC	37
4.13. PPi production changes in the absence/presence of H ₂ S.....	39
4.14. CSE and CBS level changes in VIC calcification.....	41
4.15. Interaction of hydrogen sulfide and phosphate uptake of calcified VIC.....	43
4.16. H ₂ S generation and CSE expression in human aortic valves	44
4.17. Role of H ₂ S in valvular calcification of apolipoprotein E deficient mice.....	46
5. Discussion	48
5.1. Part 1.	49
5.2. Part 2.	52
6. Summary	56
Összefoglalás	58

7. References	60
8. Key words	69
9. List of publications	70
Abstracts and presentations	73
Membership in National and International Societies	74
10. Acknowledgement	75
Appendix	76
Supplementary Figure Panels	77

Abbreviations

3-MST: 3-mercaptopyruvate sulfurtransferase

AF: Apo-ferritin

AFT: apo-ferritin

AI: isolated aortic valve with insufficiency

ALP: alkaline phosphatase

ANK1: Ankyrin G1

AP67: (4-methoxyphenyl)(pyrrolidin-1-yl) phosphinodithioc acid

AP72: 4-methoxyphenyl piperidinylphosphinodithioc acid

ApoE^{-/-}: apolipoprotein E-deficient mice

AS: stenotic aortic valve with calcification

CAVD: Calcific aortic valve disease

CBS: Cystathionine beta-synthase

CSE: Cystathionine gamma-lyase

D3T: 3H-1, 2-dithiole-3-thione

ENPP2: ectonucleotide-pyrophosphatase/phosphodiesterase family member 2

GY4137: (P-(4-Methoxyphenyl)-P-4-morpholinylphosphinodithioic acid morpholine salt)

HFT: H-ferritin

HFT222: Mutant H-ferritin222

IHC: Immunohistochemistry

IL1- β : Interleukin 1-beta

Na₂S: Sodium sulfide

NaSH: Sodium hydrosulfide

PPi: pyrophosphate

pVIC: porcine VIC

RUNX2: Runt-related transcription factor 2

Sox9: SRY (sex determining region Y)-box 9

STED: Stimulated emission depletion nanoscopy

TNF- α : Tumor necrosis factor-alpha

VEC: valvular endothelial cells

VIC: Valvular Interstitial Cells

1. Introduction

1.1. Vascular and valvular calcification

Cardiovascular calcification is a complex disease involving the major and medium-sized arteries along with the aortic valves and is accompanied with chronic kidney disease. Rudolf Ludwig Karl Virchow, the ‘father of cellular pathology’, was the first who described the phenomenon of vascular calcification with the presence of stiff, ‘bone-like’ consistency in atheroma as a degenerative process in 1858. Today it is evident that cardiovascular calcification is a well-regulated and dynamic process, implicated with an increased risk of cardiovascular morbidity and mortality. It is also well known, that the pathological progression of cardiovascular mineralization is much more pronounced in patients with diabetes and in chronic kidney disease (CKD) (Libby, Ridker et al. (2002), Davignon and Ganz (2004), Stocker and Keaney (2004), Rajamannan, Evans et al. (2011)).

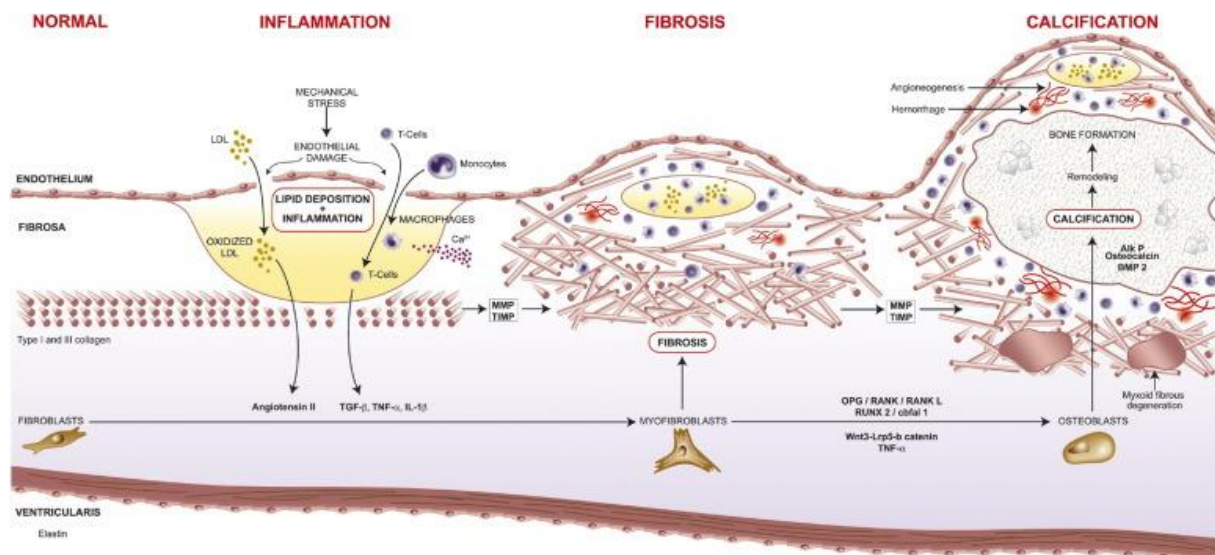


Table 1. Schematic summary of the pathological mechanism of valvular mineralization.

Different stress factors possibly result in damage to the endothelial cell layer on the surface of the valves allowing infiltration of lipids and inflammatory cells into the lower layers of the valve. Oxidative changes in the affected part of the valve, resulting from oxidation of infiltrated lipids, further increase the inflammatory activity within these lesions as proinflammatory (IL1 β) and profibrotic cytokines (TGF- β) increasingly resecreted. Matrix metalloproteinases (MMPs) and tissue inhibitors of metalloproteinases (TIMPs) contribute to a disorganized fibrous tissue, resulting in increased stiffness and thickening of the valve, also termed myxoid fibrous degeneration. In AS (aortic stenosis) mineralization of the valve begins in the early phase, this is followed by macrophage derived microvesicle secretion. Furthermore, in patients with early AS calcification accelerates as a result of increased differentiation of myofibroblast into osteoblast. Osteoblasts regulate the mineralization process of the valve by a highly regulated process akin to skeletal bone formation using many of the same mediators, such as osteocalcin (OC), alkaline phosphatase (ALP) and bone morphogenic protein (BMP2). In the later stages of the disease (end stage), a heterogeneous tissue can be observed with lamellar bone, microfractures and hemopoetic tissue within the valve. The aforementioned process of AS is followed by angiogenesis, and is localized to regions of inflammation surrounding the calcific deposits. Hemorrhage has also been demonstrated in these

new thickened vessels, and this too accelerates the disease progression. IL-1: interleukin-1-beta; LDL: low-density lipoprotein; TGF: transforming growth factor.

Calcific aortic valve disease (CAVD) is one of the most common valvular heart disease in developed countries, and is a well defined disease process (Yutzey, Demer et al. (2014)). In addition to calcification, lipid accumulation and inflammation result in an atherogenous lesion within the heart valve tissue. As demonstrated by the National Heart Lung and Blood Institute, in valvular disease inflammation is a critical initiation step (Rajamannan, Evans et al. (2011) and other research groups (Mohler, Gannon et al. (2001); Mazzone, Epistolato et al. (2004);Freeman and Otto (2005); Dweck, Boon et al. (2012); Yutzey, Demer et al. (2014)). The ratio of the calcified and non-calcified regions could guide us to determine the state of calcification (Chester (2011); Lusic, Mar et al. (2004);Mohler (2004); Speer and Giachelli (2004); Mohler, Gannon et al. (2001)). In stenotic aortic valve calcification, VIC can transdifferentiate into myofibroblast-like cells, which are identified by markers of contractility such as alpha smooth muscle actin (α -SMA), or into osteoblast-like cells: identified by upregulation of ALP activity, and increased levels of osteocalcin expression, and RUNX2 nuclear translocation into the nucleus in later stages.

In CKD patients, the elevated plasma phosphate level is one of the most potent inducer of the initiation of vascular calcification (Hruska, Mathew et al. (2008);Giachelli (2009);(Adeney, Siscovick et al. 2009)). High phosphate provokes calcification of vascular cells in a process mediated by a sodium-dependent phosphate co-transporter (Pit channels), that facilitates entry of phosphate into the cells. In calcified valves, VIC is also shown to transdifferentiate into osteoblast-like cells, determined by the increasing of osteocalcin levels, ALP activity and other osteogenic factors expression/translocation (Rajamannan, Subramaniam et al. (2003)) such as RUNX2, the osteogenic transcription factor and its nuclear translocation (Ducy (1997)). Phosphate uptake occurs via phosphate carriers Pit1 and Pit2 (Crouthamel 2013); Li, Yang et al. (2006)).

1.2. Ferritin/Ferroxidase

Iron is essential in several cellular functions. Iron overload can be potentially toxic, and is mainly modulated by the ferritin molecules. Ferritin is an iron storage protein that has antioxidant properties, and it is known to protect the endothelium/smooth muscle cells/valvular interstitial cells against the damaging effects of inflammation and calcification (Balla, Jacob et al. 1992); Sikura, Potor et al. (2019), Zarjou, Jeney et al. (2009)). Ferritin is a large molecule (450 kDa), and its function is to stores up to 4500 Fe atoms in a safe, spherical shell in a nontoxic form. Ferritin has 24 subunits of two types (heavy [H] and light [L] chain) the proportions of which depend on the iron status of the cell, the tissue, and the organ (Theil (1990)). The H-chain of ferritin has ferroxidase activity that is essential for iron incorporation and also in controlling the potentially toxic Fe (II) ions via reduction in oxidative damage (Arosio and Levi (2002)). Additionally, ferritin has various functions apart from iron storage, i.e., it is has been described as having immunomodulatory effects as summarized in a review byWang, Knovich et al. (2010).

Additionally, levels of serum ferritin are widely utilized by clinicians as a mirror of iron stores, and may signal abnormality in different diseases, e.g., infections, inflammation, cardiovascular disorders (Zarjou, Black et al. (2019)). While the connotation of iron/ferritin role in inflammation and cardiovascular diseases is not well understood and is extensively debated, in this part of this work we attempt to highlight a possible mechanism and its role in CAVD and CKD.

1.3. Role of H₂S

Hydrogen sulfide is a water soluble, colorless gas which was described first time in the 17th century (Wang (2010); Wang (2012)). Hydrogen sulfide is the novel endogenous gasotransmitter, along with nitric oxide and carbon monoxide (Wang (2002)). In mammalian tissues H₂S is mainly produced by CSE (cystathionine gamma-lyase) and CBS (cystathionine beta-synthase) from L-cysteine and homocysteine (Zhang, Wang et al. (2018)). Beltowski (2015) previously demonstrated that H₂S levels may be enhanced in vivo by conventional inorganic sulfide salts and Kang, Neill et al. (2017) have described that reaction between Lawesson's reagent and morpholine results in a new generation slow H₂S release compound GYY4137. Protonation reaction of GYY4137 results more stable H₂S releasing compounds, such as AP67 and AP72. AP72 has excellent water solubility and very slow generation of H₂S compared to the fast H₂S releasing donors such as NaSH and Na₂S (Chitnis, Njie-Mbye et al. (2013); Kang, Neill et al. (2017)); Nagy (2013)). Previously, we demonstrated that NaSH is a significant inhibitor of mineralization of vascular smooth muscle cells (Zavaczki, Jeney et al. (2011)). CSE is important for normal heart function and physiological functioning as Jiang et al, and others have concluded (Chen, Xin et al. (2007)). The development of heart disease is manifested by the disorder of H₂S production as indicated by the lower levels of plasma H₂S in patients with coronary heart disease (Jiang, Wu et al. (2005); Shen, Shen et al. (2015)). Additionally, the endogenous H₂S production by CBS also ameliorates the normal function of the brain (Abe and Kimura (1996)). Furthermore, elevation of H₂S levels is now achievable. Rose, Moore et al. (2017) recently demonstrated that H₂S play a functional role in cell-signaling and post-translational-modifications in cardiovascular system. Moreover, using siRNA or genetic animal (mouse) models to demonstrate the role of H₂S during mineralization, a mimic loss of function of genes (CSE; CBS) involved in the biosynthesis and degradation of H₂S was observed within the affected cells/tissue (Rose, Moore et al. (2017)). In this work we would like to reveal new insights into the biology of H₂S within the cardiovascular system and in cell signaling.

2. Aims of the Study

Part 1

CAVD is a complex disease mainly in the elderly. It is one of the leading causes of mortality and morbidity especially in CKD patients and in the developed countries. The progression of CAVD include the osteoblastic transdifferentiation of valvular interstitial cells (VIC) that is accompanied by bone specific gene expression, and its progression is manifested by the deposition of hydroxyapatite minerals in the affected tissue of the valve. Although, we have improved knowledge of the pathomechanisms of CAVD, the only therapeutic approach is heart valve replacement surgery. Previously, in our research laboratory demonstrated that ferritin/ferroxidase has an important role is vascular calcification. However, we have little knowledge on the role of ferritin/ferroxidase in cardiovascular mineralization.

Aims:

- Investigate the role of ferritin/ferroxidase in high phosphate induced CAVD progression in vitro and in vivo.
- Iron/ferritin role/possible mechanism in the inhibition of CAVD

Part 2

H₂S level has a crucial role in the progression of CAVD. Nonetheless, it is not known, what causes the progression of CAVD in H₂S deficiency. In this study, based on the results of the experiments outlined in Part 1 of our aims, we investigate the role of H₂S in CAVD.

Aims:

- Investigate the role of H₂S in CAVD progression.
- Examine role of exogenous exposure of H₂S donor molecules in the inhibition of CAVD.

3. Materials and Methods

3.1. Materials

All chemicals were analytical grade reagents or higher and obtained from Sigma-Aldrich, (St Louis, MO, USA). The sulfide donor molecules used in this work – GYY4137 (P-(4-Methoxyphenyl)-P-4-morpholinylphosphinodithioic acid morpholine salt), AP67 (4-methoxyphenyl) (pyrrolidin-1-yl) phosphinodithioic acid) and AP72 (4-methoxyphenyl) (piperidin-1-yl) phosphinodithioic acid) – were synthesized in-house (Kulkarni-Chitnis, Njie-Mbye et al. (2015); Li, Whiteman et al. (2008); Whiteman, Perry et al. (2015)). Sulfide stock solutions were prepared fresh daily.

3.2. Human tissue samples and cell isolation

Human aortic valve leaflets were obtained from patients undergoing valve replacement for stenosis with calcification (AS; N=52) and patients who had severe insufficiency without calcification (AI; N=28). The specimens were collected from Jan 2015 to Dec 2017 (80 patients) (Regional Research Ethical Committee, Project No.: 61538-2/2017/EKU and 4699-2016). VIC were isolated from human heart valves using collagenase (600 U/ml) (Worthington Biochemical Corp.). Cells isolated from donors were employed at passage 2 to 4. All experiments were performed on cells derived from 5 different donors.

3.3. Flow Cytometry

Cells were fixed and stained with FITC conjugated mouse anti-human CD31 antibody (Abcam; ab27333) and run on a FACScan flow cytometer. Cell population was identified and gated based on size (forward scatter, FSC) and complexity (side scatter, SSC). Isotype sample was used as control.

3.4. Animals

All the in vivo experiments adhered to the guidelines from Directive 2010/63/EU of the European Parliament on the protection of animals used for scientific purposes and by the ARRIVE guidelines: British Journal of Pharmacology, 160: 1577–1579. Animal experiments performed in this study were approved by the Scientific and Research Ethics Committee of the Scientific Council of Health of the Hungarian Government (registration number DE MÁB/157-5/2010) and are reported in accordance with the ARRIVE guidelines. C57BL/6 ApoE^{-/-} mice were maintained at the University of Debrecen under specific pathogen-free conditions in accordance with guidelines from the Institutional Ethical Committee. Mice were randomly divided into four groups. Non-high fat diet group (N=5) received a standard chow diet. To induce aortic valve calcification, mice were kept on atherogenic diet (15% fat, 1.25% cholesterol, ssniffSpezialdiäten GmbH, Soest, Germany) till the age of 8 weeks. Parallel with the atherogenic diet mice were injected intraperitoneally with AP72 (266 µmol/kg body weight; N=5) or vehicle (saline; N=9) on every other day as previously described. Aortas were collected after 8 weeks of treatment. All mice were euthanized by slow-fill compressed CO₂ asphyxiation. Atherogenic food composition (high-fat diet) was as follows: Crude Nutrients (%): Crude protein 19%; crude

fat 15.2%; crude fiber 3.4%; crude ash 6.3%; starch 25.6%; sugar 11.2%; Additives (per kg): vitamin A 15,000 IU; vitamin D3 1,000 IU; vitamin E 110 mg; vitamin K3 5 mg; vitamin C 0 mg; copper 13 mg.

3.5. Induction of calcification, calcium measurement, Alizarin Red S staining

VIC were cultured in calcification medium (2.5 mmol/L inorganic phosphate and 1.8 mmol/L calcium-chloride) with or without phenol red for 5 days. Calcium content of the supernatants was determined by QuantiChrome Calcium Assay Kit (Gentaur), normalized to protein content and expressed as $\mu\text{g}/\text{mg}$ protein. Alizarin Red S staining was used to visualize the calcium deposition. Plates were fixed with 3.7 % formaldehyde for 10 minutes followed by staining with a 2 % solution of Alizarin Red S. Photographs of the stained cells were taken with a light microscope (x10 magnification; Leica DMIL LED microscope).

3.6. Quantification of osteocalcin

ELISA kit was used (Bender MedSystem) for the quantification of osteocalcin from EDTA-solubilized extracellular matrix.

3.7. Alkaline phosphatase staining

To visualize alkaline phosphatase activity, cells were cultured in 24 well plates and fixed in Citrate-acetone solution (2:3) followed by staining with Naphtanol AS-MX –Fast Violet B solution (Sigma). Light microscope photographs were taken during the different treatments (Leica DMIL LED microscope, Leica DMC4500 camera with Leica application suite LAS Software 4.9.0).

3.8. Cell viability assay

Cells were cultured on 0.2 % collagen type I coated coverslip. NUCLEAR-ID[®] Blue/Red cell viability reagent was added to the cells at dilution 1:1000 for 30 minutes at 37 °C. Subsequently, the cells were fixed with Fluorescent Mounting Medium (Dako) on Superfrost Ultra Plus Microscope Slide (Thermo Scientific). Images were obtained with an immunofluorescence microscope (Leica DM2500 microscope, Leica DFC480 camera).

3.9. Immunofluorescence staining

Mouse monoclonal anti-human α -SMA (Santa Cruz; sc-3225; 400 ng/mL) and rabbit polyclonal anti-human von Willebrand factor antibody (Abcam; ab6994; 100 ng/mL) were used as primary antibodies to identify VIC and endothelium. Subsequently, samples were incubated with secondary antibodies, i.e., CY3-conjugated Streptavidin (Jackson Immunoresearch; 016-160-084; 1000 ng/mL) and Biotin (Jackson Immunoresearch; 715-065-150; 1000 ng/mL). For LAMP1 and H-ferritin double staining anti-human rabbit anti-human LAMP1 (Abcam; ab24170; 1000 ng/mL) and mouse anti-human H-ferritin (Santa Cruz; sc-376594; 400 ng/mL) were used with secondary antibodies anti-rabbit Alexa Fluor 488 against LAMP-1 (Thermo Fisher Scientific; A11070; 2000 ng/mL) and anti-mouse

Alexa 647 (Thermo Fisher Scientific; A21244; 4000 ng/mL) against H-ferritin. Sox9 staining was performed with rabbit anti-human Sox9 (Abcam; ab26414; 2000 ng/mL) antibody followed by the anti-rabbit Alexa Fluor 488 (Thermo Fisher Scientific; A11070; 2000 ng/mL) secondary antibody. Hoechst (0.5 ng/mL) was used to stain nuclei. Rabbit polyclonal anti-human RUNX2 (Proteintech, 20700-I-AP) was used (dilution 1:600) as a primary antibody to show RUNX2 localization in VIC. A primary antibody labeled with goat anti-rabbit Alexa 488 (Thermo Fisher Scientific, A11070) fluorophore at dilution 1:500 for 1 hour in dark at room temperature. Hoechst was used to stain nuclei. Multicolor STED imaging was acquired with STED (Stimulated Emission Depletion) Leica TCS SP8 gated STED-CW nanoscopy (Leica Microsystem Mannheim, Germany). Gated STED images were deconvolved using Huygens Professional (Scientific Volume Imaging B.V., Hilversum, Netherlands) software.

3.10. Nuclear and cytoplasmic protein extraction

Cells were cultured in growth medium and treated with or without calcification medium supplemented with 20 $\mu\text{mol/L}$ AP72. After treatment, cells were harvested with cell scraper and collected into a centrifuge tube. Pellets were washed twice with PBS followed by addition of ice-cold 1x cytoplasmic lysis buffer (20 mmol/L Tris-HCl pH 8.0, 100 mmol/L NaCl, 300 mmol/L sucrose, 3 mmol/L MgCl₂, protease inhibitor cocktail) to the pellets. Cell suspensions were incubated on ice for 15 minutes. After centrifugation, the supernatants were collected (contains cytoplasmic proteins), the pellets were washed with PBS and resuspended in ice-cold nuclear extraction buffer (20 mmol/L Tris-HCl pH 8.0, 300 mmol/L NaCl, 2 mmol/L EDTA pH 8.0, protease inhibitor cocktail). Next, the samples were drawn 5 times with 27 gauge needle for the extraction of the nuclear proteins followed by centrifugation at 8000 x g, 4°C for 20 minutes. The supernatant contains the nuclear fraction. The protein concentration of the samples was determined by the BCA Protein Detection Kit (Amersham).

3.11. Western Blot analysis

H-ferritin Western blotting was performed with rabbit anti-human H-ferritin antibody (Santa Cruz; sc-376594; 400ng/mL), followed by HRP-labeled anti-rabbit IgG antibody. To detect Pit-1, Pit2 and LAMP1 we used rabbit anti-human Pit1 antibody (Abcam; ab177147; 2000 ng/mL), rabbit anti-human Pit2 antibody (Proteintech; 12820-1-AP; 60 ng/mL) and rabbit anti-human-LAMP1 antibody (Abcam; ab24170; 1000 ng/mL), respectively. Western blot analysis for ENPP2 was performed using anti-human ENPP2 (Thermo Fisher Scientific; PA5-12478; 4000 ng/mL). Sox9 Western blot was performed with rabbit anti-human Sox9 (Abcam; ab26414; 2000 ng/mL). Western blots were performed with: rabbit anti-human Sox9 (Abcam; ab26414; 2000 ng/mL) and rabbit anti-human RUNX2 (Proteintech; 20700-I-AP; 400 ng/mL), rabbit anti-human TNF- α (Thermo Fisher Scientific; PA5-19810; 400 ng/mL), rabbit anti-human IL1- β (Invitrogen; 17h18116; 400 ng/mL), rabbit anti-human CSE at dilution 1: 600 (Proteintech, 12217-I-AP), rabbit anti-human CBS at dilution 1:600 (Proteintech, 14787-I-AP) and mouse anti-human Ankyrin G1 antibody at dilution 1:500 (Life Technologies, 338800). Complexes of

antigen-antibody were visualized with a horseradish peroxidase chemiluminescence detection system (Amersham Biosciences; RPN2109). Membranes were reprobbed with glyceraldehyde-3-phosphate dehydrogenase (GAPDH).

3.12. Quantitative Real-Time PCR (qRT-PCR)

VIC were cultured in growth media or calcification media supplemented with 20 $\mu\text{mol/L}$ AP72. Cells were harvested after 5 days. Total RNA was isolated using RNazol STAT-60 according to the manufacturer's instructions (TEL-TEST Inc., Friendswood, TX, USA). RNA concentration was measured with NanoDropTM 2000c spectrophotometer (Thermo Scientific Inc., Waltham, MA, USA). Subsequently, cDNA synthesis was performed using a high-capacity cDNA kit (Applied Biosystems, Foster City, CA). We used real-time PCR technique for quantification of mRNA levels of ENPP2 and ANK1 (Thermo Fisher Scientific Inc.) and GAPDH (Thermo Fisher Scientific Inc.). TaqMan Universal PCR Master Mix was purchased from Applied Biosystems (Applied Biosystems, Foster City, CA). Finally, we performed TaqMan quantitative PCR (40 cycles at 95° C for 15 sec. and 60° C for 1 min.) on 96-well plates with the Bio-Rad CFX96 (Bio-Rad Laboratories Inc., Hercules, California, USA) detection system. Results were expressed as mRNA expression normalized to GAPDH.

3.13. Intracellular phosphate uptake measurement

Valvular interstitial cells were cultured on 12 well plates exposed to calcification medium in the presence or absence of phenol red using D-MEM supplemented with/without AP72 (20 $\mu\text{mol/L}$) for 5 days. Cells were lysed with 0.5 % NP40 and 1 % Triton-X100. Whole cell lysate centrifuged at 12000 x g for 15 min at 4°C. The supernatant was measured by QuantiChrom quantitative colorimetric phosphate assay kit (BioAssays System) on 96-well plates at 650 nm. Phosphate uptake was normalized to the protein content of the cells.

3.14. Pyrophosphate assay

VIC were cultured in phenol red-free growth medium (D-MEM; Sigma) or calcification medium and supplemented with AP72 (20 $\mu\text{mol/L}$). Heart valve tissue (AS N=3; AI N=3) and cells were lysed with EDTA free detergent. Inorganic pyrophosphate (PPi) was measured in the extracellular fluid of the VIC using PPLightTM inorganic pyrophosphate assay (Lonza; LT-07-610). The continuous kinetic assay was employed according to the manufacturer's instruction. The luminescence was monitored for 2 hours using SynergyTMMHTX Multi-Mode Microplate Reader from BioTek Instruments (USA) with 0.1 s integrated reading time. The relative luminescence (RLU) was normalized to the protein content of the cells.

3.15. Isolation of lysosomes

To separate lysosomes, we used the Lysosome Enrichment Kit for Tissue and Cultured Cells (Thermo Fisher Scientific; 89839) and gradient ultracentrifugation. For protein analysis, lysosomes were lysed with 2 % CHAPS (Sigma Aldrich; C2632-25G) in Tris-buffered saline (TBS; 25 mmol/L Tris, 0.15 mol/L NaCl; pH 7.2), samples were

centrifuged with Beckman ultracentrifuge at 38 000 x g and the lysosomal fractions were collected from each sample.

3.16. Determination of sulfide level from AS and AI valve tissue with zinc precipitation assay

Sulfide levels were measured with zinc precipitation method as developed by Gilboa-Garber (Gilboa-Garber, 1971) and improved by Ang et al. (Ang et al., 2012). The human valves were homogenized under liquid nitrogen in PBS (pH 7.4) and were sonicated. After that the sample was centrifuged at 12 000 x g for 15 min and the lipids free clear supernatant was collected. 200 μ L of samples were mixed with 350 μ L 1% zinc acetate and 50 μ L of 1.5 mol/L sodium- hydroxide and incubated for 60 minutes on a shaker. Incubation step was followed by centrifugation at 2000 x g for 5 minutes to pellet the generated zinc sulfide. The supernatant was then removed, and the pellet washed with 1 mL of distilled water by vortexing extensively, followed by centrifugation at 2000 G for 5 minutes. The supernatant was then aspirated off and the pellet reconstituted with 160 μ L of distilled water and mixed with 40 μ L of pre-mixed dye (20 μ L of 20 mmol/L dimethyl-p-phenylene-diamine-dihydro-chloride (NNDP) in 7.2 mol/L hydrochloric acid (HCl) and 20 μ L of 30 mmol/L Iron(III) chloride (FeCl_3) in 1.2 mol/L HCl). After 10 min the absorbance of the generated methylene blue (MB) was measured with a spectrophotometer at 667 nm. Since during the reaction 1 mol/L MB formed from 1 mol/L sulfide, the concentration was determined by the MB's extinction coefficient (30 200 M⁻¹cm⁻¹). Samples were normalized for protein concentration. Results were calculated for μ mol/L generated H₂S/ mg protein at 60 minutes.

3.17. H-ferritin, Cystathionine - γ -lyase and cystathionine- β -synthase double gene silencing

H-ferritin, Cystathionine- γ -lyase (CSE) and cystathionine- β -synthase genes silencing using siRNAs (Ambion, s225998; 4392420; s3710) were performed. Briefly, valvular interstitial cells were cultured on 12 well plates in antibiotic-free medium (D-MEM, Sigma). At about 70 percent of confluence, cells were transfected with siRNA against H-ferritin, CSE and CBS (Ambion, s225998; 4390824; s289). Transfection occurred for 4 hours in minimal serum-content medium (Opti-MEM; Gibco). At the end of transfection 30% FBS containing, antibiotic free D-MEM was added. Next day, cells were washed and treated with AP72 every second day until 5 days. The sequences of the siRNAs were inserted into the Supplementary Methods.

3.18. Pharmacological inhibition of CSE and CBS

VIC were cultured in 12 well plates in growth medium or calcification medium. Inhibition of CSE, CBS and 3-MST were carried out employing pharmacological compounds: PPG; AOAA; KGA; AOAA+PPG; AOAA+KGA; PPG+KGA (20 μ mo/L of each inhibitor).

3.19. Immunohistochemistry

Heart valve tissues were fixed with formaldehyde for one day followed by TRIS buffer and embedded in paraffin wax. Subsequently, slides were deparaffinized in xylene for 5

minutes and then rehydrated. For immunohistochemistry, slides were subjected to a peroxidase-blocking reagent for 5 minutes (3% hydrogen peroxide was used to block endogenous peroxidase activity). Antigen retrieval was performed in an epitope retrieval solution (Leica RE-7113) at pH 6 using a pressure cooker (rice programs, IDA Avair 6 L pressure cooker). Double immunostaining of ALP-H-ferritin; ALP-CSE or α -SMA-CSE interaction were performed sequentially with the EnVision FLEX/HRP system. Following the first IHC staining terminating with the EnVision FLEX/HRP detection step, the incubation with the second primary monoclonal antibody was performed. In addition to DAB (brown color), the chromogen VIP was used to highlight the second IHC reaction in a different color (dark violet). For double staining experiments, methyl-green counterstaining was performed. Samples were incubated with the following primary antibodies: rabbit anti-human ALP antibody (Abcam; ab65834; 1000 ng/mL) and mouse anti-human H-ferritin antibody (Santa Cruz; sc376594; 400 ng/mL). Other IHC stains were performed with the following antibodies: rabbit anti-human TNF- α (Thermo Fisher Scientific; PA5-19810; 400 ng/mL), rabbit anti-human IL1- β (Invitrogen; 17h18116; 400 ng/mL); rabbit anti-human CSE at dilution 1: 600 (Proteintech, 12217-I-AP), rabbit anti-human CBS at dilution 1:600 (Proteintech, 14787-I-AP). Antibody binding was visualized by the Super Sensitive TM One Step Polymer-HRP IHC Detection System. The intensity and distribution of antibodies expression were assessed by light microscopy (Leica DM2500 microscope, DFC 420 camera and Leica Application Suite V3 software, Wetzlar, Germany). ALP and H-ferritin colocalization of the IHC samples were measured by Image J software.

3.20. Immunohistochemistry from mouse heart valves

Briefly, tissues were fixed in formaldehyde for one day followed by TRIS buffer and embedded in paraffin wax. Subsequently, slides were deparaffinized in xylene and then rehydrated. For immunohistochemistry, slides were subjected to the peroxidase-blocking reagent. Samples were incubated with the following primary antibodies: anti-CSE antibody at dilution 1:1000 (Proteintech, 12217-I-AP) and anti-SMA antibody at a dilution of 1:1000 (Santa Cruz; sc-32251). Antibody binding was visualized by the Super Sensitive TM One Step Polymer-HRP IHC Detection System. Liquid DAB chromogen (BG-QD630-XAKm BioGenex) was added for samples. The intensity and distribution of antibodies expression were assessed by light microscopy (Leica DM2500 microscope, DFC 420 camera and Leica Application Suite V3 software, Wetzlar, Germany).

3.21. LDH cytotoxicity assay

The cytotoxicity of the treatment was assessed by Pierce LDH Cytotoxicity Assay Kit (Thermo Scientific) according to the manufacturer's instructions.

3.22. Statistical analysis

Data were analyzed by GraphPad Prism 5.02 software (GraphPad Software Inc., 7825 Fay Avenue, Suite 230 La Jolla, CA 92037). All statistics data are expressed as mean \pm SEM. If data groups passed the normality test and equal variance test, we performed Student's t-test

or One Way ANOVA followed by Bonferroni post hoc tests as indicated in figure legends.
P<0.05 was considered significant.

4. Results

4.1. Role of iron, D3T, and apo-ferritin (AF) in mitigating VIC calcification process

Based on our previous investigations that identified induction of H-ferritin as an inhibitory mechanism against osteoblastic transition of vascular smooth muscle cells (Zarjou, Jeney et al. (2009)), we tested whether elevation of intracellular level of H-ferritin would mimic these effects in VIC. Iron and D3T were utilized to induce the expression of H-ferritin in VIC. Calcification medium alone significantly increased the extracellular calcium content of cultured VIC. Iron and D3T significantly decreased the extracellular calcium in a dose-dependent manner (Figure 1 and Supplementary Figure I. A and B) and the expression of osteocalcin, respectively. Apo-ferritin (devoid of iron) also inhibited the extracellular calcium deposition and osteocalcin level of VIC (Figure 1A middle and right panel). These observations were supported by Alizarin Red S staining after five days (Figure 1B). Next, we investigated whether inhibition of the mineralization pathway of VIC also relies on H-ferritin/ferroxidase. Indeed, we found that upregulation of H-ferritin via iron or D3T or supplementation with apo-ferritin prevents calcium deposition as well as expression of osteocalcin. Figure 1C and 1D show the elevated H-ferritin levels after exposure to iron, apo-ferritin or D3T. Supplementary Figure II. C and D show the densitometry of H-ferritin expression. To further confirm the importance of the inhibitory role of H-ferritin, we transfected VIC with small interfering RNA (siRNA) specific to H-ferritin. In the presence of H-ferritin siRNA, iron or D3T failed to inhibit calcification as reflected by the accumulation of calcium and osteocalcin (Figure 1D and E). Supplementary Figure II. A and B confirm silencing of H-ferritin expression in VIC.

To validate the ferroxidase activity's paramount role in inhibition of mineralization, we used another protein that possesses this activity, namely ceruloplasmin. As shown in Supplementary Figure III. A and B mineralization of VIC in calcifying condition was inhibited by ceruloplasmin or H-ferritin as reflected by decreased calcium content of extracellular matrix that was also confirmed by Alizarin Red S staining.

Induction of H-ferritin by iron or D3T in cells derived from healthy subjects, as well as administration of recombinant H-ferritin but not mutant H-ferritin²²² lacking ferroxidase activity, prevented mineralization of VIC as reflected by accumulation of calcium and osteocalcin in the extracellular matrix (Supplementary Figure IV. A and B).

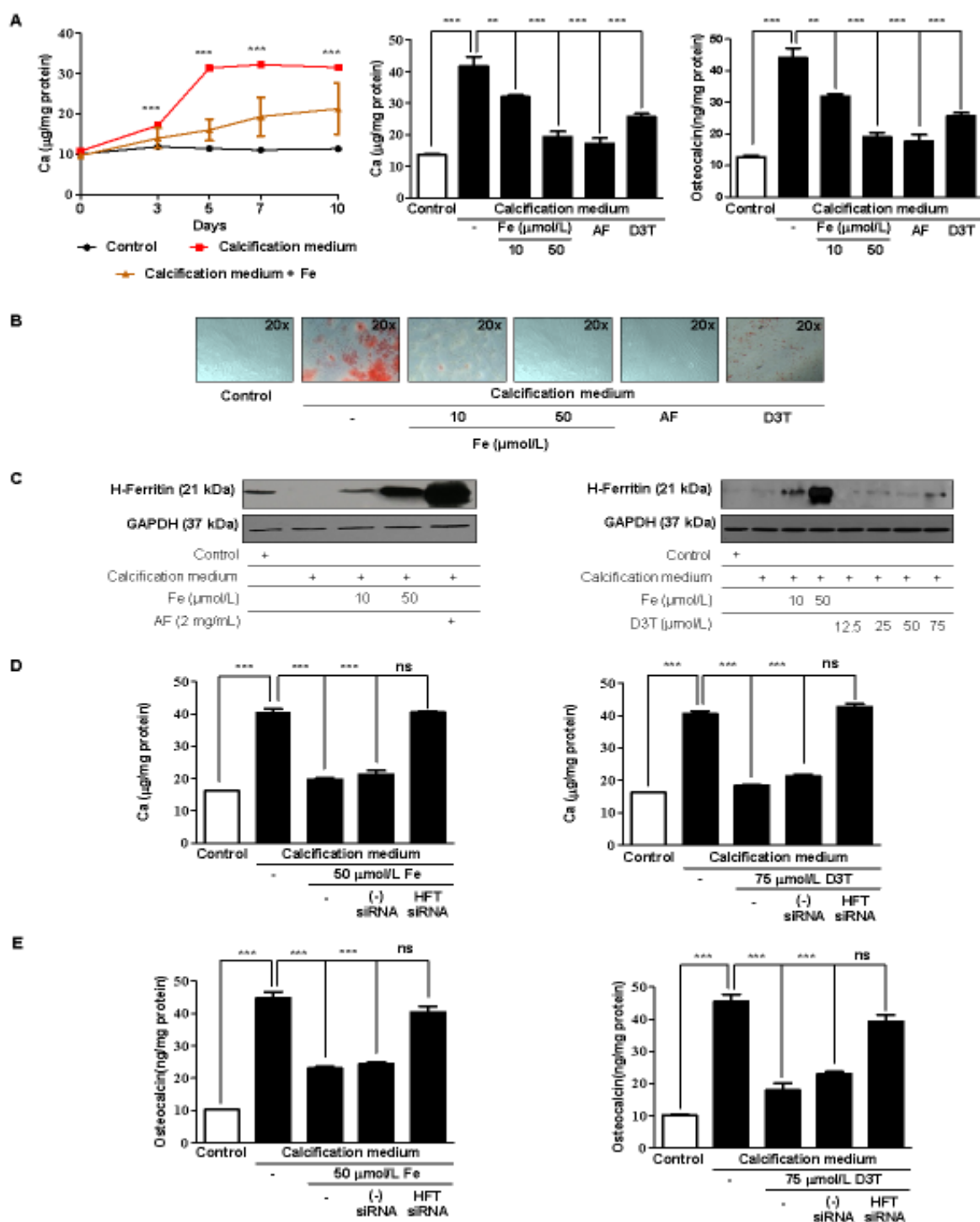


Figure 1. Calcification of valvular interstitial cells is inhibited by iron, D3T, and apo-ferritin. A) VIC were cultured in growth medium or calcification medium in the presence or absence of 10, 50 $\mu\text{mol/L}$ iron (Ammonium iron (III) citrate) and 2 mg/mL apo-ferritin. Calcium contents of the cells were measured after 0, 3, 5, 7 and ten days and normalized to protein content of the cells (left panel). Calcium content and representative images of Alizarin Red staining (Figure 1B) are shown. Figure 1 (middle panel) Calcium and Figure 1 (right panel) osteocalcin content of the cells were measured after five days incubation. Osteocalcin and calcium level were normalized to protein concentration of cells. C) Representative Western blot shows expression of H-ferritin and GAPDH of cells treated as described above. 60% confluence of VIC

were transfected with siRNA specific to H-ferritin or negative control siRNA 24 hours before the experiment. Cells were cultured in growth medium or calcification medium in the presence or absence of iron or D3T for five days. D) Calcium deposition, E) Osteocalcin level was measured. Graphs analyzed by One Way ANOVA, Bonferroni's Multiple Comparison Test and show mean \pm SEM of three independent experiments. Not significant (ns), ** $P < 0.001$, *** $P < 0.0001$.

4.2. Calcification potential of VIC derived from isolated insufficient aortic valve and stenotic aortic heart valves

We investigated whether the origin of VIC (cells derived from the aortic valve with insufficiency (AI) or stenotic valve leaflets (AS)) may influence the calcification potential of these cells. Supplementary Figure V. shows that cells from stenotic valve tissue have greater ability to transdifferentiate into osteoblast-like cells as indicated by the higher level of extracellular calcium deposition and the accumulation of calcium binding protein, osteocalcin (Supplementary Figure V. A and V. B). Furthermore, we found that the inhibitory effect of iron and apo-ferritin on mineralization was more pronounced in AI valve cells compared to AS VIC. In Supplementary Figure V. we demonstrate that calcium accumulation and osteocalcin levels were higher in AS compared to AI VIC. Interestingly, iron exposure could not inhibit mineralization in the AS stage VIC compared to AI VIC. However, apo-ferritin treatment could inhibit calcification regardless of the degree of valvular disease. This is likely explained by the high concentration of apo-ferritin and may suggest that significantly higher levels of iron may exert similar effects. Osteocalcin, the marker of osteoblastic activity, also corroborated the above findings and its levels suggested that apo-ferritin had a paramount effect on its expression than iron (Supplementary Figure V. B). Macroscopic images from AI and AS valves are shown in the Supplementary Figure V. C.

4.3. Effect of iron, apo-ferritin and D3T in localization of RUNX2 under calcific condition of VIC

Runt-related transcription factor 2 (RUNX2) is a key determinant of osteoblast activity (Komori, Yagi et al. (1997)) and implicated in the pathogenesis of vascular mineralization (Steitz, Speer et al. (2001)). Therefore, we investigated whether regulation of osteoblastic differentiation of VIC by ferritin occurs via modulation of RUNX2. We examined cultured VIC by immunocytochemistry and by Western blot (Figure 2A and 2B) and found nuclear translocation of RUNX2 in cells maintained in calcification medium. On the contrary, treatment of VIC with iron, apo-ferritin or D3T prevented translocation of RUNX2 into the nucleus (Figure 2A and 2B). Colocalization rate of RUNX2 bound to DNA in the nucleus (Hoechst staining) is shown in Figure 2A. Furthermore, we also tested the location of RUNX2 by immunostaining in VIC derived from AS and its expression from whole protein lysates derived from AS valves as compared to AI valves (Figure 2C and 2D). We found that RUNX2 is located in AS sample's nuclear region. Conversely, nuclear location of RUNX2 was not detected in AI derived VIC (Figure 2D). Moreover, silencing of H-ferritin gene resulted in increased translocation of RUNX2 into the nucleus (Supplementary Figure VI). Lower magnification images of RUNX2 immunostaining with antibody controls are shown in Supplementary Figure VII.

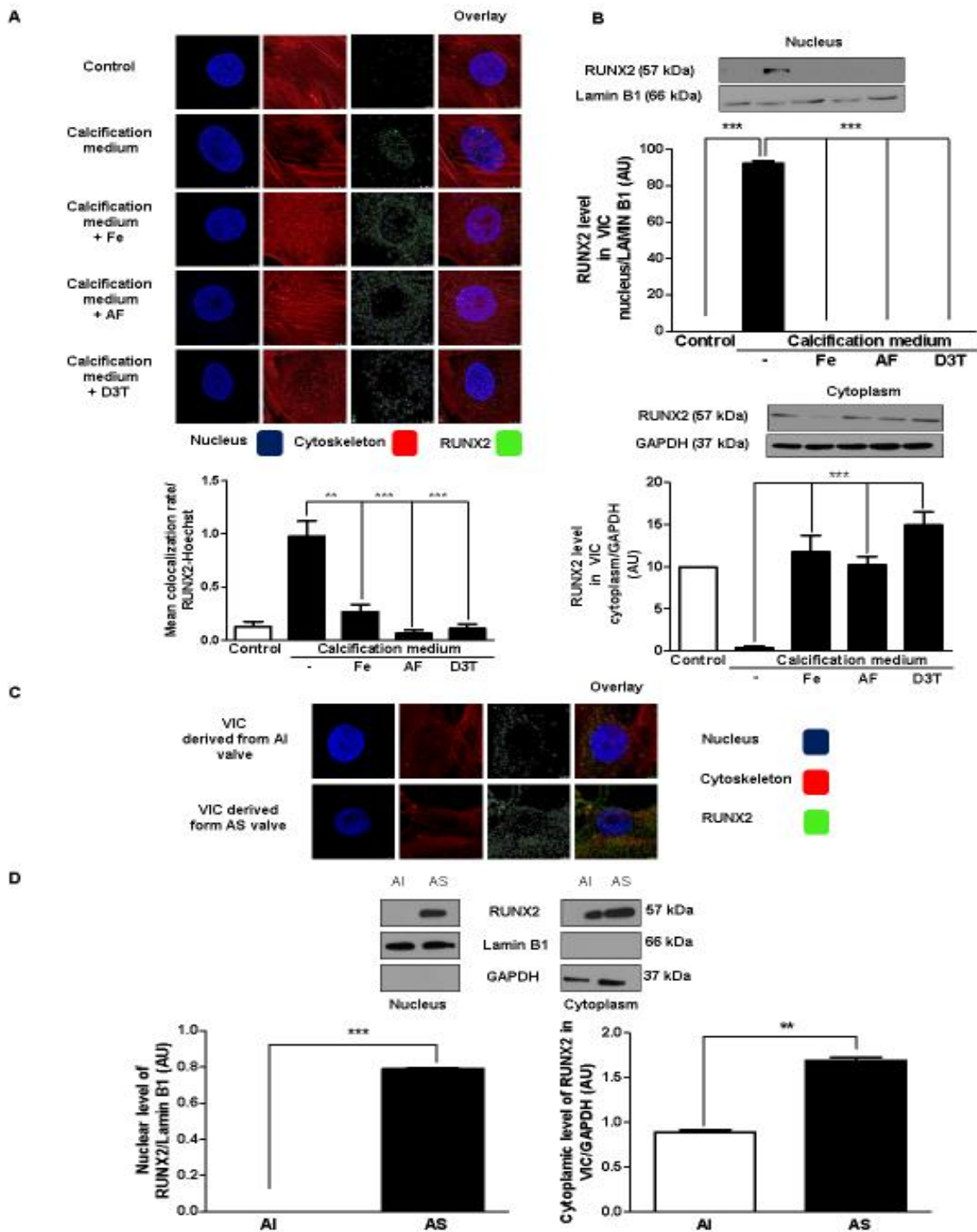


Figure 2. Nuclear translocation of RUNX2 is prevented by iron, apo-ferritin and D3T.

A) VIC were cultured with 50 $\mu\text{mol/L}$ iron (Ammonium iron(III) citrate), 2 mg/mL apo-ferritin, 75 $\mu\text{mol/L}$ D3T added into the calcification medium and localization of transcription factor RUNX2 was examined (green). Colocalization of RUNX2 and Hoechst was measured. B) Representative Western blot of RUNX2 from isolated nucleus and cytoplasm of VIC. Samples were normalized for GAPDH and Lamin B1. C) RUNX2 immunostainings of VIC derived from AI or AS valves are shown. Brightness was adjusted by 40%. D) RUNX2 protein level isolated from AI and AS tissues. Results were normalized to Lamin B1 and GAPDH. Images were obtained employing immunofluorescence-confocal STED nanoscopy. Representative staining is shown from at least three independent experiments. Results were analyzed by One Way ANOVA, Bonferroni's Multiple Comparison Test (Figure 2A-C) and Paired t-test (Figure 2D) and are shown as mean values \pm SEM of at least three independent experiments. ** $P < 0.001$; *** $P < 0.0001$.

4.4. Sox9 in valvular mineralization

Since RUNX2 activity was previously revealed to be antagonized by Sox9 in VIC (Cheng and Genever (2010)), we investigated the location of Sox9 in cultured VIC by immunocytochemistry and Western blot analysis. In cells cultured in growth medium Sox9 existed in the nucleus, while under calcific conditions nuclear Sox9 was barely detectable (Figure 3A and 3B). In contrast, nuclear location of Sox9 was maintained in cells cultured in calcification medium supplemented with iron, apo-ferritin and D3T. Moreover, we also collected human heart valves of AS exhibiting calcification for comparison to AI without calcification. Western blot analysis showed the nuclear presence of Sox9 in AI valve samples. On the contrary, nuclear Sox9 in AS valves was below the detection level (Figure 3C). Lower magnification images of Sox9 immunostaining with antibody controls are shown in Supplementary Figure VIII.

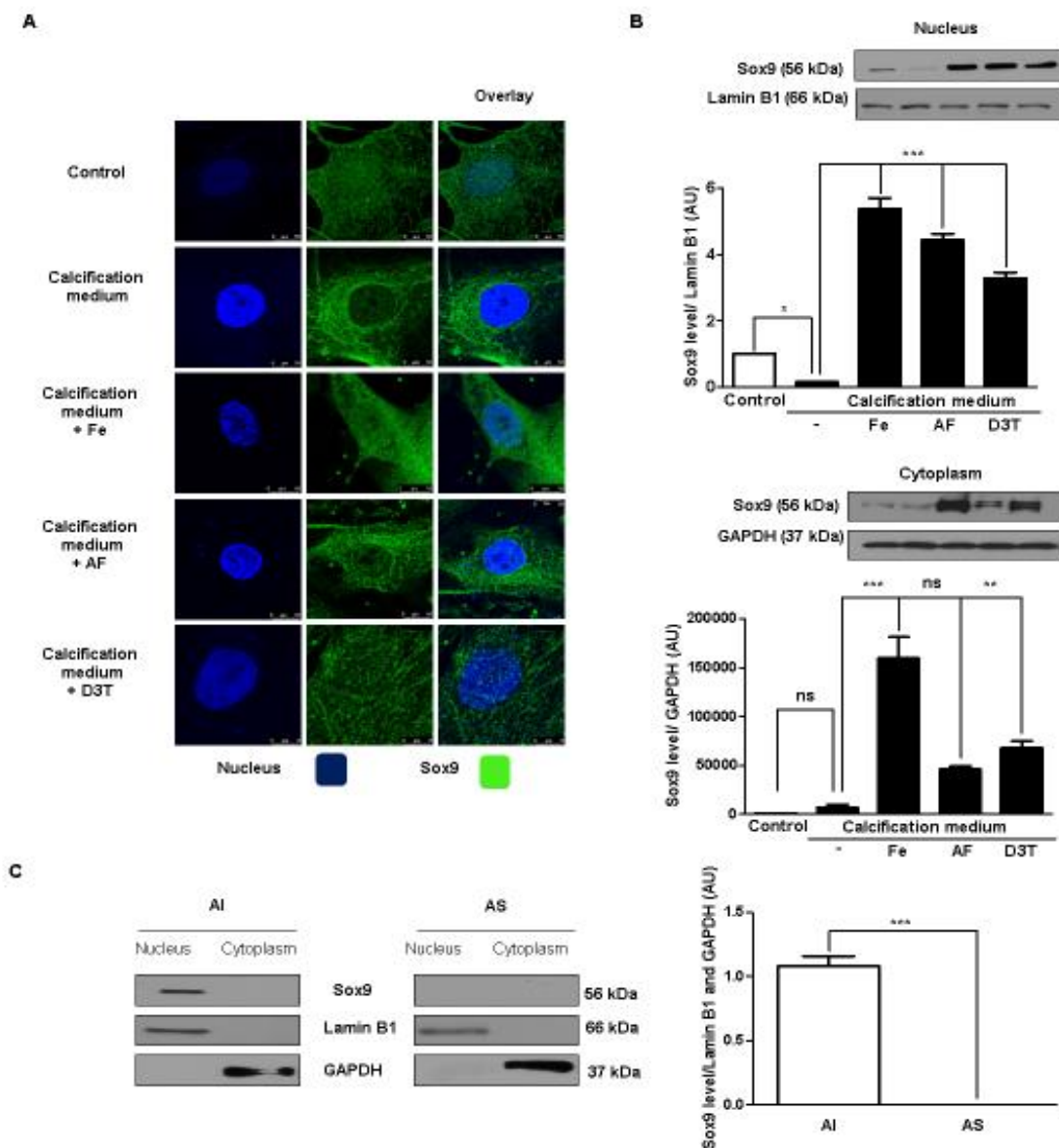


Figure 3. Calcifying milieu inhibits Sox9 nuclear localization. VIC were cultured in growth medium or calcification medium in the presence or absence of 10, 50 $\mu\text{mol/L}$ iron (Ammonium iron (III)

citrate) and 2 mg/mL apo-ferritin. A) Localization of Sox9 was shown (stained green) by immunostaining. Images were obtained employing immunofluorescence-confocal STED nanoscopy. B) Sox9 protein expression from isolated nucleus and cytoplasm fraction also shown. Results were normalized to Lamin B1 and GAPDH. C) Co-localization of Sox9 in VIC. Representative staining is shown from at least three independent experiments. Data were analyzed by One Way ANOVA, Bonferroni's Multiple Comparison Test (Figure 3A-B)) and Paired t-test (Figure 3C) and shows the average of three separate experiments performed in duplicate. ** P<0,001; ***P < 0.0001.

4.5. Regulation of VIC phosphate uptake by iron, apo-ferritin, D3T and H-ferritin

Nuclear translocation of RUNX2 was shown to be regulated by intracellular phosphate level (Jono, McKee et al. (2000); Fujita, Izumo et al. (2001)). To test whether H-ferritin affects intracellular phosphate levels in VIC maintained in normal condition or calcification medium we treated VIC with iron, apo-ferritin or D3T. As shown in Figure 4A significantly lower intracellular phosphate levels were found in cells exposed to iron, apo-ferritin or D3T compared to cells growing in calcific condition alone. Importantly, lysosomal phosphate level was also decreased to the control level in response to iron exposure in cells cultured in calcification medium (Figure 4B). Accordingly, expression of Pit1 (the membrane-associated channels responsible for the phosphate transport) was attenuated after treatment of VIC with iron, apo-ferritin or D3T (Figure 4C). In addition, Pit2 expression was diminished in response to ferritin induction (Figure 4D). Exogenous H-ferritin also decreased Pit1 protein expression in VIC cells derived from AS tissues (Figure 4E).

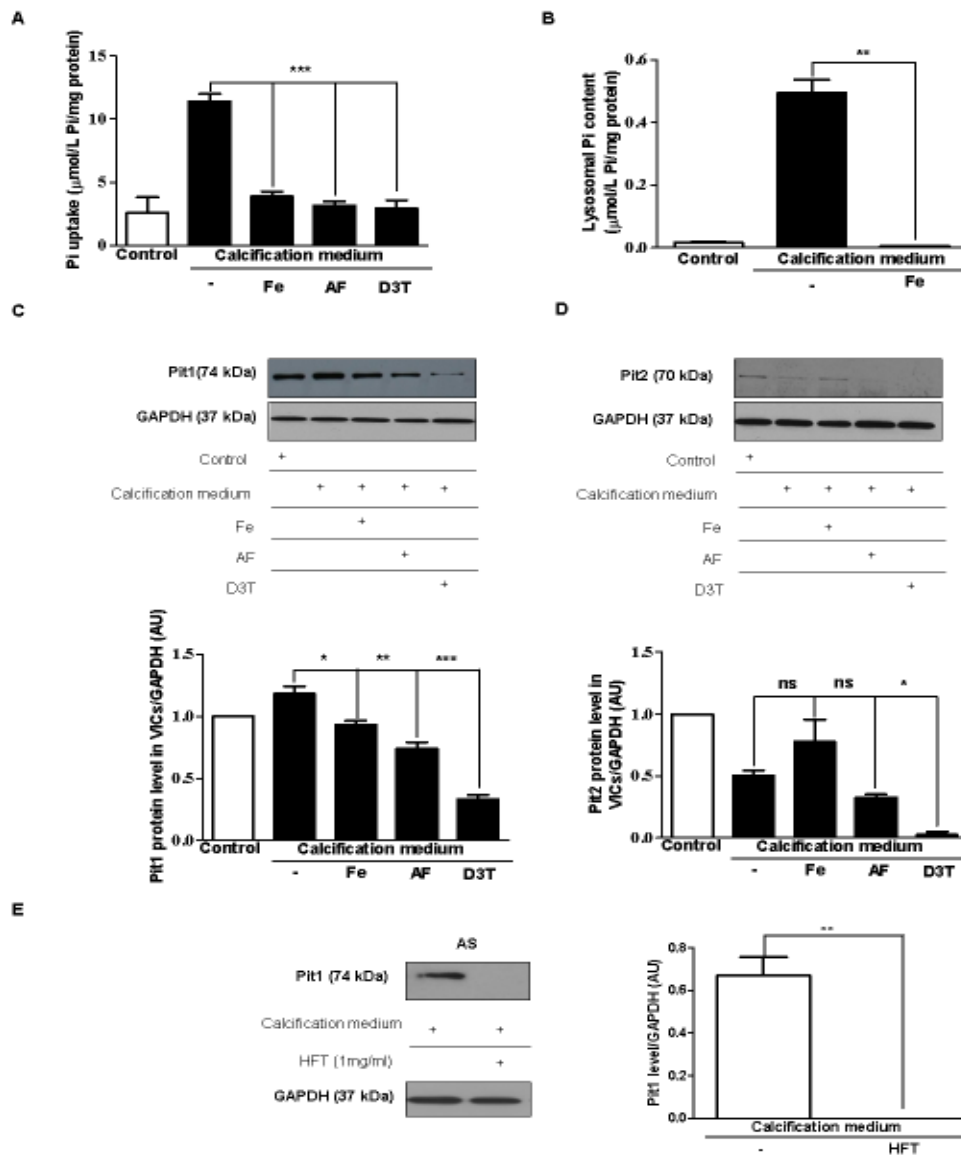


Figure 4. Phosphate uptake by valvular interstitial cells is reduced by iron, apo-ferritin, and D3T. A) Cells were cultured in a normal or calcific environment exposed to iron, or apo-ferritin, and D3T and phosphate content was determined using QuantiChrom quantitative colorimetric assay. B) VIC were cultured in growth medium or calcification medium in the presence or absence of iron (Ammonium iron (III) citrate). After isolation of lysosomes, phosphate level was measured. VIC were cultured with 50 µmol/L iron (Ammonium iron (III) citrate), 2 mg/mL apo-ferritin, 75 µmol/L D3T and C) Pit1 and D) Pit2 Western blotting was performed in the same experiments. E) VIC derived AS valves were cultured in calcific condition alone or supplemented with H-ferritin. Pit1 Western blots were carried out and normalized to the protein content of the samples. Results were analyzed by One Way ANOVA, Bonferroni's Multiple Comparison Test and are shown as mean values ± SEM of at least three independent experiments. *P < 0.05; **P < 0.001; ***P < 0.0001.

4.6. H-ferritin and inorganic phosphate association in the lysosome under calcific conditions

Apo-ferritin has a hollow internal cavity which can accommodate iron in a ferric oxyhydrophosphate complex (de Silva, Guo et al. (1993)). Through the action of ferroxidase, it is capable of storing iron and phosphate (2250 and 380 atoms, respectively). The amount of iron and phosphate within the core of ferritin are not related to different subunit composition. Double immunostaining against LAMP1 (lysosome marker) and H-ferritin (Figure 5B) revealed maximal co-localization (Figure 5C). Furthermore, inside the fused lysosomes (shown by arrows) a significant accumulation of ferritin is evident. To confirm this finding, we isolated lysosomes from cultured and treated VIC, and tested for H-ferritin/LAMP1 in different conditions: in the growth medium; calcification medium alone, or supplemented with iron. In iron-treated cells, we found a markedly increased H-ferritin level inside the lysosome (Figure 5A), which is demonstrated by the co-localization rate of H-ferritin and LAMP1 (Figure 5C). Lower magnification images of LAMP1- H-ferritin immunostaining with antibody controls were shown in Supplementary Figure IX.

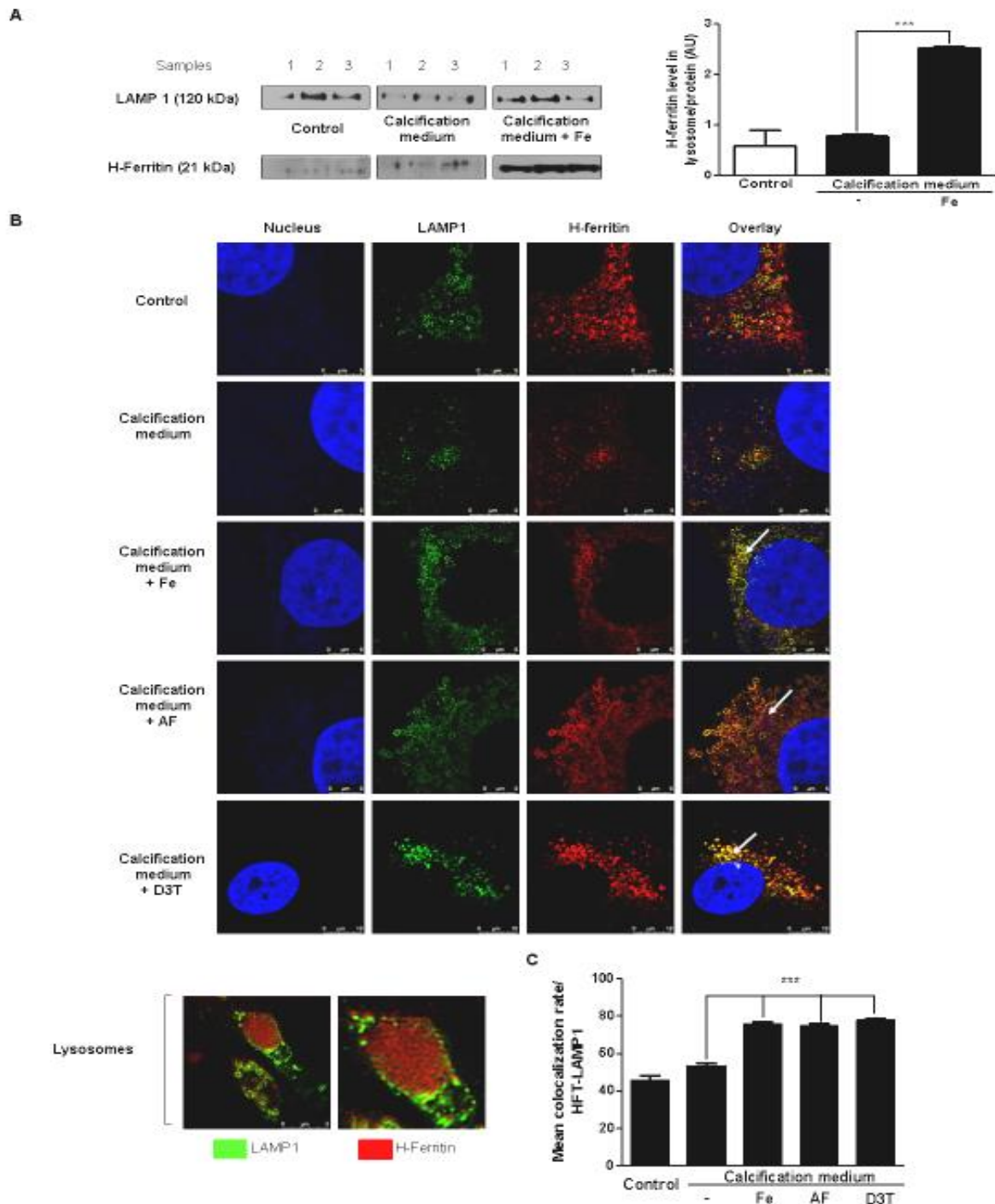


Figure 5. Lysosomal localization of H-ferritin in cells exposed to iron, apo-ferritin or D3T.

A) VIC were cultured in growth medium or calcification medium in the presence or absence of iron (Ammonium iron (III) citrate). Western blot analysis for H-ferritin and LAMP1 derived from the isolated lysosome. B) VIC were cultured in growth medium or calcification medium in the presence or absence of iron (Ammonium iron (III) citrate), apo-ferritin or D3T. Double immunofluorescence staining of VIC for LAMP1 and H-ferritin are shown. Images were obtained employing immunofluorescence-confocal microscope and STED nanoscopy. Representative staining is shown from at least three independent experiments. Results were analyzed by One Way ANOVA, Bonferroni's Multiple Comparison Test and are shown as mean values \pm SEM of at least three independent experiments. ***P < 0.0001.

4.7. Role of extracellular pyrophosphate in the inhibition of valvular calcification

Pyrophosphate (PPi) is also a key inhibitor of mineralization through binding to nascent hydroxyapatite crystals (Fleisch and Bisaz (1962); Terkeltaub (2001)). Therefore, we analyzed the changes of the level of pyrophosphate compared with the calcification medium. Iron/apo-ferritin/D3T treatment significantly increased the level of pyrophosphate contrary to cultured cells in calcification medium (Figure 6A). Since, the major pyrophosphate generating ectoenzyme is the ENPP2 we examined whether ENPP2 expression correlated with PPi level. Similarly to PPi, a decrease in ENPP2 expression was observed under calcification condition. Intriguingly, elevated expression of ENPP2 and higher PPi level were found in cells exposed to iron, apo-ferritin and D3T as compared to those cultured in calcification medium alone (Figure 6C). Moreover, treatment of cells with H-ferritin also increased ENPP2 protein level in VIC derived from AS tissues (Figure 6E). To confirm the importance of H-ferritin in controlling the pyrophosphate generation, we transfected VIC with small interfering RNA (siRNA) specific to H-ferritin. In the presence of H-ferritin siRNA, iron and also H-ferritin failed to enhance PPi level (Figure 6B and 6D). Expression of Ankyrin G1 protein was not altered by ferritin (data not shown).

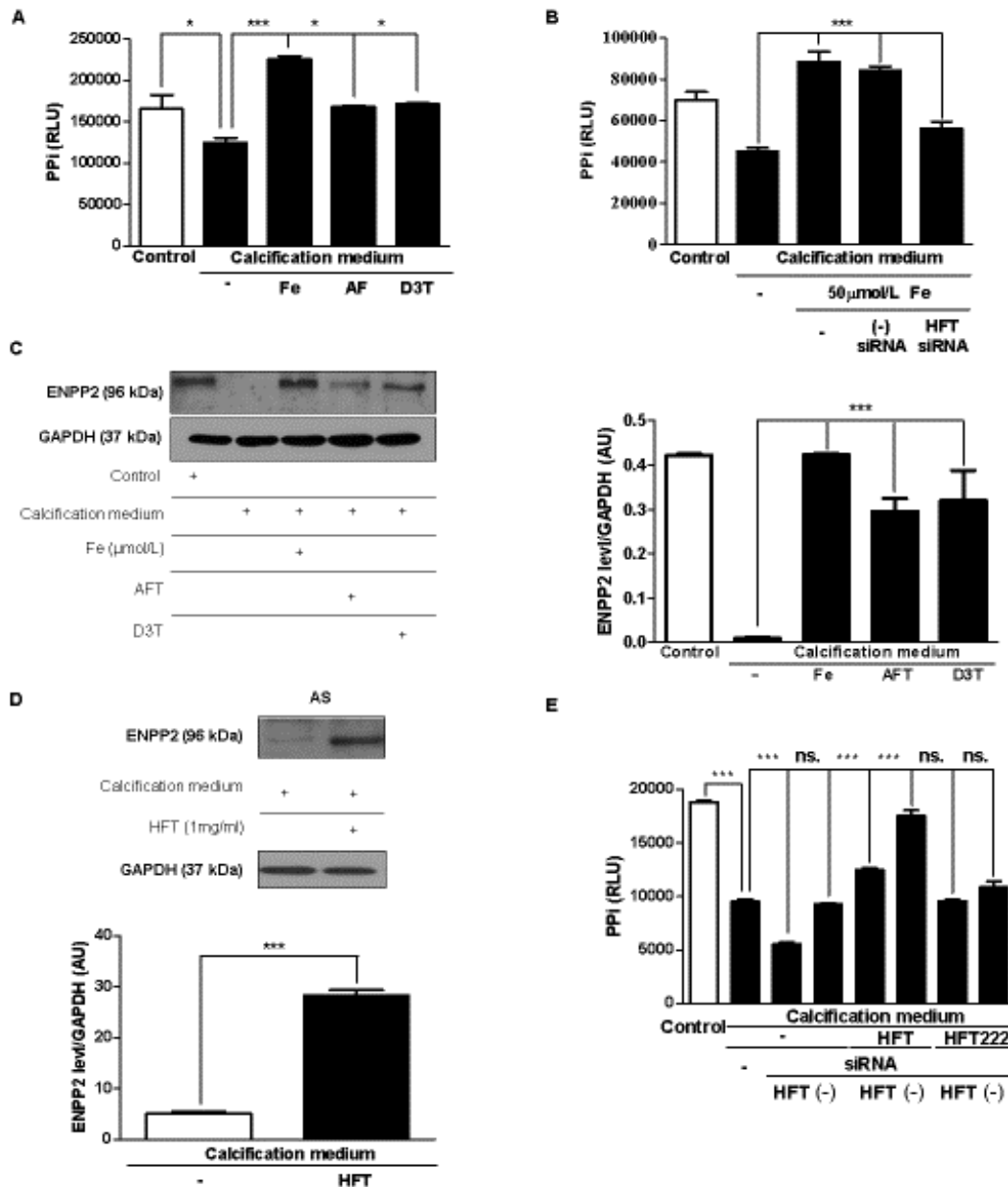


Figure 6. Pyrophosphate generation and ENPP expression are enhanced in VIC by iron, apo-ferritin and D3T. A) VIC were cultured in growth or calcification medium supplemented with 50 μmol/L iron (Ammonium iron (III) citrate), 2 mg/mL apo-ferritin or 75 μmol/L D3T for five days and pyrophosphate level was measured. B) VIC were transfected with siRNA specific to H-ferritin or negative control siRNA prior to iron exposure and pyrophosphate level was measured. C) ENPP2 expression in VIC was assessed by Western blot analysis. D) ENPP2 Western blot were shown. AS tissues derived VIC cells were cultured in calcific condition alone or treated with H-ferritin. Samples were normalized to the protein content of the cells. E) PPI level changes after H-Ferritin silencing were shown. VIC cells were transfected with siRNA against H-Ferritin. Samples were treated in the next day with 1 mg/mL of H-Ferritin and 1 mg/mL H-Ferritin 222 (mutant ferritin without ferroxidase activity) for 3 days. Data were analyzed by One Way ANOVA, Bonferroni's Multiple Comparison Test and are shown as mean values ± SEM of three separate experiments performed in duplicate. Not significant (ns), *P < 0.05; ***P < 0.0001.

4.8. H-ferritin and ALP expression in stenotic aortic valve

The above findings prompted us to examine whether the expression of ferritin is altered in VIC in CAVD. Therefore, Western blot analysis was performed for H-ferritin from patients' tissue lysate samples of AS and AI. Significantly higher level of H-ferritin was present in AS when compared to AI valves (Figure 7A). To localize H-ferritin in CAVD dual immunohistochemistry investigation (ALP and H-ferritin) was carried out. As shown in Figure 7B, ALP⁺ and H-ferritin⁺ cells were present in the affected valve from the endothelial surface to the calcific core. In the distant surface area more H-ferritin and less ALP staining was observed in cells, the ratio was 2.3:1 \pm 0.41, respectively. Expression of ALP and H-ferritin progressively increased toward the core and the ratio of H-ferritin to ALP decreased to 0.6 \pm 0.15 at the zone close to the calcific core of AS. In AI valves the staining for ALP and H-ferritin was even and moderate, the ratio of H-ferritin to ALP was 2.2:1 \pm 0.65 (Figure 7B).

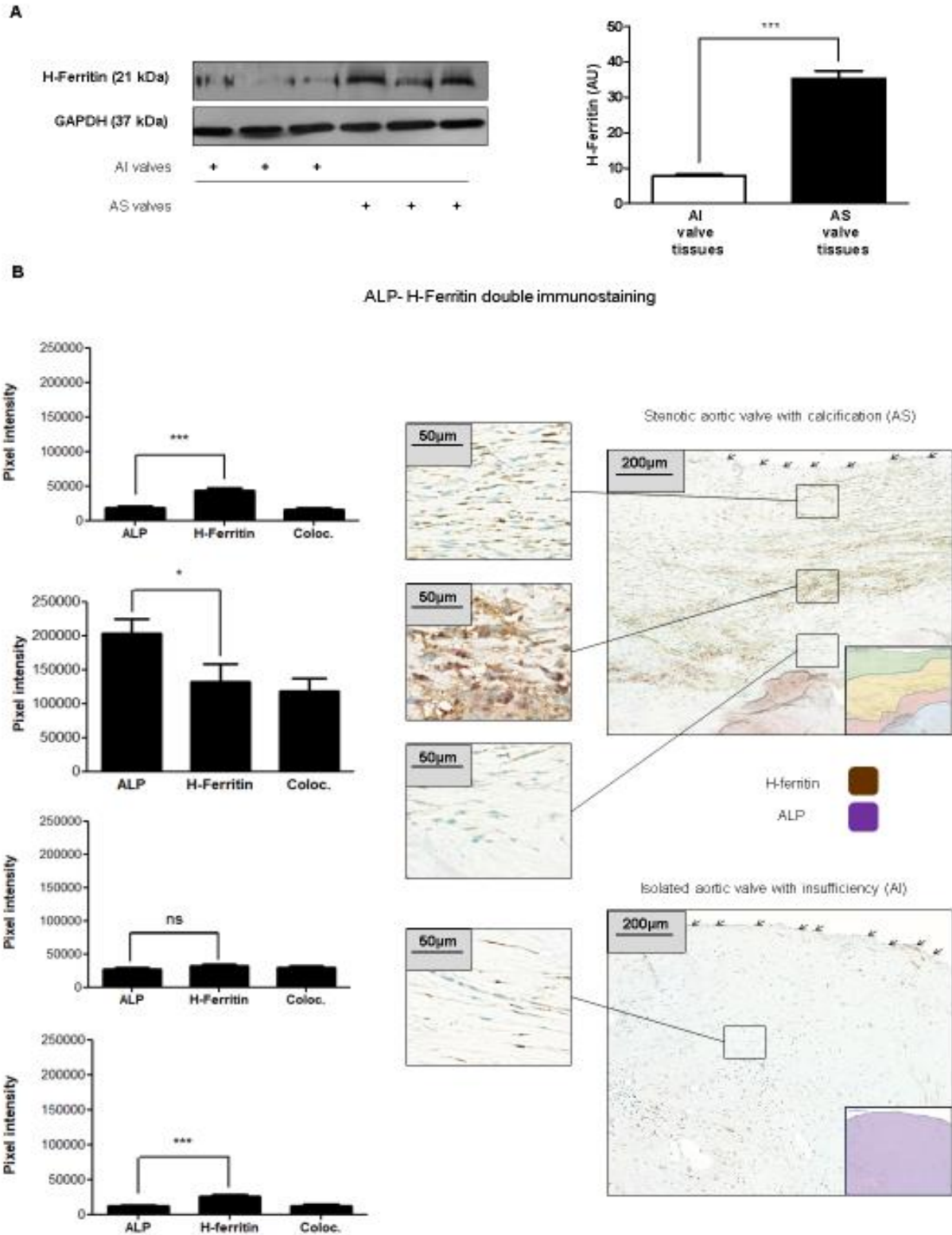


Figure 7. H-ferritin expression in AI and AS heart valves. A) H-ferritin expression in AI and AS heart valve tissue was assessed by Western blot analysis. B) The AI and AS valve sections were stained for ALP and H-ferritin. ALP, H-ferritin and colocalization rate of ALP and H-ferritin are shown as pixel intensity from AS and AI samples (left panels). Arrows show endothelial layer. Scale bars show 200 µm at 12.5x magnification and 50µm at 50x magnification. Results were analyzed by Unpaired t-test and are shown as mean values \pm SEM of at least three independent experiments.

4.9. Association between increased level of H-ferritin and inflammation in AS valves

Our previous findings highlight the question as to whether the elevated H-ferritin expression is due to iron exposure. To answer this question, we stained AS valves with Prussian blue (specific iron staining) and as shown in Figure 8A iron was absent in the highly calcified region. Torti et al. previously demonstrated that inflammatory cytokines upregulate the expression of H-ferritin in the absence of iron (Torti, Kwak et al. (1988); Tsuji, Miller et al. (1991)). Moreover, inflammation is implicated in the progression of CAVD (Rajamannan, Evans et al. (2011)). Therefore, we performed immunohistochemistry (Figure 9A) and Western blot analysis (Figure 9B) for inflammatory markers, TNF- α and IL1- β on human healthy and AS tissue. Importantly, elevated H-ferritin expression corroborated the increased protein level of TNF- α and IL1- β in AS tissues as compared to healthy aortic valves (Figure 9).

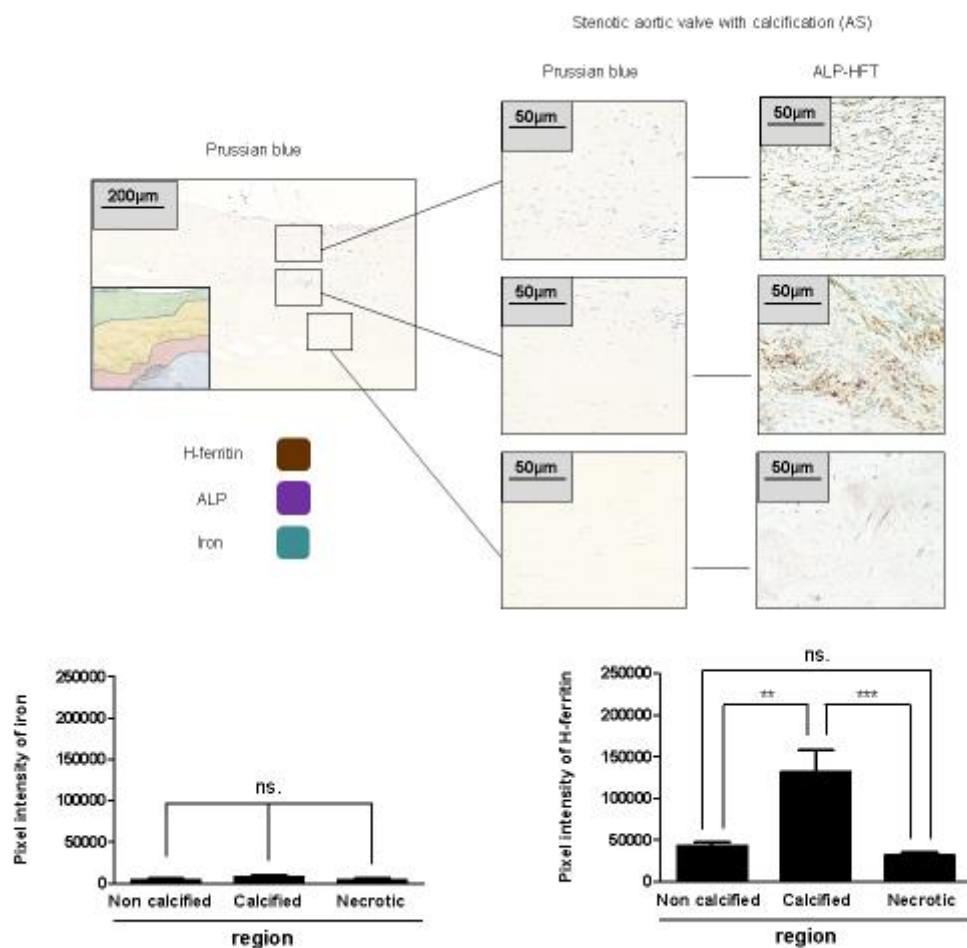


Figure 8. Increased H-ferritin levels in AS valve without accumulation of iron. A) Prussian blue (left panel) and H-ferritin-ALP (right panel) staining were performed on AS valves (N=3). Scale bars (200 µm at 12.5x magnification and 50µm at 50x magnification) and pixel intensity of iron and H-ferritin staining were shown. Representative stains were shown from at least three independent experiments. Results were analyzed by unpaired t-test and are shown as mean values \pm SEM of at least three independent experiments.

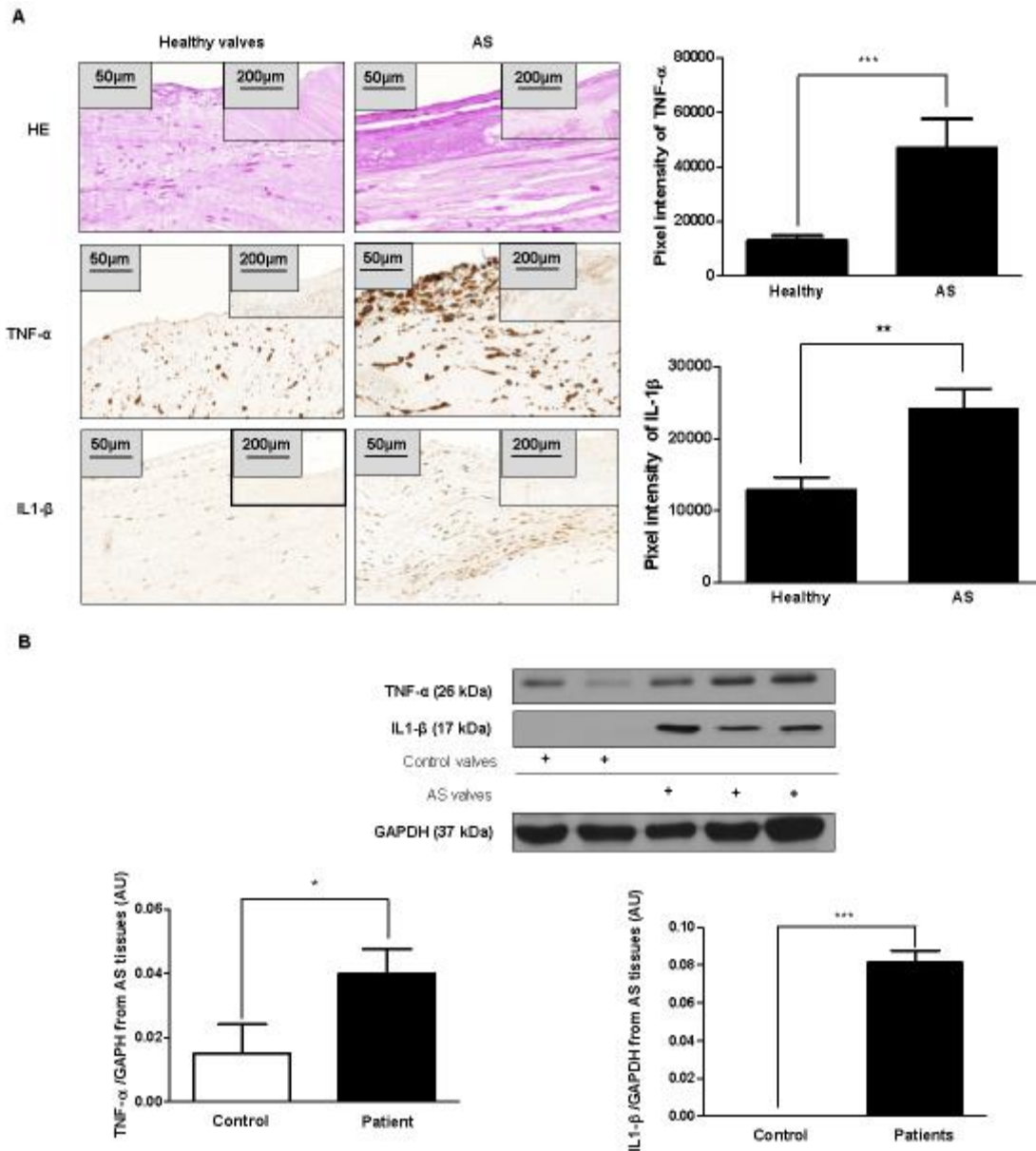


Figure 9. Increased expression of inflammatory markers in AS valves. A) Hematoxylin and eosin (upper panels); TNF- α ; and IL1- β IHC staining were performed on healthy heart valves derived from the Department of Forensic Institute, University of Debrecen (left column; N=3) and on AS valves with calcification (right column, N=9). Scale bars (200 μ m at 12.5x magnification and 50 μ m at 50x magnification) and pixel intensity of IHC staining were shown. Representative staining was shown from at least three independent experiments. B) Western blots (TNF- α and IL1- β) from AS tissues were shown. Protein expressions were normalized to GAPDH. Results were analyzed by One Way ANOVA, Bonferroni's Multiple Comparison Test (Figure 8B) and were shown as mean values \pm SEM of at least three independent experiments. **P < 0.001; ***P < 0.0001.

4.10. Function of H-ferritin in the development of inflammation of heart valve

To test whether ferritin/ferroxidase system has the potential to act against inflammation in CAVD, we treated VIC cells derived from AS tissue with H-ferritin. We found that H-ferritin exposure inhibited the expression of TNF- α and IL1- β (Figure 10A). Figure 10B shows the possible mechanisms for the beneficial role of ferritin/ferroxidase in CAVD.

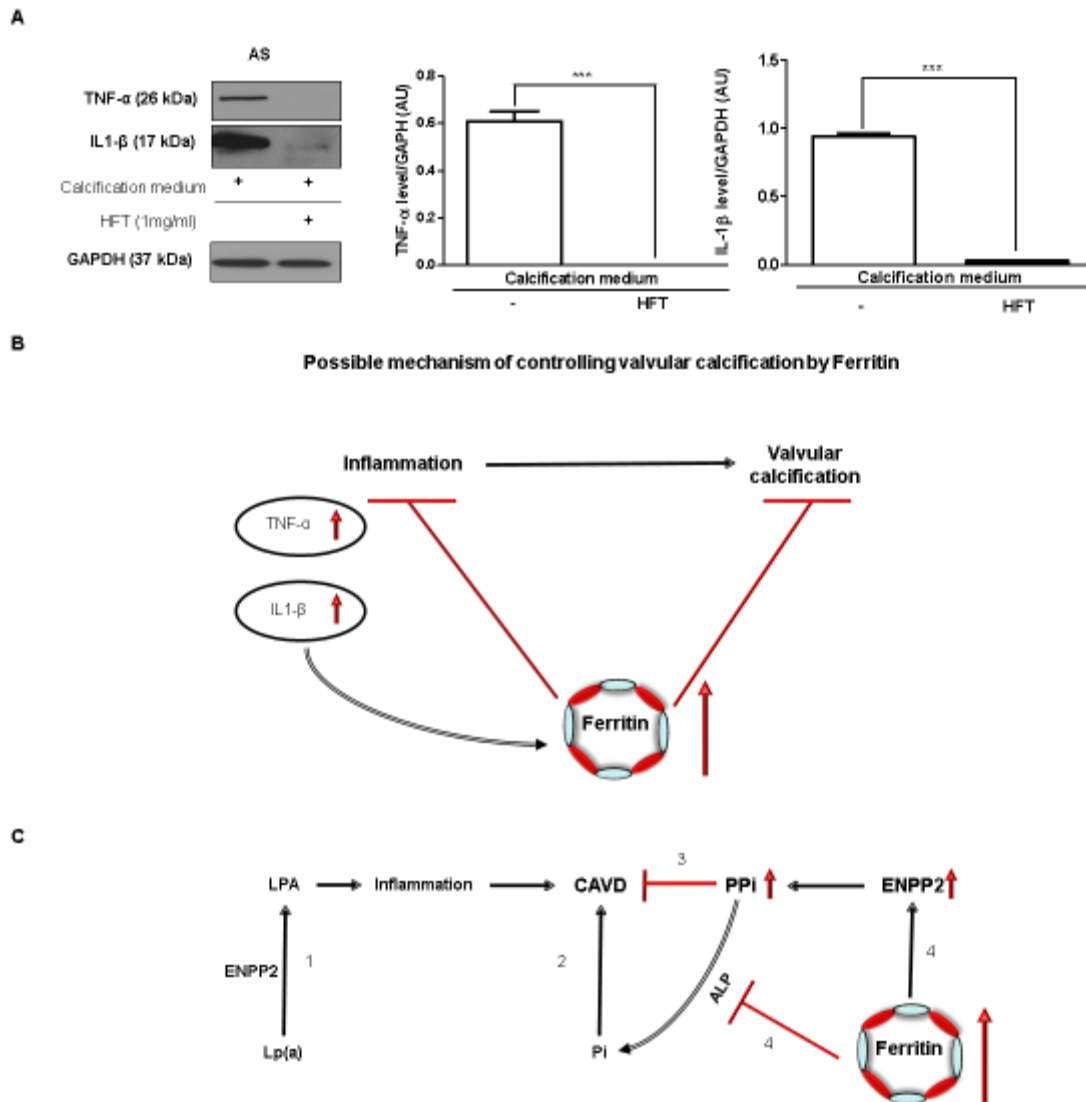


Figure 10. H-ferritin inhibits the expression of TNF- α and IL1- β in VIC derived from AS. VIC were cultured in calcification medium or supplemented with 1mg/mL H-ferritin. A) Western blot was performed and the following antibodies were used: anti-human TNF- α ; anti-human IL1- β . B) TNF- α and IL1- β protein level in AS valve tissue. (N=3). B) Role of H-ferritin in the inflammatory process and valvular calcification. C) (1) Lp (a) is a risk factor of calcific aortic valve disease (CAVD) via inducing inflammation. (2) Pi is risk factor of calcific aortic valve disease. (3) PPi antagonizes valvular mineralization. (4) H-ferritin inhibits valvular mineralization via elevating PPi and decreasing Pi by the induction of ENPP2 and the inhibition of ALP activity. Data were analyzed by One Way ANOVA, Bonferroni's Multiple Comparison Test and samples were derived from four separate experiments performed in triplicates and shown as mean \pm SEM ***P < 0.0001.

Part2

4.11. H₂S function in the calcification of valvular interstitial cells *in vitro*

The potential of different H₂S donors for inhibition of calcification of valvular interstitial cells isolated from human aortic valves were investigated. Cells were cultured in calcific condition containing 2.5 mmol/L inorganic phosphate and 1.8 mmol/L calcium-chloride. VIC were treated with H₂S: the simple sulfide salts NaSH and Na₂S that instantaneously generates H₂S via pH-dependent salt dissociation and novel slow-release sulfide donors (AP67 and AP72) and the more commonly used donor GYY4137 (synthesized in-house). As expected, the osteoblastic transition of VIC occurred in calcifying environment, which is reflected by the extracellular accumulation of calcium (Figure 11), and the increased expression of osteocalcin and ALP (Figure 12). Particularly, all H₂S donors decreased calcium deposition in a dose-responsive fashion (Figure 11). NaSH reached the maximum inhibition at 150 μmol/L (Figure 11A), Na₂S and GYY4137 attenuated calcification at 100 μmol/L (Figure 11B and C), while AP67 suppressed calcification at 50 μmol/L (Figure 11D) concentration compared to calcification medium without H₂S supplementation. Among the H₂S donors, AP72 fully abrogated calcium deposition in the extracellular matrix of VIC at 20 μmol/L concentration (Figure 11E-F). Moreover, osteocalcin accumulation and expression of ALP in VIC along with calcium deposition were also prevented by AP72 (20 μmol/L; Supplementary Figure XII. A-C). Similarly, other fast (NaSH, Na₂S) and slow (GYY4137, AP67) sulfide releasing molecules significantly attenuated the osteocalcin secretion (Supplementary Figure X.A). ALP and Alizarin Red S staining showed pronounced osteoblastic transformation of VIC in the calcific environment and this effect was prevented by AP72 (Supplementary Figure XII. C-D). As demonstrated in Supplementary Figure XII.E, AP72 did not exhibit any cytotoxic effects on VIC at the applied dose. We observed a “U” shape curve in the inhibition of mineralization. Use of H₂S donors at concentrations in excess of that stated above resulted in a concentration-dependent decline in protection. Then, we selected from these studies the most effective H₂S donor (AP72) for further investigation to explore the mechanism by which H₂S regulates the calcification processes.

Phenol was shown to capture H₂S (Huang, Zhang et al. (2017)), so we tested if AP72 affects calcification at lower concentrations in phenol red-free medium as compared to calcification medium with phenol red. In phenol red free condition, AP72 significantly inhibited calcification of VIC at concentration of 2.5 nmol/L to 5 μmol/L (Supplementary Figure X. B). Respectively, osteocalcin accumulation was prevented and phosphate uptake was also decreased by AP72 in condition without phenol red (Figure 12A-B). Alkaline phosphatase and Alizarin Red S staining indicated the inhibitory effect of AP72 at a concentration of 2 μmol/L (Figure 12D-E). In Supplementary Figure XII, in phenol red containing medium AP72 exhibited inhibitory effect on calcification in VIC at one order magnitude higher concentration. At the most effective concentrations of the sulfide donor molecules did not caused cytotoxicity in VIC (Supplementary Figure X. C).

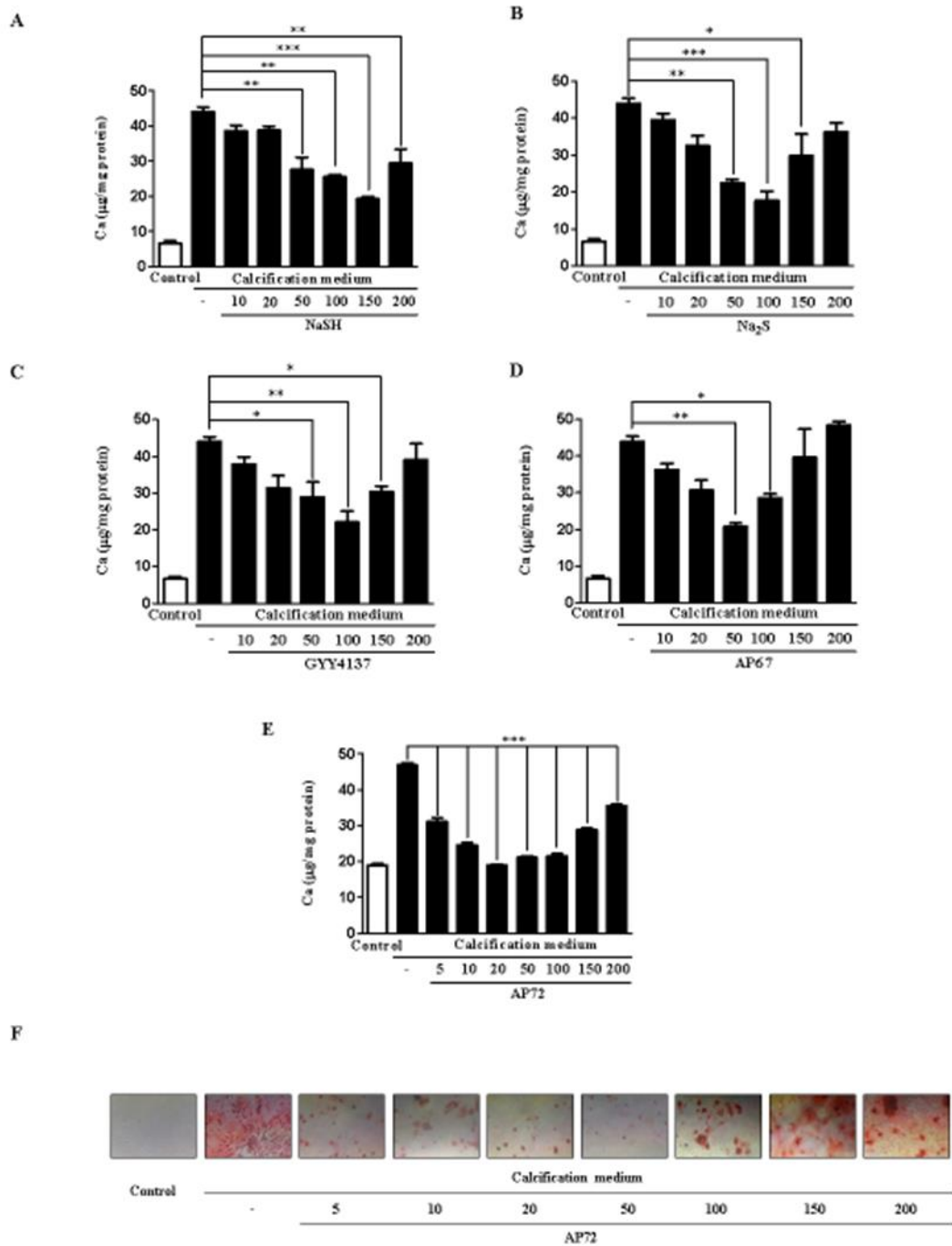
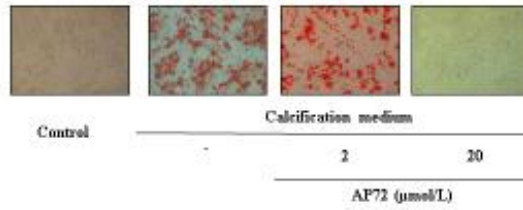
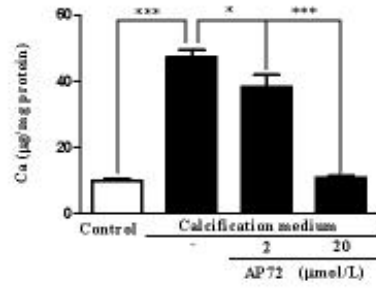


Figure 11. H₂S donors dose-dependently inhibit the calcification of VIC. Calcium contents of VIC was shown in growth medium or calcification medium after 5 days treatment with A) NaSH; B) Na₂S; C) GYY4137; D) AP67 (10-200 µmol/L) or with E) AP72 (5-200 µmol/L). F) Alizarin Red S staining of VIC. Graph shows means ±SEM of five independent experiments. *P < 0.05; **P < 0.01; ***P < 0.001.

A



B

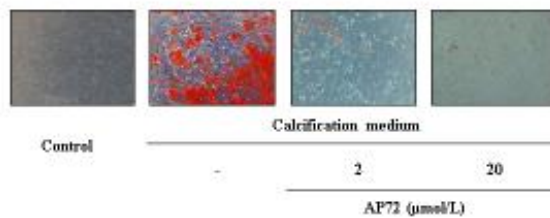
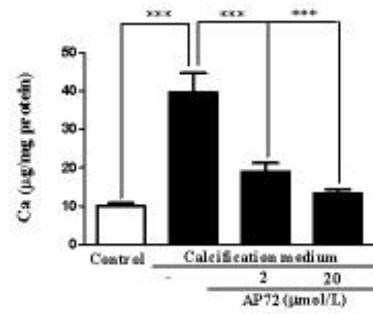


Figure 12. Phenol red impairs anti-calcification effect of H₂S. Cultured VIC in A) phenol red containing D-MEM (Sigma) or B) phenol red free media were supplemented with AP72 (2 µmol/L; 20 µmol/L) for 5 days and calcium content of the cells was measured and normalized to protein content of the cells. Alizarin Red S staining represents the microscopic image of calcium deposition of extracellular matrix. Graph shows mean ±SEM of five separate experiments. *P < 0.05; ***P < 0.001.

4.12. Association of AP72 source and RUNX2 localization under calcification of VIC

RUNX2 is the key transcription factor of the early osteoblastic differentiation of vascular smooth muscle cells and VIC. We were curious whether cultured VIC in calcification medium affected by AP72 treatment how determined the localization of RUNX2. Immunofluorescence staining demonstrated that RUNX2 was located in the cytoplasm of VIC cultured in growth medium (control medium) (Figure 13A; upper panels). Phosphate exposure of VIC triggered the translocation of RUNX2 from the cytoplasm to the nucleus (Figure 13A; middle panels). As demonstrated in Figure 13A (lower panel) AP72 prevented the appearance of RUNX2 in the nucleus of VIC maintained in calcification medium. To support our immunofluorescence observation, we examined RUNX2 translocation by Western blot analysis using from cytoplasm and nucleus fractions of VIC. We found that RUNX2 appeared in the nucleus in response to calcification medium (Figure 13B; left panel) while its level was decreased in the cytoplasmic fraction (Figure 13B; right panel). Moreover, AP72 treatment prevented the translocation of RUNX2 into the nucleus of VIC exposed to phosphate (Figure 13B).

We also examined the nuclear location of the RUNX2 in VIC derived from human valves with visible calcification (AS) and without calcification (AI). Confocal microscopy and Western blot analysis revealed that RUNX2 was mainly located in the nucleus of VIC derived from AS human valve tissue. On the contrary, RUNX2 was detected in the cytoplasm of VIC derived from AI tissue (Figure 13C-D). Importantly, exposure of cells to 200 $\mu\text{mol/L}$ of AP72 did not restrain the nuclear translocation of RUNX2 from the cytoplasm to the nucleus (Supplementary Figure XIII).

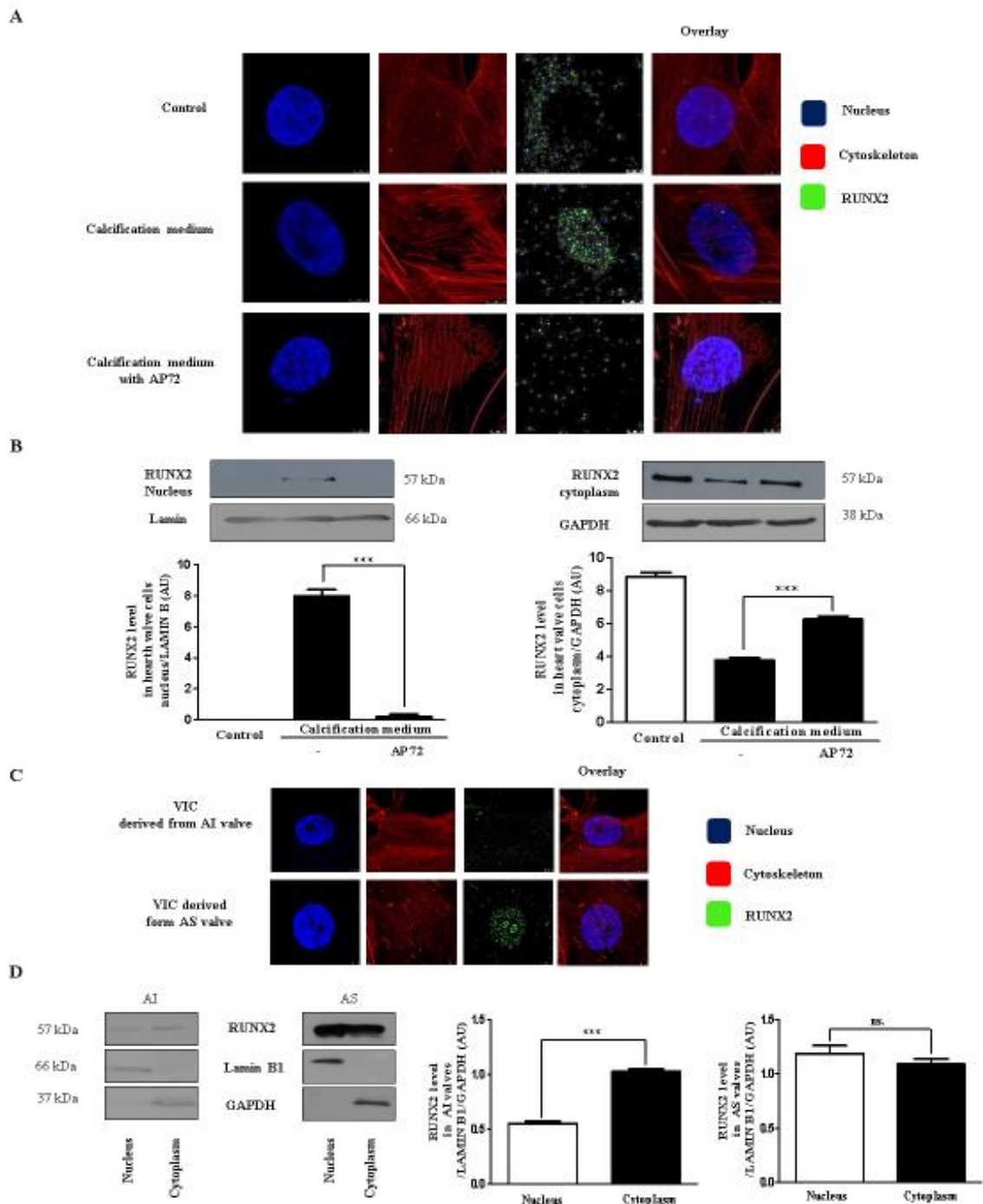


Figure 13. AP72 prevents nuclear translocation of RUNX2. VIC were grown on coverslips were exposed to growth medium or calcification medium alone or supplemented with AP72 (20 $\mu\text{mol/L}$) for 2 days. A) Cells were stained for DNA (Hoechst 33258, blue), RUNX2 (green, Alexa Flour 488), and F-actin (cytoskeleton, red, iFlour 647). Images are obtained employing an immunofluorescence-confocal STED nanoscope. B) RUNX2 expression in cytoplasmic and nuclear fraction of VIC. The band intensities are normalized for Laminin B1 in case of nuclear extracts and for GAPDH in case of cytoplasm extracts. C) RUNX2 localization in AI and AS derived VIC samples. Images are obtained employing an immunofluorescence confocal STED nanoscope. D) Protein levels of RUNX2 in AI and AS tissue lysates are shown. Representative staining and protein analysis are shown from at least five independent experiments. Not significant (ns); *** $P < 0.001$.

4.13. P_i production changes in the absence/presence of H₂S

P_i is a well-known anti-calcification molecule, regulated by ENPP2 and ANK1. Accordingly, we tested whether H₂S may control P_i production by regulating the expression of ENPP2 and ANK1 in VIC. Figure 14A shows that the expression of ENPP2 was decreased in VIC cultured in calcification medium as compared to control. Exposure of cells with AP72 abolished such an effect. ENPP expression was significantly elevated above the level observed in control cells (Figure 14A). Furthermore, the level of ANK1 protein in VIC maintained under calcifying conditions did not change compared to cells grown in growth medium. In contrast, AP72 induced ANK1 expression at both mRNA and protein levels in VIC (Figures 14B). Consequently, the amount of generated P_i decreased in cells grown under calcifying conditions (Figure 14C). Using AP72 supplementation P_i generation increased significantly in VIC compared to both cells cultured in control growth medium or calcification medium without any treatment (Figure 14C). GYY4137 and AP67 were also tested for affecting P_i level in VIC. These H₂S donors enhanced the P_i level lesser than AP72 (Figure 14C). The fast sulfide releasing molecules (NaSH and Na₂S) were able to enhance the P_i level only to the baseline (Supplementary Figure XIV). Additionally, our measurements in human heart valve tissue samples indicated significantly lower ENPP2 protein levels and lower P_i content in AS valve specimens as compared to AI valves samples (Figure 14D-E).

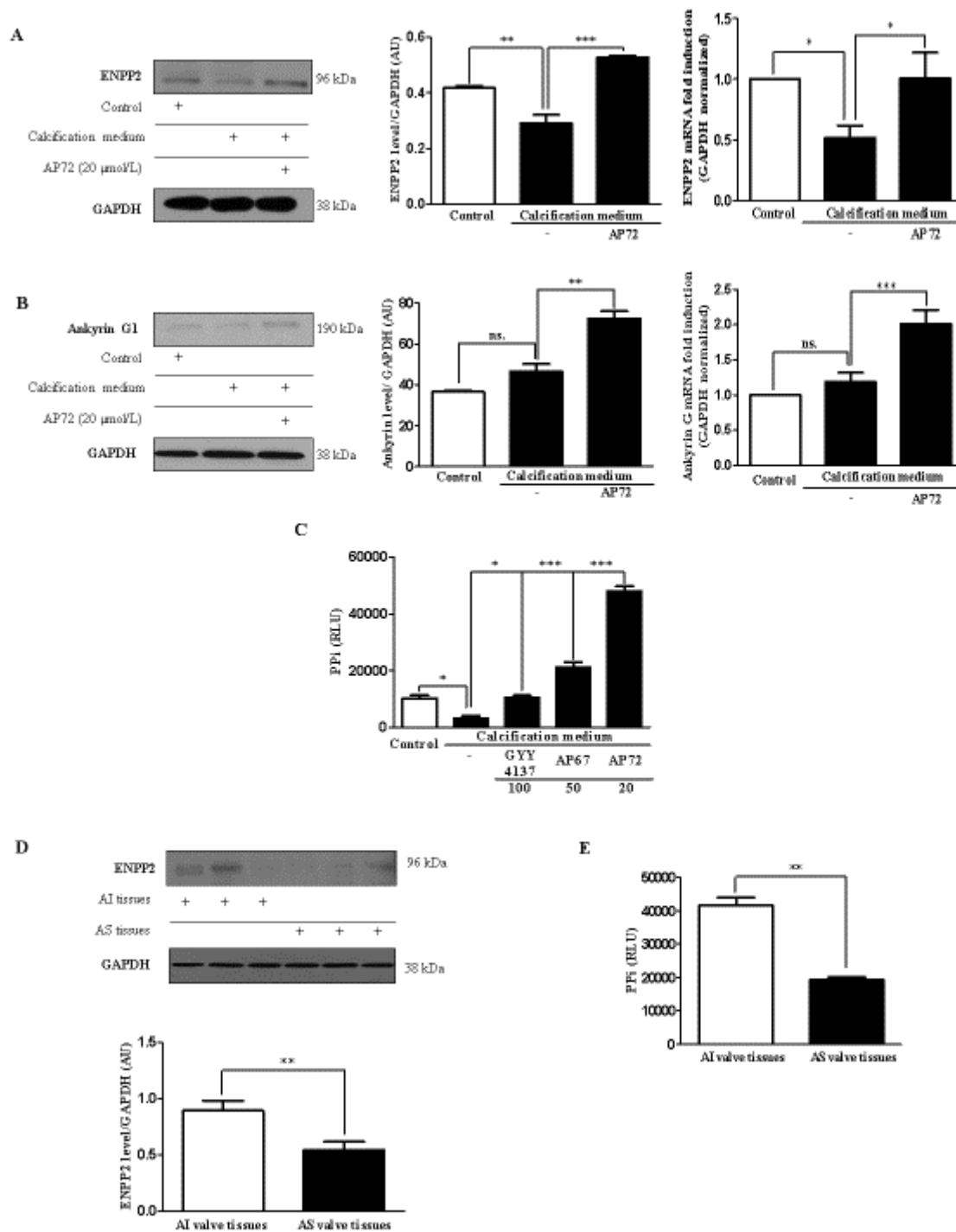


Figure 14. AP72 enhances generation of PPi. VIC were cultured in growth medium or calcification medium alone or supplemented with AP72 (20 $\mu\text{mol/L}$) for 5 days. Differences in A) ENPP2 protein and mRNA levels, B) ANK1 protein and mRNA levels, C) Pyrophosphate level measured using a PPiLight pyrophosphate detection kit are presented. D) Representative ENPP2 Western blot from AI and AS tissue lysate of heart valves. E) Pyrophosphate levels of heart valve tissues were measured using a pyrophosphate detection kit. Graph shows mean \pm SEM of five independent experiments. Not significant (ns); * $P < 0.05$; ** $P < 0.01$; *** $P < 0.001$.

4.14. CSE and CBS level changes in VIC calcification

To investigate potential anti-calcification effects of endogenously produced H₂S we silenced CSE production in VIC using small interfering RNA (siRNA). We found that CSE silencing (Figure 15A; right panel) did not significantly enhance the calcium accumulation under calcifying conditions (Figure 15A; left panel). Intriguingly, we observed that CSE silencing increased the expression of CBS, which is another pyridoxal 5'-phosphate (PLP or vitamin B6) dependent transsulfuration enzyme involved in endogenous sulfide production (Figure 15B). Thus, we performed double silencing against CSE and CBS to test whether calcium deposition in extracellular matrix was affected. We observed an increase in mineralization after CSE and CBS were concomitantly silenced in VIC (Figure 15C) suggesting that transsulfuration pathways are likely to control calcification. Next, we performed experiments with pharmacological inhibitors of CSE (PPG) together with CBS (AOAA) in calcifying condition in VIC. We found that pharmacological inhibition of CSE with CBS increased the amount of extracellular calcium deposition (Figure 15D). Moreover, we tested all three synthetic inhibitors for CSE (PPG), CBS (AOAA) and 3-MST (KGA) alone, or in combination. Calcium depositions of CSE/CBS double silenced VIC are shown inhibition of CSE and CBS altered calcification in VIC (Supplementary Figure XV. A). Furthermore, AOAA+PPG; AOAA+LKGS and PPG+LKGS pharmacological inhibitors significantly reduced the H₂S production in VIC (Supplementary Figure XV. B). To our surprise, nuclear translocation of RUNX2 was not influenced by double silencing of CSE and CBS in calcification medium (Supplementary Figure XVII). Moreover, we monitored the progression of calcification in extracellular matrix on the first and third days. On the first day we did not find significant alteration in the calcium content of VIC maintained in calcifying condition compared to control. In contrast, we detected a significantly increased extracellular calcium content in VIC silenced with CSE/CBS siRNA (Figure 15E). Mineralization was more robust in the double silenced VIC by day three (Figure 15E). As shown in Supplementary Figure XVI.B, production of H₂S was lowered in calcifying condition compared to cells cultured in growth media, and that was further decreased by double silencing for CSE and CBS. Finally, we examined the expression of 3-MST in VIC treated with CSE/CBS siRNA. We found that siRNA specific to CSE and CBS decreased 3-MST protein level in VIC (Supplementary Figure XVI. C).

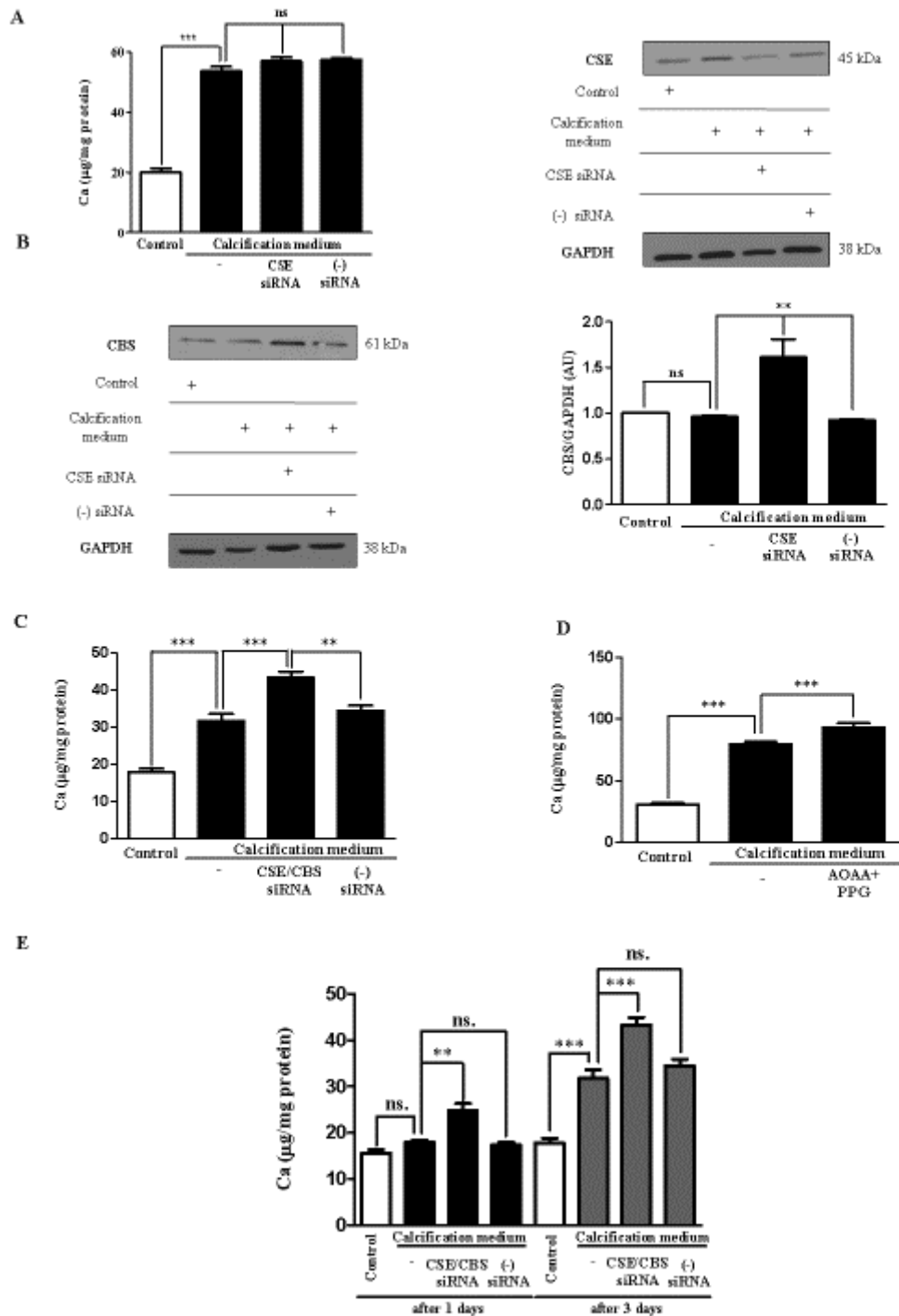


Figure 15. Concomitant silencing of pharmacological inhibition of CSE and CBS increases calcification of VIC. VIC were cultured in growth medium or calcification medium. Cystathionine- γ -lyase (CSE) and CSE/CBS (cystathionine- β -synthase) double gene silencing using siRNA was performed. A) Calcium content, B) CSE and CBS levels of VIC after silencing of CSE are shown. Figure 5C shows the calcium content of CSE/CBS double silenced samples. Figure 5D shows the calcium contents of pharmacological inhibition of CSE and CBS. E) Calcium depositions of CSE/CBS double silenced VIC were shown. Graph shows mean \pm SEM of five independent experiments. Not significant (ns); ** $P < 0.01$; *** $P < 0.001$.

4.15. Interaction of hydrogen sulfide and phosphate uptake of calcified VIC

Cellular phosphate uptake is a key event in the process of mineralization, therefore next we measured intracellular phosphate levels in VIC and observed a significant elevation in cells cultured in calcification medium compared to cells kept in control medium (Figure 16A). Exposure of VIC to AP72 diminished this increase in phosphate content to the level observed in control cells (Figure 16A). In order to explain the inhibition of phosphate uptake, we measured the expression of phosphate channels (Pit1; Pit2) in VIC maintained in calcification medium in the presence or absence of AP72. We found that AP72 did not affect the expression of Pit1 and Pit2 channels (Figure 16B-C). Thus, we hypothesize that sulfide induced posttranslational modification of these channels might affect phosphate uptake. Measurements to support or disprove this hypothesis are underway.

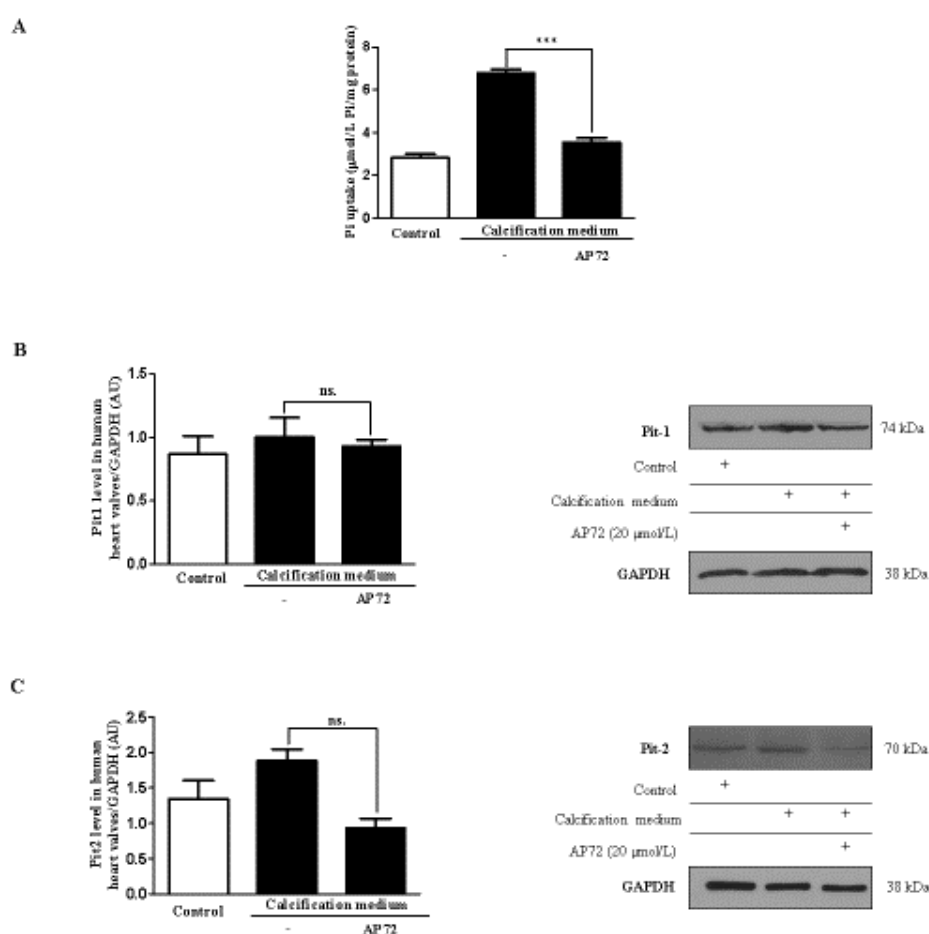


Figure 16. Hydrogen sulfide donor leads to inhibition of phosphate transport. Cells were cultured in a normal or calcific environment exposed to AP72 (20 µmol/L) for 5 days. A) Phosphate content was determined using QuantiChrom quantitative colorimetric assay. B) Pit1 and C) Pit2 Western blotting was performed and normalized to GAPDH. Results are shown as mean values ± SEM of at least five independent experiments. Not significant (ns); ***P < 0.001.

4.16. H₂S generation and CSE expression in human aortic valves

In the human body, CSE was claimed to be one of the main endogenous hydrogen sulfide producing proteins. By Western blot analyzes we investigated the expression of CSE in tissue lysates of human AS and AI valves. We found higher expression of CSE in AS valves with massive calcification as compared to AI valves known to lack calcification (Figure 17A). In contrast, sulfide levels that can be precipitated by Zn²⁺ under alkaline conditions from tissue lysates of valves were markedly, and significantly lower in calcified AS specimens compared to not calcified AI specimens (Figure 17B). Next, we performed dual immunohistochemistry analyses (CSE-SMA and CSE-ALP) on human AI and AS valves to localize CSE. In Figure 17 shows less SMA⁺ and more CSE⁺ cells were present in calcified AS tissue than in AI tissue (upper panels). ALP-CSE double staining revealed the appearance of ALP⁺ cells expressing high levels of CSE protein in AS valve samples, while ALP⁺ cells were not detected in AI valve (Figure 17C; lower panels).

The potential of osteoblastic differentiation was dependent upon the origin of VIC. Under the same calcifying condition VIC derived from AS exhibited earlier mineralization than AI. The higher CSE level found in AI was accompanied by delayed calcification (Figure 17C). Human CSE recombinant protein was used as a control for the CSE Western blot (Supplementary Figure XVII. B).

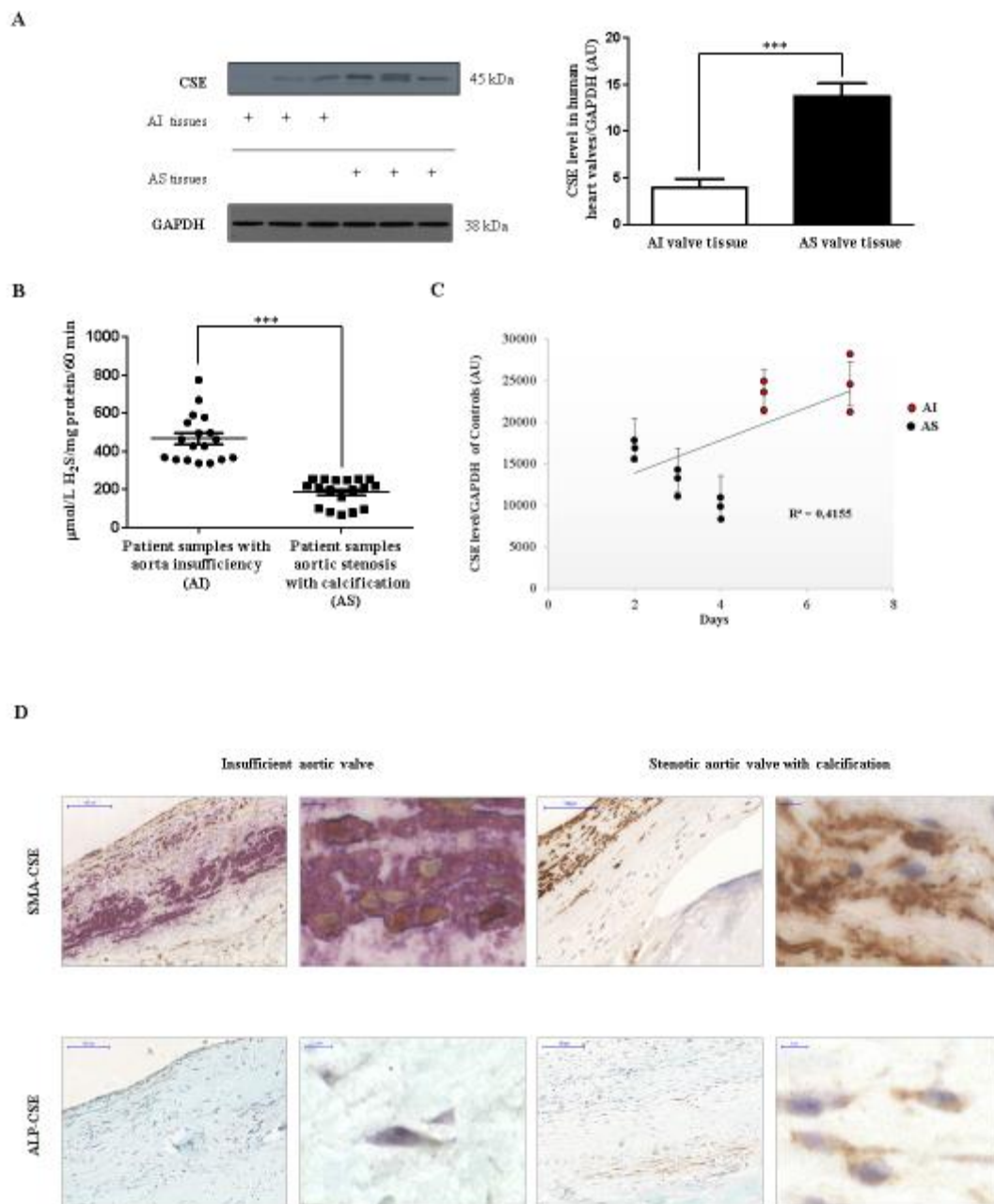


Figure 17. Expression of CSE in human aortic valves. A) Western blot of CSE protein from AS valve (N=12) lysates and AI valve (N=9) lysates (left panel) were performed. Representative CSE protein levels of three AS and three AI valves lysates were shown. Relative CSE levels were assessed by densitometry analyses of band intensities of CSE Western blots normalized to GAPDH (panel right). B) Zn²⁺ precipitated sulfide content under alkaline conditions was measured in AI (N=18) and AS (N=18) valve tissues normalized to protein content of the individual samples. C) VIC derived from different AI (N=6) and AS (N=9) patients were cultured in calcification medium. CSE expression was measured after the initiation of calcification. VIC from AI tissues were shown in red, VIC from AS tissues were shown in black. Results were normalized to GAPDH of the samples. D) Double immunohistochemistry of CSE-SMA and CSE-ALP was shown with two different magnification (x400 magnification and x1000 magnification). Results are shown as mean values \pm SEM of the experiments. ***P < 0.001.

4.17. Role of H₂S in valvular calcification of apolipoprotein E deficient mice

Von Kossa staining demonstrates (Figure 18; middle panels) that calcific nodules appeared in aortic heart valves of ApoE^{-/-} mouse, which were kept on a high-fat diet (second column; middle panel) as opposed to ApoE^{-/-} mouse on standard chow diet, where no valvular calcification was observed (first column; middle panel). ApoE^{-/-} mouse on a high-fat diet exhibited an expansion of extracellular matrix in aortic valve compared to those received standard diet (upper panels). To demonstrate the benefit of H₂S in vivo, we administered AP72 intraperitoneally (266 μmol/kg body weight) and assessed valvular calcification in ApoE^{-/-} mice on a high-fat diet. AP72 significantly inhibited the development of calcific nodules in aortic valves (third column; middle panels) and decreased the expansion of extracellular matrix (third column; upper panels). Similarly, to human aortic stenosis the amount of CSE⁺ cells in calcified aortic valves of mice fed with the high-fat diet was increased as compared to in aortic valves of mice on a regular diet (lower panels). Consequently, the administration of exogenous H₂S lowered the total measured expression of CSE in aortic valves of mice fed with a high-fat diet (third column; lower panels). Alpha-SMA staining demonstrated that AP72 maintained the phenotype of valvular interstitial cells in the aortic valve (Figure 18).

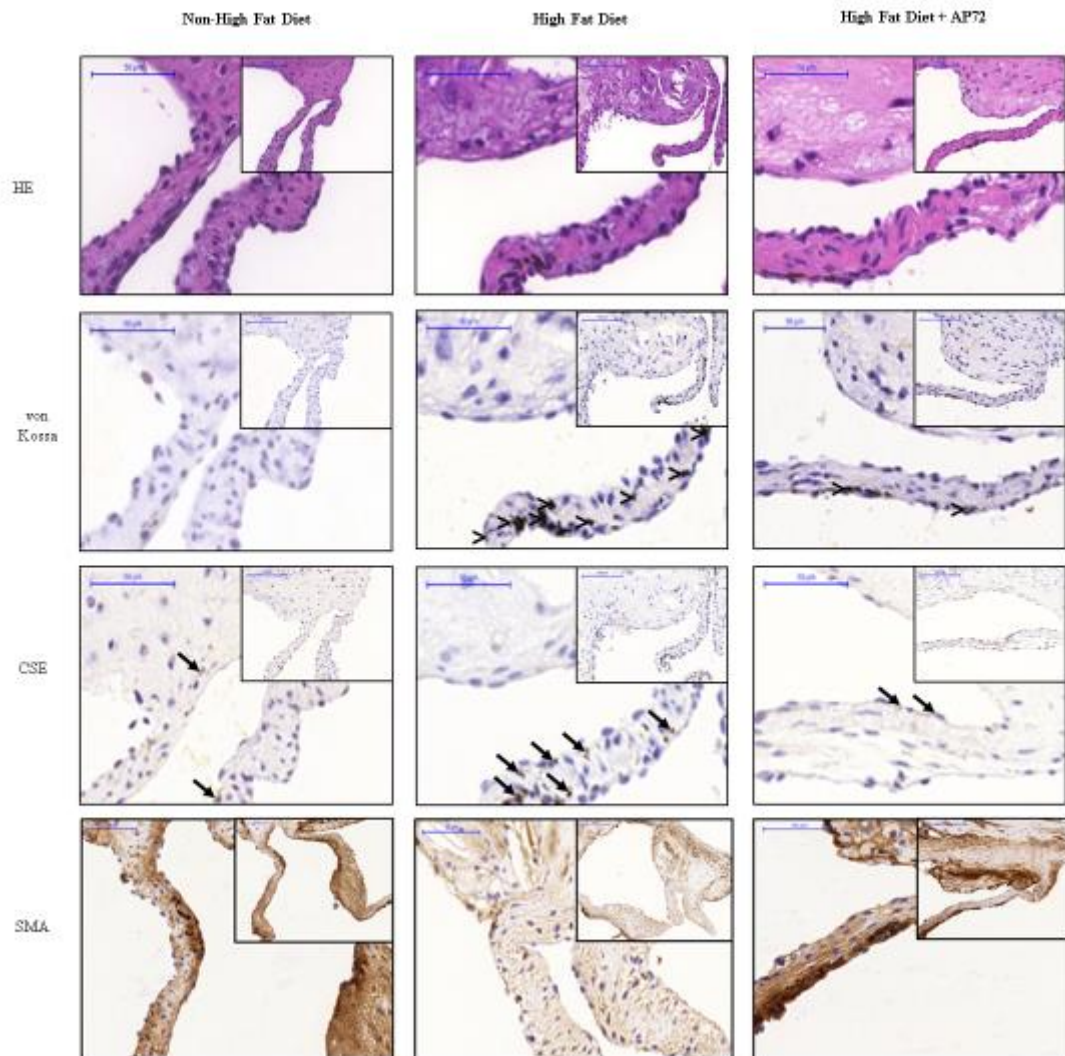


Figure 18. Hydrogen sulfide inhibits valvular calcification in ApoE^{-/-} knockout mice. Hematoxylin and eosin (upper panels); von Kossa (middle panels), CSE (second middle panels) and alpha smooth muscle actin (alpha-SMA; lower panels) staining was performed on aortic valves of mice kept on normal diet (1st column; N=5), on high-fat diet (2nd column, N=9); and on high-fat diet treated with AP72 (3rd column; N=5). Comparison (>) designates calcified region and arrow indicate CSE positive cells.

5. Discussion

Our findings are the first as regards to the relationship between the disrupted iron metabolism, a frequent complication of CKD, and valvular calcification. In our work we report how cellular iron metabolism may regulate the mineralization and osteoblastic transformation of human VIC when cultured in calcification medium. Consequently, with previous reports in vascular smooth muscle cells (Zarjou, Jeney et al. (2009); Becs, Zarjou et al. (2016)) and bioprosthetic tissues (Carpentier, Carpentier et al. (1995)) we confirm reduction of the calcification process of VIC through the combined mechanism of H-ferritin induction via iron, D3T or apo-ferritin (Primiano, Kensler et al. (1996)). These new results and observations also confirm previously reported findings that the elevated inorganic phosphate and calcium levels induced the mineralization of VIC (Mathieu, Voisine et al. (2005); Block (2000); London, Pannier et al. (2000)). We used extracellular calcium level, Alizarin Red S staining, osteocalcin content, ALP staining, and pyrophosphate level as surrogates of VIC transformation into osteoblast-like cells and validate the predominant inhibitory role of H-ferritin induction in this process. Particularly, our data suggest that upregulation of intracellular H-ferritin (irrespective of the inducer) prevents nuclear translocation of RUNX2 that is considered the main transcription factor and regulator of osteogenesis (Komori, Yagi et al. (1997); Speer, Li et al. (2010); Steitz, Speer et al. (2001)).

Calcific aortic valve disease (CAVD), mostly in CKD and the elderly, is the most common valvular heart disease (Freeman and Otto (2005)). The prevalence of CAVD is expected to rise with the increase of life expectancy (Freeman and Otto (2005); Mohler, Gannon et al. (2001); O'Brien, Kuusisto et al. (1995)). Actually, compared to the general population, patients with CKD with adjusted cardiovascular disease risk factors have about 10-20 fold higher mortality (Mathieu, Voisine et al. (2005); Block (2000)). One of the major contributors to such elevated risk of cardiovascular-related mortality in this group of patients is vascular and valvular calcification (Moradi, Sica et al. (2013)). Valvular abnormalities predispose patients to increased risk of thromboembolism, arrhythmias, and infective endocarditis (London, Pannier et al. (2000); Maher, Young et al. (1987); Wang, Wang et al. (2003); Di Iorio, Bortone et al. (2006)). High phosphate level in plasma is an important risk factor of CAVD and it has been demonstrated in multiple studies to act as a key regulator of vascular calcification (Adeney, Siscovick et al. (2009); Giachelli (2009); Hruska, Mathew et al. (2008)). Elevated phosphate level stimulates mineralization of vascular cells in a sodium-dependent phosphate co-transporters mediated process, which promote the entry of phosphate into the cells (Zarjou, Jeney et al. (2009)). The increased phosphate uptake induces osteoblastic transition of vascular smooth muscle cells via a process that is attended by translocation of RUNX2 from the cytosol into the nucleus required for osteoblast differentiation, bone matrix gene expression, and, consequently, bone mineralization (Komori (2006); Zarjou, Jeney et al. (2009)). ALP, another important enzyme in early osteogenesis and osteocalcin, a major non-collagenous protein found in bone matrix that is indicated to the regulation of mineralization (Zarjou, Jeney et al. (2009)). Nowadays, the emerging idea that therapies targeting the molecular processes of

aortic valve calcification (Yutzey, Demer et al. (2014)) could increase the durability of surgically implanted and transcatheter bioprosthetic valves (Leopold (2012)).

5.1. Part 1

Ferritin is an abundant and highly conserved three-dimensional protein and plays a major role in intracellular iron handling (Finazzi and Arosio (2014);Coffman, Parsonage et al. (2009)). The family of ferritins is similar to spherical shells with the capability to sequester and store a large amount of iron in a soluble and bioavailable form. Ferritin has 24 subunits (two types: H, heavy and L, light chain) whose proportions depend on the iron status of the cells, tissue or organ. Only the H-ferritin has ferroxidase activity that can oxidize Fe^{2+} to Fe^{3+} facilitating the safe incorporation of iron into the shell. Iron is stored in an internal cavity in a ferric oxyhydrophosphate complex (de Silva, Guo et al. (1993)). High amounts of iron and phosphate are stored within the core of ferritin (Juan and Aust (1998)). The main functions of ferritin are to depot, sequester and allow availability of iron when needed (Finazzi and Arosio (2014);Alkhateeb and Connor (2010)). In the past decade, our understanding of the role of ferritin and its function has markedly enhanced, and there is significantly more insight into the role of ferritin in the regulation of iron metabolism and homeostasis (Pietsch, Chan et al. (2003); Coffman, Parsonage et al. (2009); Alani, Tamimi et al. (2014); Zarjou, Bolisetty et al. (2013)). Expression of H-ferritin is controlled at a translational level by iron via the iron regulatory element/iron regulatory protein machinery. This pathway involves the iron-dependent change in activity of the iron regulatory proteins 1 and 2. In condition of low iron level these proteins bind to the iron-responsive element of mRNA at the 5'UTR of the ferritin transcripts inhibiting their translation, whereas in high iron they lose affinity and translation is derepressed (Kuhn (2015)). Particularly, the transcriptional control of the H-ferritin is also linked to oxidative stress and it is affected through the binding of Nrf2/Small Maf protein to conserved antioxidant-responsive element (Theil, Behera et al. (2013)). H-ferritin induction is mediated by Nrf2 in response to D3T (Pietsch, Chan et al. (2003)).

Previously, we concluded that iron and H-ferritin prevented calcification and osteoblastic transformation of vascular smooth muscle cells induced by the high level of inorganic phosphate (Zarjou, Jeney et al. (2009); Zarjou, Jeney et al. (2010); Arosio, Ingrassia et al. (2009)). Here we report that H-ferritin and is also a key mediator in inhibition of VIC calcification. Importantly, our findings suggest that this inhibitory mechanism is an active process whereby primary osteoblast-specific genes are attenuated in response to H-ferritin induction. Given the clinical significance of these findings and the potential of targeting ferritin induction as a novel therapeutic approach, we were encouraged to examine the role of D3T in this context. D3T has a chemopreventive effect in cancer medicine (Zhang and Munday (2008)). Using various strategies including H-ferritin gene silencing, we discussed that D3T mimics the inhibitory properties of iron, apo-ferritin further highlighting the central role of H-ferritin in this process. Moreover, these inhibitory effects are also replicated by ceruloplasmin, another protein with ferroxidase activity. Our findings forecasted the close relationship between intracellular iron metabolism and osteoblastic activity. Interestingly, Western blot and histological

panel of H-ferritin (Figure 7A) revealed significant differences in the expression of intracellular ferritin levels in the AS valve section compared to the AI valve tissue section. Double immunostaining of heart valve sections (Figure 7B) further corroborated these observations. Furthermore, we found that calcified areas of the valves were deficient in ferritin expression (Figure 7B) and such expression was limited to areas that were devoid of mineralization. In contrast, as supposed these calcified regions exhibited robust ALP staining (Figure 7B) highlighting their acquired osteoblastic status. These results may propose an adaptive response where induction of H-ferritin works as a major stratagem to prevent the osteoblastic transition of VIC.

For instance, Raaz et al. investigated the role of RUNX2 as a potential mediator and therapeutic target of aortic fibrosis and aortic stiffening in diabetes mellitus. They found that RUNX2, as a previously unrecognized inducer of vascular fibrosis in the setting of diabetes mellitus, promotes arterial stiffness irrespective of calcification (Raaz, Schellinger et al. (2015)). Furthermore, it has been shown that RUNX2 overexpression induces aortic media fibrosis, increased aortic stiffness, and elevated pulse pressure. These results identify upregulation of RUNX2 as a maladaptive response during injury to the vasculature, uremic milieu, and hyperglycemic conditions (Di Iorio, Bortone et al. (2006)). Moreover, we demonstrated that RUNX2 was manifested in the nucleus of AS valve tissue cells with calcification cultured in normal condition compared to AI valve cells, where RUNX2 localized in the cytoplasmic region of the cells (Figure 2C and 2D). Increasing body of evidence highlights the key role of osteogenic transcription factor RUNX2 in cardiovascular calcification in CKD patients (Hosen, Coucke et al. (2014)). These findings demonstrate that nuclear localization of RUNX2 shows the early transformation into osteoblast-like cells of VIC. RUNX2 and Sox9 were revealed to interact physically in intact cells where Sox9 inhibits the transactivation of RUNX2. In addition, RUNX2 effects reciprocal inhibition on Sox9 activity. Sox9 was shown to induce a dose-dependent degradation of RUNX2 (Lincoln, Kist et al. (2007); Peacock, Levay et al. (2010); Huk, Austin et al. (2016); Cheng and Genever (2010)).

In our studies, we also found a reciprocal and counter-regulatory interaction between RUNX2 and Sox9. In calcifying condition nuclear Sox9 level in VIC was decreased, conversely, RUNX2 level was increased. Respectively, cells of stenotic aortic valve with calcification exhibited higher level of nuclear RUNX2 and lower level of Sox9 as compared to isolated aortic valve with insufficiency. Particularly, treatment of VIC with iron, apo-ferritin and D3T enhanced the presence of Sox9 in nucleus and maintained nuclear RUNX2 at low level. These findings demonstrate that one of the targets for ferritin (iron and D3T) to inhibit mineralization of VIC is mediated by modulation of Sox9 and subsequently RUNX2. Alternatively, inhibition of phosphate uptake (Figure 4A) via decreasing the expression of Pit1 and Pit2 channels (Figure 4C and D) by ferritin may also administered to the attenuation of RUNX2 nuclear translocation, thereby preventing osteoblastic phenotype transition, the appearance of osteoblastic phenotype, as reflected by ALP, osteocalcin expression and the development of the hydroxyapatite crystals. The predominant role of ferroxidase activity of ferritin is confirmed by enhanced RUNX2

nuclear translocation resulting in osteoblastic transformation of VIC after silencing the H-ferritin gene (Supplementary Figure V). Respectively, exogenous H-ferritin decreased the expression of Pit1 channel and subsequently lowered phosphate uptake in VIC (Figure 4E and Supplementary Figure VI. C). Even if lysosomal localization of ferritin/ferroxidase induced by iron or D3T is demonstrated, some caveat is acknowledged. The mechanism by which H-ferritin/ferroxidase activity alters the expression of Pit1 and Pit2 channels and the activity of RUNX2 and its subcellular localization, have not been explored in our studies.

In 1955 Christian de Duve was the first who described that lysosomes are membrane-bound organelles. They have a single-bilayer lipid membrane that limits their acidic lumen. Lysosomes contain several types of hydrolases that are allocated to the degradation of specific substrates. The lysosomal membrane-proteins are involved the transport of substances into and out of the lumen, acidification of the lysosomal lumen, and fusion of the lysosome with other cellular structures (Saftig and Klumperman (2009)). Mancias et al. revealed that nuclear receptor coactivator 4 is required for delivery of ferritin to lysosomes (Mancias, Wang et al. (2014)) and alternative lysosomal transport has also been described (Goodwin, Dowdle et al. (2017)). Accordingly, we tested whether the excess intracellular phosphate could be depleted by ferritin and transported into the lysosome. Ferritin has a hollow internal cavity for storing iron and phosphate (2250 and 380 atoms, respectively). We found that H-ferritin and the main protein of the lysosome LAMP1 could interact, and such interaction may play a crucial role in the general homeostasis of the cells including phosphate level (Figure 4).

The pyrophosphate level of plasma is an endogenous inhibitor of vascular calcification, which is reduced in end-stage renal disease and correlates inversely with arterial calcification (Lomashvili, Narisawa et al. 2014)). ENPP2 is the major extracellular pyrophosphate generating protein. Genetic deficiency of ENPP2 causes generalized arterial calcification of infancy (GACI), which is a lethal cardiovascular calcification disease (Nitschke, Baujat et al. (2012)). In our study, we concluded that decreased ENPP2 expression accompanied by lower PPi generation under calcification condition. Exposure of cells to iron, Apo-ferritin D3T and H-ferritin upregulated ENPP2 and eventually enhanced the production of PPi (Figure 6). A drop in PPi level occurred after silencing the expression of H-ferritin in VIC exposure by iron. These data propose that ferritin may also act via ENPP2 and PPi to control mineralization of VIC.

Lipoprotein(a) [Lp(a)] was associated with calcific aortic valve disease (CAVD) as the Mendelian randomization studies (Thanassoulis, Campbell et al. (2013);Arsenault, Boekholdt et al. (2014), Kamstrup, Tybjaerg-Hansen et al. (2014)) have highlighted. Oxidized phospholipids with a high content in lysophosphatidylcholine were transported by Lp(a). ENPP2 is present in the Lp(a) fraction in circulation and also expressed by VIC in CAVD. ENPP2 interacts on lysophosphatidylcholine and catalyzes the extracellular production of lysophosphatidic acid, a pro-osteogenic agonist likely via the LPA1 receptor (Mathieu, Arsenault et al. (2017)). In our studies H-ferritin elevate the biogenesis of PPi via increasing the expression of ENPP2 and decreasing ALP level, the major enzyme degrading PPi. The control of ENPP2 activity to generate PPi versus lysophosphatidic acid

may perform a key regulatory mechanism mediating the anti-calcification actions by H-ferritin (Figure 10C).

Furthermore, we found that H-ferritin is highly expressed in VIC of AS valve, and the level increases toward the calcific core. The relative dominance of H-ferritin over ALP in the intact area of valves might represent an adaptive response to the calcifying milieu in CAVD. What prompts and triggers expression of H-ferritin in this context remains to be fully elucidated. The pathogenesis of CAVD is complex, and its manifestations developed after long-term exposure to risk factors, leading to altered activation of signaling pathways important in the development of valves and bone (Dutta and Lincoln (2018)). NHLBI working group concluded that CAVD is an active and well-regulated inflammatory disease, however specific pathobiological mechanisms are not fully understood (Rajamannan, Evans et al. (2011)). In previous studies were shown that inflammatory cytokines induce H-ferritin expression (Torti, Kwak et al. (1988);Tsuji, Miller et al. (1991)). In our work, we also found that elevation H-ferritin expression was accompanied by inflammatory markers as TNF- α and IL1- β in AS tissues without the accumulation of iron (Figure 9A-B). Furthermore, H-ferritin decreased the expression of TNF- α and IL1- β in VIC derived from human AS valve (Figure 10A). These data may suggest a potential role of H-ferritin in controlling the inflammatory process in CAVD (Figure 10B).

Finally, we report for the first time a novel role of ferritin/ ferroxidase system in the context of human VIC mineralization and transdifferentiation into osteoblast-like cells. The chemical exposure of D3T and its inhibitory role via H-ferritin induction may be a potential preventive measure in cardiovascular calcification. Moreover, these findings will provide a novel platform for more in-depth research into the process of physiological and pathological bone formation and identify previously unknown targets to alleviate the detrimental consequences of cardiovascular calcification in CKD.

5.2. Part 2

In our previous work, the elevation of CSE expression was demonstrated in human atheroma, derived from the carotid artery with lipid accumulation without calcification (Potor, Nagy et al. (2018)). Presently, we observed that CSE expression was higher in human AS valves known to be associated with calcification as compared to AI valves lacking calcification (Figure 15A). In AS valves, ALP+ cells were shown to exhibit CSE positivity (Figure 17A). Importantly, suggesting that loss of CSE activity and/or H₂S bioavailability might exacerbate the progression of mineralization of VIC, we observed decreased H₂S generation in AS heart valve tissue (Figure 17B) compared to AI valves. Thus, to investigate whether endogenous H₂S production had an anti-calcification effect, we silenced CSE gene in VIC isolated from human aortic valves without calcification then cultured the cells in high phosphate containing medium. Based on the previously observed protecting roles of sulfide administration we supposed that CSE silencing would enhance VIC calcification. Surprisingly, there was no increase in the calcium deposition after silencing CSE expression (Figure 15A). Nandi and Mishra previously reported the

interaction of the expression CSE/CBS, and demonstrated that CBS deficiency upregulates CSE protein levels (Nandi and Mishra (2017)). Hence, we investigated the expression of CBS in CSE silenced VIC and, importantly, CSE silencing resulted in increased CBS protein expression in VIC (Figure 15B). Next, we employed double silencing against CSE/CBS and surprisingly obtained a further increase in calcium accumulation in the extracellular matrix of VIC cultured in high phosphate containing medium (Figure 15C). Furthermore, we followed the progression of calcification we found that CSE/CBS silenced VIC showed earlier calcification compared to cells maintained in calcification medium without siRNA (Figure 15E). Exposure of VIC by the synthetic CSE inhibitor (PPG) together with CBS inhibitor (AOAA) also promote the formation of the extracellular calcium deposition (Figure 15D). The finding that lower expression of CSE found in AS compared to AI also support the protective role of CSE in calcification is associated with higher calcification rate of VIC (Figure 17C). These results are consequent with the notion that there is impaired H₂S bioavailability and/or defective endogenous H₂S production in CAVD and strategies which overcome this loss of H₂S, such as H₂S delivery molecules, represent a novel strategy for preventing, delaying and/or reversing mineralization of VIC in CAVD susceptible individuals. Even though, it has to be noted that CSE and CBS are transsulfuration enzymes working hand in hand in cysteine production from homocysteine via their canonical activities. Cys metabolic pathways (also including the oxidative catabolism as well as the reverse transsulfuration pathways, which can produce H₂S) are highly orchestrated and fine-tuned to –among other reasons- keep steady-state Cys levels in a narrow concentration range. In cysteine catabolism hydrogen sulfide and homeostatic impact of sulfite have a crucial role. Thus, the CSE/CBS double knockdown cell line is exhibit impaired cysteine formation and expected to produce less endogenous H₂S. To the better understanding and the relative contributions of these processes need further investigations.

To obtain insight into the contribution of endogenous sulfide production how to prevent mineralization of VIC, we employed several H₂S generating molecules. We used ‘instant’ H₂S generate donors: NaSH and Na₂S in aqueous solution as well as slow sulfide release donor molecules (GYY4137, AP67 and AP72). (It is important to note that total donor concentrations do not represent the total amount of released sulfide and all slow donors have different sulfide releasing potential.) Moreover, slow-releasing H₂S donors were increasingly recognized and potentially better mimic the effects of the endogenous H₂S buffer system, because of their slow generation of low sulfide levels (Nagy (2013); Whiteman, Perry et al. (2015)). Particularly, we also demonstrated that AP72 the slow H₂S releasing molecules (Nagy (2013)) exhibited a greater inhibition on the calcification compared to GYY4137, possibly cause the rate of H₂S release from AP72 is faster than that of GYY4137, a poorly efficient H₂S donor (Whiteman, Perry et al. (2015)). It is important to note that phenols are susceptible to absorbing high amount of H₂S from liquids (Huang, Zhang et al. (2017)). Accordingly, in our experiments in VIC mineralization inhibited by AP72 at one order magnitude lower concentration in phenol red-free media. Sun et al. previously demonstrated the importance of RUNX2 in bone and in arterial calcification. They concluded that role of RUNX2 was important in regulating

the expression of many factors, such as RANKL, which is the key protein in the interplay between vein smooth muscle cells and macrophages and contributes to the pathogenesis of vascular calcification and atherosclerosis (Lin, Chen et al. (2015); Sun, Byon et al. (2012)). Furthermore, in calcification process phosphate uptake of the cells was elevated followed by nuclear translocation of the RUNX2 from the cytoplasm to the nucleus. Inhibiting phosphate uptake (Figure 16A) – possibly via posttranslational modification of Pit channels by H₂S- H₂S attenuated RUNX2 translocation and thereby prevents the development of the osteoblastic phenotype (Figure 13), as reflected by ALP, OC protein expression and the appearance of the hydroxyapatite crystals (Figure 12).

Plasma PPI acts as an endogenous inhibitor of vascular calcification, and inversely correlate with arterial calcification and reduced levels of PPI were observed in end-stage renal disease (Lomashvili, Narisawa et al. (2014)). Since, we were curious whether H₂S could affect the regulation of PPI generation; a recent observation that could provide a new pathway to inhibit VIC calcification in CAVD. Indeed, lower level of ENPP2 protein and PPI were observed in human calcified valves of AS, compared to AI valve tissue (Figure 14A; C and D) and we showed that by the exposure of AP72 the expression of ENPP2 is markedly upregulated (Figure 14A) resulting in an increased production of PPI in VIC (Figure 14C). Furthermore, ANK1 channel protein expression, which contributed to the extracellular localization of PPI from the cytoplasm, was increased by the AP72 treatment (Figure 14B). All together, the regulation of PPI generation by H₂S represents a novel additional mechanism to control calcification.

ApoE^{-/-} mouse is the most widely studied animal model for atherosclerosis (Massy, Ivanovski et al. (2005); Rattazzi, Bennett et al. (2005)). We demonstrated that after a high-fat diet, a most pronounced calcification occurred and seen in the aortic arch and in the aorta and aortic valves. Our recent study, and our development of ApoE^{-/-} mice aortic valves mineralization by high-fat diet was strongly associated with the increase of extracellular matrix and the formation of hydroxyapatite nodules and expansion of extracellular matrix in the heart valves was prevented by AP72. Furthermore, we also observed that the expression of CSE in VIC was increased in mice on high-fat diet similarly to human aortic stenosis. Potor et al. previously demonstrated, that several triggers could be identified for inducing CSE expression in resident cells of atherosclerotic lesions including plaque lipids, oxidized low-density lipoprotein, tumor necrosis factor- α , and interleukin-1 β (Potor, Nagy et al. (2018)). Therefore, the induction of CSE might represent an adaptive cellular response to lipid deposition and inflammation, serving as a clinical hallmark of CAVD. In vascular calcification, when vascular smooth muscle cells were shown to transform into osteoblast-like cells, they lose their smooth muscle actin (Johnson, Leopold et al. (2006)). Immunostaining of the aortic valves of ApoE^{-/-} mice demonstrated that AP72 treatment preserved alpha smooth muscle actin (Figure 17, lower panels). In agreement with our hypothesis that CAVD is a condition of disturbed H₂S bioavailability, we found a deficiency in the generation of H₂S in human AS valves in spite of the elevated expression of CSE. Bibli et al. concluded that the phosphorylation of Ser377 of CSE results in a markedly decrease in H₂S production which may indicate the

inactivation of the enzyme (Bibli, Hu et al. (2019)). Such a therapeutic supplementation of H₂S by H₂S donor molecules (like AP72 or other novel compounds that are currently under pre-clinical or clinical investigation by us and others) may offer a novel approach to prevent valvular calcification in CAVD and related conditions.

We described three separate and new anti-calcification effects by H₂S i, inhibiting phosphate uptake, ii, preventing nuclear translocation of RUNX2 iii, increasing pyrophosphate level. Even though all these pathways are important and related to each other (Table 2.), some contradictions are acknowledged. AP72 has a slight but significant evidence of anti-calcification action at 200 μmol/L, however did not affect nuclear translocation of RUNX2 indicating the importance of pyrophosphate for preventing the formation of mineralized nodules in extracellular matrix.

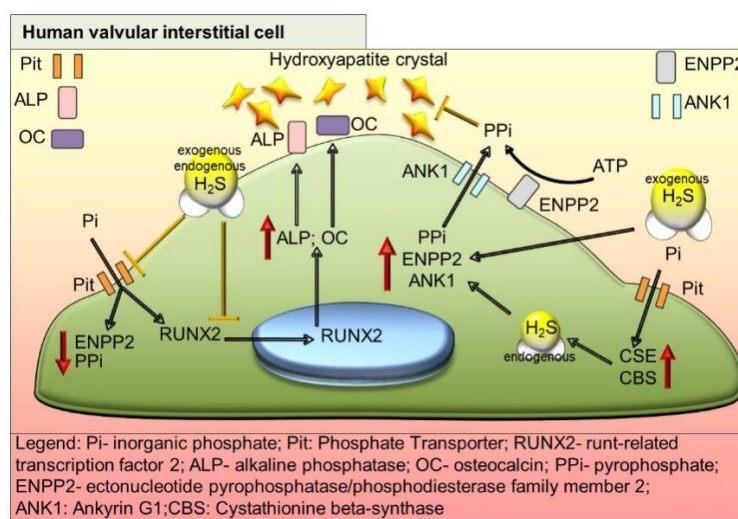


Table 2. Role of H₂S in mineralization of heart valves. During valvular mineralization, exogenous H₂S is able to inhibit phosphate uptake of valvular interstitial cells, thus protecting VIC from RUNX2 nuclear translocation, the initiation step of osteoblastic differentiation. Pyrophosphate (PPi) level (key endogenous regulator of calcification) is also elevated by enhanced ENPP2 and ANK1 expression by exogenous addition of H₂S donor molecule AP72.

In conclusion, our studies the first which provide evidence how endogenous H₂S limits calcification of valvular interstitial cells. Pharmacologically, by novel H₂S releasing molecules generated H₂S may have a potential to control in heart valves calcification and osteoblastic differentiation.

6. Summary

The studies that are presented in this thesis focused on two different but very important molecules in the development of CAVD. In Part 1 we focused on our previous findings to understand the molecular mechanism of the inhibitory role ferritin/ferroxidase of the high phosphate induced development of CAVD. Our results suggested that ferritin/ferroxidase is not just a potent inhibitor of the cardiovascular mineralization; it is inducible exogenously by different drugs such as D3T. In Part 2 we sought to investigate the role of H₂S in valvular mineralization induced by high phosphate. We provide strong evidence that H₂S level changes during the progression of CAVD caused by the possible structural deficiency (sulphydration of Serin residues) (Bibli, Hu et al. (2019)) of H₂S producing enzyme CSE. Moreover, the lack of H₂S could be replaced by H₂S releasing donor molecules and perhaps be possible a therapeutic approach in the future (Sikura, Potor et al. (2019)). These studies were the first to provide two different mechanistic insights in the same clinical condition (CAVD) and offer novel pharmaceutical avenues that may lead to innovative therapeutic modalities.

The relationship between iron homeostasis/H₂S balance and valvular calcification has never been explored and their role in mineralization is poorly understood. Although most patients with CKD or CAVD, may require renal or heart valve (or both) replacement, complications in these cases include cardiovascular calcification, deranged iron homeostasis and deficiency of H₂S. In patient with CKD iron accumulation can be observed in reticuloendothelial cells that are accompanied by higher levels of ferritin in plasma. This increase results from the iron sequestration of reticuloendothelial cells and its availability to the other cells is significantly lower. This mechanism results in depletion of intracellular ferritin and subsequent anemia of chronic, inflammatory disease. In the first part of our observations we suggest that the derangement of iron metabolism possibly facilitated by high phosphate induced valvular calcification may be controlled (induction of ferroxidase) by oral administration of D3T to prevent mineralization of the cardiovascular system. In the second part, we propose that CAVD is a condition of disturbed H₂S bioavailability. The observed deficiency in the generation of H₂S in human calcified stenotic valves is accompanied with elevated expression of CSE. The development of heart disease is manifested by the disorder of H₂S production as indicated by the lower levels of plasma H₂S in patients with coronary heart disease (Jiang, Wu et al. (2005);(Shen, Shen et al. 2015)). The replacement of the absence H₂S is achievable by a reaction between Lawesson's reagent and morpholine resulting in a new generation slow H₂S release compound (GYY4137). Protonation reaction of GYY4137 results more stable H₂S releasing compounds such as AP67 and AP72. Although the link between valvular calcification and H₂S homeostasis is not characterized, our results demonstrate a therapeutic approach against CAVD from a new perspective. In conclusion, improved insight and better understanding of the pathogenesis of CAVD may help develop effective strategies to prevent or decrease iron and/or H₂S deficiency manifested clinical cardiovascular conditions.

Novel findings

1. H-ferritin induces by iron and 3H-1, 2-dithiole-3-thione inhibits mineralization and osteoblastic differentiation of human valvular interstitial cells.
2. H-ferritin enhances nuclear localization of transcription factor Sox9, and as a reciprocal effect it reduces nuclear accumulation of RUNX2.
3. H-ferritin inhibits cellular phosphate uptake and lysosomal phosphate accumulation via decreasing the expression of phosphate channels and localization of lysosomal H-ferritin with high phosphate binding capacity, as well as enhances pyrophosphate generation via up-regulating ENPP2.
4. Histological analysis of stenotic aortic valve revealed high expression of H-ferritin and its relative dominance over ALP in the intact non-calcified regions.
5. H-ferritin decreases the expression of inflammatory markers (TNF- α ; IL1- β) in VIC derived from human AS valve.
6. CSE and CBS derived H₂S and H₂S releasing donors inhibit mineralization of aortic valve.
7. Anti-calcification function occurs via inhibiting phosphate uptake, preventing nuclear translocation of RUNX2, increasing pyrophosphate level.
8. H₂S releasing donors and CSE/CBS derived H₂S has therapeutic potentials in calcific aortic valve disease.

Összefoglalás

A dolgozatban bemutatott tanulmányok két különféle, a CAVD progressziója szempontjából rendkívül fontos molekulákat mutatnak be. Az 1. részben laboratóriumunk korábbi eredményeire összpontosítottuk, melynek célja, hogy megértsük a ferritin / ferroxidáz gátló szerepének molekuláris mechanizmusát a magas foszfáttal indukált CAVD-ben. Eredményeink arra utaltak, hogy a ferritin / ferroxidáz nem csupán a kardiovaszkuláris mineralizáció hatékony gátlója, hanem különféle gyógyszerek, például a D3T által exogén módon indukálható. A 2. részben szintén egy, laborunk korábbi munkájának megállapítása található: az endogen H₂S szint mineralizációs körülmények között csökken. Az endogen H₂S szint és a meszesedés közötti kapcsolat kevésbé ismert, viszont az utóbbi években kutatott terület. Munkánkban célunk volt részletesebben megvizsgálni a H₂S szerepét magas foszfát által kiváltott szívbillentyű mineralizációban. Eddigi eredményeink alapján megállapítottuk, hogy a H₂S endogen szintje a CAVD előrehaladtával csökken, mely feltehetőleg a H₂S-t termelő CSE enzim struktúrális módosulásával magyarázható (Bibli, Hu et al. (2019)). A szervezetben kialakuló kénhidrogénszint-deficiencia pótolható kénhidrogént felszabadító donor molekulákkal, amelyek a jövőben mint lehetséges terápiás gyógyszerek válhatnak elérhetővé (Sikura, Potor et al. (2019)). A dolgozat témájául szolgáló két közlemény az első olyan munkák, amelyek két különböző molekula mechanizmusába nyújtanak betekintést ugyanabban a klinikai állapotban (CAVD), valamint elsőként kínálnak új gyógyszerészeti lehetőségeket, innovatív terápiás módszereket a CAVD és a kardiovaszkuláris megbetegedések gyógyításában.

A vas homeosztázis / H₂S egyensúly és a szívbillentyűk meszesedése közötti kapcsolatot még nagyon kevesen vizsgálták, és a szívbillentyű mineralizáció pathomechanizmusának ismerete még gyerekcipőben jár. Noha a legtöbb kardiovaszkuláris megbetegedés, jelen esetekben a kardiovaszkuláris rendszer mineralizációja a szervezet vasháztartásának felborulása és/vagy H₂S hiány következtében alakul ki, a terápiás kezelés hiányában a CKD-ben vagy CAVD-ben szenvedő betegeknél a vese vagy a szívbillentyűk (vagy mindkettő) transzplantációja a legtöbb esetben elkerülhetetlen. Vas esetében a CKD-s betegekben a retikuloendoteliális sejtekben vas felhalmozódása figyelhető meg, amelyet magasabb ferritin szint kísér a plazmában. Ez a növekedés a retikuloendoteliális sejtek vas szekretációjának következménye, mely által a vas hozzáférhetősége a többi sejt számára szignifikánsan alacsonyabb. Ez a mechanizmus az intracelluláris ferritin kimerülését és krónikus, gyulladós betegség kialakulását és az ezt követő vérszegénységet eredményezi. Megfigyeléseink első részében összefoglaltuk, hogy a vas metabolizmusának rendellenessége nagymértékben hozzájárul a magas foszfát indukálta szívbillentyű-kalcifikáció kialakulásához. A D3T orálisan adagolt terápiájával azonban (ferroxidáz rendszer indukciója) a szívbillentyűk/szív-érrendszer meszesedése megelőzhető.

A tanulmány második részében demonstráltuk, hogy a CAVD kialakulása során a szervezet endogen kénhidrogén ellátása szenved zavart. Meszes humán szívbillentyűkben a H₂S képződésében tapasztalt deficienciát a CSE enzim magas szintű expressziója kísérte. Számos tanulmány kimutatta, hogy a H₂S termelés hiánya szívbetegségek kialakulásához

vezet, ahogy azt, a szívkoszorúér betegségben szenvedő betegek plazmájában mérhető alacsonyabb H₂S szintje is jelzi (Jiang, Wu et al. (2005);(Shen, Shen et al. 2015)). A H₂S hiánya exogén módon pótolható egy, a Lawesson reagensből és a morfolin reakciójából származtatható, új generációs, lassú kénhidrogén felszabadulást biztosító vegyületek által (GYY4137). A GYY4137 protonációs reakciója pedig még stabilabb H₂S-felszabadító vegyületeket eredményez, mint például AP67 és AP72. Habár a valvuláris kalcifikáció és az endogén H₂S homeosztázis közötti kapcsolat kevésbé ismert, bemutatott eredményeink egy másik szempontból megközelíthető stabil terápiás eljárást kínálnak CAVD gyógyításában. Nem utolsó sorban eredményeink azáltal hogy részletes betekintést nyújtanak a CAVD patogenezisébe, új lehetőségeket kínálnak a vas- és/vagy az endogén kénhidrogén hiány okozta klinikai kardiovaszkuláris állapotok kialakulásának megelőzéséhez vagy csökkentésére irányuló jobb tervezési stratégiák kifejlesztéséhez.

Új eredmények

1. A H-ferritin/ferroxidáz vas vagy 3H-1,2-ditioil-3-tion (D3T) által indukálva gátolja a human szívbillentyűk intersticiális sejtjeinek mineralizációját, osteoblasztos differenciációját.
2. A H-ferritin elősegíti a Sox9 transzkripciós faktor nukleáris transzlokációját, azáltal, hogy csökkenti a RUNX2 nukleáris felhalmozódását.
3. A H-ferritin gátolja a szívbillentyű sejtek foszfátfelvételt és a lizoszomális foszfát-felhalmozódást azáltal, hogy csökkenti a foszfát csatornák expresszióját; a H-ferritin foszfátkötő képessége által a ferritin-foszfát komplexet lizoszomálisan lokalizálja, valamint fokozza a pirofoszfát képződést az ENPP2 indukciójával.
4. A stenotikus aorta billentyűk szövettani elemzése igazolta a H-ferritin magas expresszióját és relatív dominanciáját az ALP felett, azokban a régiókban, ahol mineralizáció nem volt detektálható.
5. A H-ferritin csökkenti a gyulladáshoz kapcsolódó markerek (TNF- α és IL1- β) expresszióját a humán AS szívbillentyűkből származó VIC sejtekben.
6. CSE és CBS eredetű H₂S és a kénhidrogént felszabadító donormolekulák gátolják az aorta billentyűk mineralizációját.
7. Az anti-kalcifikációs hatások a foszfátfelvétel gátlásával, a RUNX2 nukleáris transzlokációjának megakadályozásával, a pirofoszfát szintjének megemlése által valósulnak meg.
8. H₂S felszabadító donorok és a CSE / CBS eredetű H₂S terápiás potenciállal rendelkeznek a meszes aorta billentyű betegségben (CAVD).

7. References

- Abe, K. and H. Kimura (1996). "The possible role of hydrogen sulfide as an endogenous neuromodulator." J Neurosci **16**(3): 1066-1071.
- Adeney, K. L., D. S. Siscovick, J. H. Ix, S. L. Seliger, M. G. Shlipak, N. S. Jenny and B. R. Kestenbaum (2009). "Association of serum phosphate with vascular and valvular calcification in moderate CKD." J Am Soc Nephrol **20**(2): 381-387.
- Alani, H., A. Tamimi and N. Tamimi (2014). "Cardiovascular co-morbidity in chronic kidney disease: Current knowledge and future research needs." World J Nephrol **3**(4): 156-168.
- Alkhateeb, A. A. and J. R. Connor (2010). "Nuclear ferritin: A new role for ferritin in cell biology." Biochim Biophys Acta **1800**(8): 793-797.
- Arosio, P., R. Ingrassia and P. Cavadini (2009). "Ferritins: a family of molecules for iron storage, antioxidation and more." Biochim Biophys Acta **1790**(7): 589-599.
- Arosio, P. and S. Levi (2002). "Ferritin, iron homeostasis, and oxidative damage." Free Radic Biol Med **33**(4): 457-463.
- Arsenault, B. J., S. M. Boekholdt, M. P. Dube, E. Rheaume, N. J. Wareham, K. T. Khaw, M. S. Sandhu and J. C. Tardif (2014). "Lipoprotein(a) levels, genotype, and incident aortic valve stenosis: a prospective Mendelian randomization study and replication in a case-control cohort." Circ Cardiovasc Genet **7**(3): 304-310.
- Balla, G., H. S. Jacob, J. Balla, M. Rosenberg, K. Nath, F. Apple, J. W. Eaton and G. M. Vercellotti (1992). "Ferritin: a cytoprotective antioxidant strategem of endothelium." J Biol Chem **267**(25): 18148-18153.
- Becs, G., A. Zarjou, A. Agarwal, K. E. Kovacs, A. Becs, M. Nyitrai, E. Balogh, E. Banyai, J. W. Eaton, P. Arosio, M. Poli, V. Jeney, J. Balla and G. Balla (2016). "Pharmacological induction of ferritin prevents osteoblastic transformation of smooth muscle cells." J Cell Mol Med **20**(2): 217-230.
- Beltowski, J. (2015). "Hydrogen sulfide in pharmacology and medicine--An update." Pharmacol Rep **67**(3): 647-658.
- Bibli, S. I., J. Hu, F. Sigala, I. Wittig, J. Heidler, S. Zukunft, D. I. Tsilimigras, V. Randriamboavonjy, J. Wittig, B. Kojonazarov, C. Schurmann, M. Siragusa, D. Siuda, B. Luck, R. Abdel Malik, K. A. Filis, G. Zografos, C. Chen, D. W. Wang, J. Pfeilschifter, R. P. Brandes, C. Szabo, A. Papapetropoulos and I. Fleming (2019). "Cystathionine gamma Lyase Sulfhydrates the RNA Binding Protein Human Antigen R to Preserve Endothelial Cell Function and Delay Atherogenesis." Circulation **139**(1): 101-114.
- Block, G. A. (2000). "Prevalence and clinical consequences of elevated Ca x P product in hemodialysis patients." Clin Nephrol **54**(4): 318-324.

- Carpentier, S. M., A. F. Carpentier, L. Chen, M. Shen, L. J. Quintero and T. H. Witzel (1995). "Calcium mitigation in bioprosthetic tissues by iron pretreatment: the challenge of iron leaching." Ann Thorac Surg **60**(2 Suppl): S332-338.
- Chen, C. Q., H. Xin and Y. Z. Zhu (2007). "Hydrogen sulfide: third gaseous transmitter, but with great pharmacological potential." Acta Pharmacol Sin **28**(11): 1709-1716.
- Cheng, A. and P. G. Genever (2010). "SOX9 determines RUNX2 transactivity by directing intracellular degradation." J Bone Miner Res **25**(12): 2680-2689.
- Chester, A. H. (2011). "Molecular and cellular mechanisms of valve calcification." Aswan Heart Centre Science & Practice Series **2011**(1): 4.
- Chitnis, M. K., Y. F. Njie-Mbye, C. A. Opere, M. E. Wood, M. Whiteman and S. E. Ohia (2013). "Pharmacological actions of the slow release hydrogen sulfide donor GYY4137 on phenylephrine-induced tone in isolated bovine ciliary artery." Exp Eye Res **116**: 350-354.
- Coffman, L. G., D. Parsonage, R. D'Agostino, Jr., F. M. Torti and S. V. Torti (2009). "Regulatory effects of ferritin on angiogenesis." Proc Natl Acad Sci U S A **106**(2): 570-575.
- Crouthamel (2013). "Sodium-Dependent Phosphate Cotransporters and Phosphate-Induced Calcification of Vascular Smooth Muscle Cells."
- Davignon, J. and P. Ganz (2004). "Role of endothelial dysfunction in atherosclerosis." Circulation **109**(23 Suppl 1): Iii27-32.
- de Silva, D., J. H. Guo and S. D. Aust (1993). "Relationship between iron and phosphate in mammalian ferritins." Arch Biochem Biophys **303**(2): 451-455.
- Di Iorio, B. R., S. Bortone, C. Piscopo, P. Grimaldi, E. Cucciniello, E. D'Avanzo, F. Mondillo, N. Cillo and V. Bellizzi (2006). "Cardiac vascular calcification and QT interval in ESRD patients: is there a link?" Blood Purif **24**(5-6): 451-459.
- Ducy (1997). "Osf2/Cbfa1: A Transcriptional Activator of Osteoblast Differentiation."
- Dutta, P. and J. Lincoln (2018). "Calcific Aortic Valve Disease: a Developmental Biology Perspective." Curr Cardiol Rep **20**(4): 21.
- Dweck, M. R., N. A. Boon and D. E. Newby (2012). "Calcific aortic stenosis: a disease of the valve and the myocardium." J Am Coll Cardiol **60**(19): 1854-1863.
- Finazzi, D. and P. Arosio (2014). "Biology of ferritin in mammals: an update on iron storage, oxidative damage and neurodegeneration." Arch Toxicol **88**(10): 1787-1802.
- Fleisch, H. and S. Bisaz (1962). "Mechanism of calcification: inhibitory role of pyrophosphate." Nature **195**: 911.
- Freeman, R. V. and C. M. Otto (2005). "Spectrum of calcific aortic valve disease: pathogenesis, disease progression, and treatment strategies." Circulation **111**(24): 3316-3326.

Fujita, T., N. Izumo, R. Fukuyama, T. Meguro, H. Nakamuta, T. Kohno and M. Koida (2001). "Phosphate provides an extracellular signal that drives nuclear export of Runx2/Cbfa1 in bone cells." Biochem Biophys Res Commun **280**(1): 348-352.

Giachelli, C. M. (2009). "The emerging role of phosphate in vascular calcification."

Kidney Int **75**(9): 890-897.

Goodwin, J. M., W. E. Dowdle, R. DeJesus, Z. Wang, P. Bergman, M. Kobylarz, A. Lindeman, R. J. Xavier, G. McAllister, B. Nyfeler, G. Hoffman and L. O. Murphy (2017). "Autophagy-Independent Lysosomal Targeting Regulated by ULK1/2-FIP200 and ATG9." Cell Rep **20**(10): 2341-2356.

Hosen, M. J., P. J. Coucke, O. Le Saux, A. De Paepe and O. M. Vanakker (2014).

"Perturbation of specific pro-mineralizing signalling pathways in human and murine pseudoxanthoma elasticum." Orphanet J Rare Dis **9**: 66.

Hruska, K. A., S. Mathew, R. Lund, P. Qiu and R. Pratt (2008). "Hyperphosphatemia of chronic kidney disease." Kidney Int **74**(2): 148-157.

Huang, K., X.-M. Zhang, L.-S. Zhou, D.-J. Tao and J.-P. Fan (2017). "Highly efficient and selective absorption of H₂S in phenolic ionic liquids: A cooperative result of anionic strong basicity and cationic hydrogen-bond donation." Chemical Engineering Science **173**: 253-263.

Huk, D. J., B. F. Austin, T. E. Horne, R. B. Hinton, W. C. Ray, D. D. Heistad and J. Lincoln (2016). "Valve Endothelial Cell-Derived Tgfbeta1 Signaling Promotes Nuclear Localization of Sox9 in Interstitial Cells Associated With Attenuated Calcification." Arterioscler Thromb Vasc Biol **36**(2): 328-338.

Jiang, H. L., H. C. Wu, Z. L. Li, B. Geng and C. S. Tang (2005). "[Changes of the new gaseous transmitter H₂S in patients with coronary heart disease]." Di Yi Jun Yi Da Xue Xue Bao **25**(8): 951-954.

Johnson, R. C., J. A. Leopold and J. Loscalzo (2006). "Vascular calcification: pathobiological mechanisms and clinical implications." Circ Res **99**(10): 1044-1059.

Jono, S., M. D. McKee, C. E. Murray, A. Shioi, Y. Nishizawa, K. Mori, H. Morii and C. M. Giachelli (2000). "Phosphate regulation of vascular smooth muscle cell calcification." Circ Res **87**(7): E10-17.

Juan, S. H. and S. D. Aust (1998). "Iron and phosphate content of rat ferritin heteropolymers." Arch Biochem Biophys **357**(2): 293-298.

Kamstrup, P. R., A. Tybjaerg-Hansen and B. G. Nordestgaard (2014). "Elevated lipoprotein(a) and risk of aortic valve stenosis in the general population." J Am Coll Cardiol **63**(5): 470-477.

Kang, J., D. L. Neill and M. Xian (2017). "Phosphonothioate-Based Hydrogen Sulfide Releasing Reagents: Chemistry and Biological Applications." Front Pharmacol **8**: 457.

- Komori, T. (2006). "Regulation of osteoblast differentiation by transcription factors." J Cell Biochem **99**(5): 1233-1239.
- Komori, T., H. Yagi, S. Nomura, A. Yamaguchi, K. Sasaki, K. Deguchi, Y. Shimizu, R. T. Bronson, Y. H. Gao, M. Inada, M. Sato, R. Okamoto, Y. Kitamura, S. Yoshiki and T. Kishimoto (1997). "Targeted disruption of *Cbfa1* results in a complete lack of bone formation owing to maturational arrest of osteoblasts." Cell **89**(5): 755-764.
- Kuhn, L. C. (2015). "Iron regulatory proteins and their role in controlling iron metabolism." Metallomics **7**(2): 232-243.
- Kulkarni-Chitnis, M., Y. F. Njie-Mbye, L. Mitchell, J. Robinson, M. Whiteman, M. E. Wood, C. A. Opere and S. E. Ohia (2015). "Inhibitory action of novel hydrogen sulfide donors on bovine isolated posterior ciliary arteries." Exp Eye Res **134**: 73-79.
- Leopold, J. A. (2012). "Cellular mechanisms of aortic valve calcification." Circ Cardiovasc Interv **5**(4): 605-614.
- Li, L., M. Whiteman, Y. Y. Guan, K. L. Neo, Y. Cheng, S. W. Lee, Y. Zhao, R. Baskar, C. H. Tan and P. K. Moore (2008). "Characterization of a novel, water-soluble hydrogen sulfide-releasing molecule (GYY4137): new insights into the biology of hydrogen sulfide." Circulation **117**(18): 2351-2360.
- Li, X., H. Y. Yang and C. M. Giachelli (2006). "Role of the sodium-dependent phosphate cotransporter, Pit-1, in vascular smooth muscle cell calcification." Circ Res **98**(7): 905-912.
- Libby, P., P. M. Ridker and A. Maseri (2002). "Inflammation and atherosclerosis." Circulation **105**(9): 1135-1143.
- Lin, M. E., T. Chen, E. M. Leaf, M. Y. Speer and C. M. Giachelli (2015). "Runx2 Expression in Smooth Muscle Cells Is Required for Arterial Medial Calcification in Mice." Am J Pathol **185**(7): 1958-1969.
- Lincoln, J., R. Kist, G. Scherer and K. E. Yutzey (2007). "Sox9 is required for precursor cell expansion and extracellular matrix organization during mouse heart valve development." Dev Biol **305**(1): 120-132.
- Lomashvili, K. A., S. Narisawa, J. L. Millan and W. C. O'Neill (2014). "Vascular calcification is dependent on plasma levels of pyrophosphate." Kidney Int **85**(6): 1351-1356.
- London, G. M., B. Pannier, S. J. Marchais and A. P. Guerin (2000). "Calcification of the aortic valve in the dialyzed patient." J Am Soc Nephrol **11**(4): 778-783.
- Lusis, A. J., R. Mar and P. Pajukanta (2004). "Genetics of atherosclerosis." Annu Rev Genomics Hum Genet **5**: 189-218.
- Maher, E. R., G. Young, B. Smyth-Walsh, S. Pugh and J. R. Curtis (1987). "Aortic and mitral valve calcification in patients with end-stage renal disease." Lancet **2**(8564): 875-877.

- Mancias, J. D., X. Wang, S. P. Gygi, J. W. Harper and A. C. Kimmelman (2014). "Quantitative proteomics identifies NCOA4 as the cargo receptor mediating ferritinophagy." Nature **509**(7498): 105-109.
- Massy, Z. A., O. Ivanovski, T. Nguyen-Khoa, J. Angulo, D. Szumilak, N. Mothu, O. Phan, M. Daudon, B. Lacour, T. B. Drueke and M. S. Muntzel (2005). "Uremia accelerates both atherosclerosis and arterial calcification in apolipoprotein E knockout mice." J Am Soc Nephrol **16**(1): 109-116.
- Mathieu, P., B. J. Arsenault, M. C. Boulanger, Y. Bosse and M. L. Koschinsky (2017). "Pathobiology of Lp(a) in calcific aortic valve disease." Expert Rev Cardiovasc Ther **15**(10): 797-807.
- Mathieu, P., P. Voisine, A. Pepin, R. Shetty, N. Savard and F. Dagenais (2005). "Calcification of human valve interstitial cells is dependent on alkaline phosphatase activity." J Heart Valve Dis **14**(3): 353-357.
- Mazzone, A., M. C. Epistolato, R. De Caterina, S. Storti, S. Vittorini, S. Sbrana, J. Gianetti, S. Bevilacqua, M. Glauber, A. Biagini and P. Tanganelli (2004). "Neoangiogenesis, T-lymphocyte infiltration, and heat shock protein-60 are biological hallmarks of an immunomediated inflammatory process in end-stage calcified aortic valve stenosis." J Am Coll Cardiol **43**(9): 1670-1676.
- Mohler, E. R., 3rd (2004). "Mechanisms of aortic valve calcification." Am J Cardiol **94**(11): 1396-1402, a1396.
- Mohler, E. R., 3rd, F. Gannon, C. Reynolds, R. Zimmerman, M. G. Keane and F. S. Kaplan (2001). "Bone formation and inflammation in cardiac valves." Circulation **103**(11): 1522-1528.
- Moradi, H., D. A. Sica and K. Kalantar-Zadeh (2013). "Cardiovascular burden associated with uremic toxins in patients with chronic kidney disease." Am J Nephrol **38**(2): 136-148.
- Nagy, P. (2013). "Kinetics and mechanisms of thiol-disulfide exchange covering direct substitution and thiol oxidation-mediated pathways." Antioxid Redox Signal **18**(13): 1623-1641.
- Nandi, S. S. and P. K. Mishra (2017). "H₂S and homocysteine control a novel feedback regulation of cystathionine beta synthase and cystathionine gamma lyase in cardiomyocytes." Sci Rep **7**(1): 3639.
- Nitschke, Y., G. Baujat, U. Botschen, T. Wittkampf, M. du Moulin, J. Stella, M. Le Merrer, G. Guest, K. Lambot, M. F. Tazarourte-Pinturier, N. Chassaing, O. Roche, I. Feenstra, K. Loechner, C. Deshpande, S. J. Garber, R. Chikarmane, B. Steinmann, T. Shahinyan, L. Martorell, J. Davies, W. E. Smith, S. G. Kahler, M. McCulloch, E. Wraige, L. Loidi, W. Hohne, L. Martin, S. Hadj-Rabia, R. Terkeltaub and F. Rutsch (2012). "Generalized arterial calcification of infancy and pseudoxanthoma elasticum can be caused by mutations in either ENPP1 or ABCC6." Am J Hum Genet **90**(1): 25-39.

- O'Brien, K. D., J. Kuusisto, D. D. Reichenbach, M. Ferguson, C. Giachelli, C. E. Alpers and C. M. Otto (1995). "Osteopontin is expressed in human aortic valvular lesions." Circulation **92**(8): 2163-2168.
- Peacock, J. D., A. K. Levay, D. B. Gillaspie, G. Tao and J. Lincoln (2010). "Reduced sox9 function promotes heart valve calcification phenotypes in vivo." Circ Res **106**(4): 712-719.
- Pietsch, E. C., J. Y. Chan, F. M. Torti and S. V. Torti (2003). "Nrf2 mediates the induction of ferritin H in response to xenobiotics and cancer chemopreventive dithiolethiones." J Biol Chem **278**(4): 2361-2369.
- Potor, L., P. Nagy, G. Mehes, Z. Hendrik, V. Jeney, D. Petho, A. Vasas, Z. Palinkas, E. Balogh, A. Gyetvai, M. Whiteman, R. Torregrossa, M. E. Wood, S. Olvaszto, P. Nagy, G. Balla and J. Balla (2018). "Hydrogen Sulfide Abrogates Hemoglobin-Lipid Interaction in Atherosclerotic Lesion." Oxid Med Cell Longev **2018**: 3812568.
- Primiano, T., T. W. Kensler, P. Kuppusamy, J. L. Zweier and T. R. Sutter (1996). "Induction of hepatic heme oxygenase-1 and ferritin in rats by cancer chemopreventive dithiolethiones." Carcinogenesis **17**(11): 2291-2296.
- Raaz, U., I. N. Schellinger, E. Chernogubova, C. Warnecke, Y. Kayama, K. Penov, J. K. Hennigs, F. Salomons, S. Eken, F. C. Emrich, W. H. Zheng, M. Adam, A. Jagger, F. Nakagami, R. Toh, K. Toyama, A. Deng, M. Buerke, L. Maegdefessel, G. Hasenfuss, J. M. Spin and P. S. Tsao (2015). "Transcription Factor Runx2 Promotes Aortic Fibrosis and Stiffness in Type 2 Diabetes Mellitus." Circ Res **117**(6): 513-524.
- Rajamannan, N. M., F. J. Evans, E. Aikawa, K. J. Grande-Allen, L. L. Demer, D. D. Heistad, C. A. Simmons, K. S. Masters, P. Mathieu, K. D. O'Brien, F. J. Schoen, D. A. Towler, A. P. Yoganathan and C. M. Otto (2011). "Calcific aortic valve disease: not simply a degenerative process: A review and agenda for research from the National Heart and Lung and Blood Institute Aortic Stenosis Working Group. Executive summary: Calcific aortic valve disease-2011 update." Circulation **124**(16): 1783-1791.
- Rajamannan, N. M., M. Subramaniam, D. Rickard, S. R. Stock, J. Donovan, M. Springett, T. Orszulak, D. A. Fullerton, A. J. Tajik, R. O. Bonow and T. Spelsberg (2003). "Human aortic valve calcification is associated with an osteoblast phenotype." Circulation **107**(17): 2181-2184.
- Rattazzi, M., B. J. Bennett, F. Bea, E. A. Kirk, J. L. Ricks, M. Speer, S. M. Schwartz, C. M. Giachelli and M. E. Rosenfeld (2005). "Calcification of advanced atherosclerotic lesions in the innominate arteries of ApoE-deficient mice: potential role of chondrocyte-like cells." Arterioscler Thromb Vasc Biol **25**(7): 1420-1425.
- Rose, P., P. K. Moore and Y. Z. Zhu (2017). "H2S biosynthesis and catabolism: new insights from molecular studies." Cell Mol Life Sci **74**(8): 1391-1412.
- Saftig, P. and J. Klumperman (2009). "Lysosome biogenesis and lysosomal membrane proteins: trafficking meets function." Nat Rev Mol Cell Biol **10**(9): 623-635.

Shen, Y., Z. Shen, S. Luo, W. Guo and Y. Z. Zhu (2015). "The Cardioprotective Effects of Hydrogen Sulfide in Heart Diseases: From Molecular Mechanisms to Therapeutic Potential." Oxid Med Cell Longev **2015**: 925167.

Sikura, K. E., L. Potor, T. Szerafin, M. Oros and P. Nagy (2019). "Hydrogen sulfide inhibits calcification of heart valves; implications for calcific aortic valve disease."

Sikura, K. E., L. Potor, T. Szerafin, A. Zarjou, A. Agarwal, P. Arosio, M. Poli, Z. Hendrik, G. Mehes, M. Oros, N. Posta, L. Beke, I. Furtos, G. Balla and J. Balla (2019). "Potential Role of H-Ferritin in Mitigating Valvular Mineralization." Arterioscler Thromb Vasc Biol **39**(3): 413-431.

Speer, M. Y. and C. M. Giachelli (2004). "Regulation of cardiovascular calcification." Cardiovasc Pathol **13**(2): 63-70.

Speer, M. Y., X. Li, P. G. Hiremath and C. M. Giachelli (2010). "Runx2/Cbfa1, but not loss of myocardin, is required for smooth muscle cell lineage reprogramming toward osteochondrogenesis." J Cell Biochem **110**(4): 935-947.

Steitz, S. A., M. Y. Speer, G. Curinga, H. Y. Yang, P. Haynes, R. Aebersold, T. Schinke, G. Karsenty and C. M. Giachelli (2001). "Smooth muscle cell phenotypic transition associated with calcification: upregulation of Cbfa1 and downregulation of smooth muscle lineage markers." Circ Res **89**(12): 1147-1154.

Stocker, R. and J. F. Keaney, Jr. (2004). "Role of oxidative modifications in atherosclerosis." Physiol Rev **84**(4): 1381-1478.

Sun, Y., C. H. Byon, K. Yuan, J. Chen, X. Mao, J. M. Heath, A. Javed, K. Zhang, P. G. Anderson and Y. Chen (2012). "Smooth muscle cell-specific runx2 deficiency inhibits vascular calcification." Circ Res **111**(5): 543-552.

Terkeltaub, R. A. (2001). "Inorganic pyrophosphate generation and disposition in pathophysiology." Am J Physiol Cell Physiol **281**(1): C1-c11.

Thanassoulis, G., C. Y. Campbell, D. S. Owens, J. G. Smith, A. V. Smith, G. M. Peloso, K. F. Kerr, S. Pechlivanis, M. J. Budoff, T. B. Harris, R. Malhotra, K. D. O'Brien, P. R. Kamstrup, B. G. Nordestgaard, A. Tybjaerg-Hansen, M. A. Allison, T. Aspelund, M. H. Criqui, S. R. Heckbert, S. J. Hwang, Y. Liu, M. Sjogren, J. van der Pals, H. Kalsch, T. W. Muhleisen, M. M. Nothen, L. A. Cupples, M. Caslake, E. Di Angelantonio, J. Danesh, J. I. Rotter, S. Sigurdsson, Q. Wong, R. Erbel, S. Kathiresan, O. Melander, V. Gudnason, C. J. O'Donnell and W. S. Post (2013). "Genetic associations with valvular calcification and aortic stenosis." N Engl J Med **368**(6): 503-512.

Theil, E. C. (1990). "The ferritin family of iron storage proteins." Adv Enzymol Relat Areas Mol Biol **63**: 421-449.

Theil, E. C., R. K. Behera and T. Tosha (2013). "Ferritins for Chemistry and for Life." Coord Chem Rev **257**(2): 579-586.

Torti, S. V., E. L. Kwak, S. C. Miller, L. L. Miller, G. M. Ringold, K. B. Myambo, A. P. Young and F. M. Torti (1988). "The molecular cloning and characterization of murine ferritin heavy chain, a tumor necrosis factor-inducible gene." J Biol Chem **263**(25): 12638-12644.

Tsuji, Y., L. L. Miller, S. C. Miller, S. V. Torti and F. M. Torti (1991). "Tumor necrosis factor-alpha and interleukin 1-alpha regulate transferrin receptor in human diploid fibroblasts. Relationship to the induction of ferritin heavy chain." J Biol Chem **266**(11): 7257-7261.

Wang, A. Y., M. Wang, J. Woo, C. W. Lam, P. K. Li, S. F. Lui and J. E. Sanderson (2003). "Cardiac valve calcification as an important predictor for all-cause mortality and cardiovascular mortality in long-term peritoneal dialysis patients: a prospective study." J Am Soc Nephrol **14**(1): 159-168.

Wang, R. (2002). "Two's company, three's a crowd: can H₂S be the third endogenous gaseous transmitter?" Faseb j **16**(13): 1792-1798.

Wang, R. (2010). "Hydrogen sulfide: the third gasotransmitter in biology and medicine." Antioxid Redox Signal **12**(9): 1061-1064.

Wang, R. (2012). "Physiological implications of hydrogen sulfide: a whiff exploration that blossomed." Physiol Rev **92**(2): 791-896.

Wang, W., M. A. Knovich, L. G. Coffman, F. M. Torti and S. V. Torti (2010). "Serum ferritin: Past, present and future." Biochim Biophys Acta **1800**(8): 760-769.

Whiteman, M., A. Perry, Z. Zhou, M. Bucci, A. Papapetropoulos, G. Cirino and M. E. Wood (2015). "Phosphinodithioate and Phosphoramidodithioate Hydrogen Sulfide Donors." Handb Exp Pharmacol **230**: 337-363.

Yutzey, K. E., L. L. Demer, S. C. Body, G. S. Huggins, D. A. Towler, C. M. Giachelli, M. A. Hofmann-Bowman, D. P. Mortlock, M. B. Rogers, M. M. Sadeghi and E. Aikawa (2014). "Calcific aortic valve disease: a consensus summary from the Alliance of Investigators on Calcific Aortic Valve Disease." Arterioscler Thromb Vasc Biol **34**(11): 2387-2393.

Zarjou, A., L. M. Black, K. R. McCullough, T. D. Hull, S. K. Esman, R. Boddu, S. Varambally, D. S. Chandrashekar, W. Feng, P. Arosio, M. Poli, J. Balla and S. Bolisetty (2019). "Ferritin Light Chain Confers Protection Against Sepsis-Induced Inflammation and Organ Injury." Front Immunol **10**: 131.

Zarjou, A., S. Bolisetty, R. Joseph, A. Traylor, E. O. Apostolov, P. Arosio, J. Balla, J. Verlander, D. Darshan, L. C. Kuhn and A. Agarwal (2013). "Proximal tubule H-ferritin mediates iron trafficking in acute kidney injury." J Clin Invest **123**(10): 4423-4434.

Zarjou, A., V. Jeney, P. Arosio, M. Poli, P. Antal-Szalmás, A. Agarwal, G. Balla and J. Balla (2009). "Ferritin prevents calcification and osteoblastic differentiation of vascular smooth muscle cells." J Am Soc Nephrol **20**(6): 1254-1263.

Zarjou, A., V. Jeney, P. Arosio, M. Poli, E. Zavaczki, G. Balla and J. Balla (2010). "Ferritin ferroxidase activity: a potent inhibitor of osteogenesis." J Bone Miner Res **25**(1): 164-172.

Zavaczki, E., V. Jeney, A. Agarwal, A. Zarjou, M. Oros, M. Katko, Z. Varga, G. Balla and J. Balla (2011). "Hydrogen sulfide inhibits the calcification and osteoblastic differentiation of vascular smooth muscle cells." Kidney Int **80**(7): 731-739.

Zhang, L., Y. Wang, Y. Li, L. Li, S. Xu, X. Feng and S. Liu (2018). "Hydrogen Sulfide (H₂S)-Releasing Compounds: Therapeutic Potential in Cardiovascular Diseases." Front Pharmacol **9**: 1066.

Zhang, Y. and R. Munday (2008). "Dithiolethiones for cancer chemoprevention: where do we stand?" Mol Cancer Ther **7**(11): 3470-3479.

8. Key words

Aortic valve

AP72

Apolipoprotein E knockout mice

Calcification

D3T

Ferritin

H₂S

Inflammation

9. List of publications



Registry number: DEENK/177/2019.PL
Subject: PhD Publikációs Lista

Candidate: Katalin Éva Sikura
Neptun ID: U71BBT
Doctoral School: Kálmán Laki Doctoral School
MTMT ID: 10055770

List of publications related to the dissertation

1. **Sikura, K. É.**, Potor, L., Szerafin, T., Oros, M., Nagy, P., Méhes, G., Hendrik, Z., Zarjou, A., Agarwal, A., Posta, N., Torregrossa, R., Whiteman, M., Fürtös, I., Balla, G., Balla, J.: Hydrogen sulfide abrogates heart valve calcification: implications for calcific aortic valve disease.
Br. J. Pharmacol. [Epub ahead of print], 2019.
DOI: <http://dx.doi.org/10.1111/bph.14691>
IF: 6.81 (2017)
2. **Sikura, K. É.**, Potor, L., Szerafin, T., Zarjou, A., Agarwal, A., Arosio, P., Poli, M., Hendrik, Z., Méhes, G., Oros, M., Posta, N., Beke, L., Fürtös, I., Balla, G., Balla, J.: Potential Role of H-Ferritin in Mitigating Valvular Mineralization.
Arterioscler. Thromb. Vasc. Biol. 39 (3), 413-431, 2019.
DOI: <http://dx.doi.org/10.1161/ATVBAHA.118.312191>
IF: 6.086 (2017)





List of other publications

3. Becs, G., Zarjou, A., Agarwal, A., **Sikura, K. É.**, Becs, Á., Nyitrai, M., Balogh, E., Bányai, E., Eaton, J. W., Arosio, P., Poli, M., Jeney, V., Balla, J., Balla, G.: Pharmacological induction of ferritin prevents osteoblastic transformation of smooth muscle cells.
J. Cell. Mol. Med. 20 (2), 217-230, 2016.
DOI: <http://dx.doi.org/10.1111/jcmm.12682>
IF: 4.499
4. Szemán-Nagy, G., Turáni, M., **Sikura, K. É.**, Bánfalvi, G.: Chromatin Changes upon Silver Nitrate Treatment in Human Keratinocyte HaCaT and K562 Erythroleukemia Cells.
In: Cellular effects of heavy metals. Ed.: Gáspár Bánfalvi, Springer, Milton Keynes, 195-217, 2011.

Total IF of journals (all publications): 17,395

Total IF of journals (publications related to the dissertation): 12,896

The Candidate's publication data submitted to the iDEa Tudóstér have been validated by DEENK on the basis of the Journal Citation Report (Impact Factor) database.

07 May, 2019



Abstracts and presentations

1. Magyar Szabadgyök-Kutató Társaság VII. Kongresszusa, 2013; Debrecen, Hungary. *Kovács Katalin Éva, Jeney Viktória, Szerafin Tamás, Balla József, Humán szívbílyentyűk kalcifikációjának gátlása a ferritin rendszeren keresztül.*
2. Magyar Szívsebészeti Társaság XXII. Kongresszusa; 2015.; Szeged, Hungary. *Kovács Katalin Éva, Szerafin Tamás, Hendrik Zoltán, Balla György, Balla József, Humán valvuláris interstitialis sejtek mineralizációs folyamatai.*
3. Scientific Congress of the Society of Hungarian Cardiologists; May, 2015; Balatonfüred, Hungary. *Katalin Éva Sikura, Tamás Szerafin, Zoltán Hendrik, György Balla, József Balla, Mineralization process of human heart valve interstitial cells.*
4. 9th International Conference on Heme Oxygenase. November, 2016; Prague, Czech Republic. *Katalin Éva Sikura, Tamás Szerafin, Abolfazl Zarjou, Anupam Agarwal, Gerardo Alvarado, Zoltán Hendrik, György Balla, József Balla, Targeting H-ferritin to mitigate valvular mineralization.*
5. Magyar Szabadgyök-Kutató Társaság Kongresszusa, 2017. Gödöllő, Hungary. *Sikura Katalin Éva, Potor László, Hendrik Zoltán, Posta Niké, Oros Melinda, Balla György, Balla József, A ferritin rendszer és a szabadgyökök.*
6. Cardiovascular Research Days, 2018. Debrecen, Hungary. *Katalin Éva Sikura, Tamás Szerafin, Abolfazl Zarjou, Anupam Agarwal, Gerardo Alvarado, Gábor Méhes, Zoltán Hendrik, László Potor, Melinda Oros, György Balla, József Balla, Targeting H-ferritin to mitigate valvular mineralization.*
7. Magyar Szívsebészeti Társaság XXV. Kongresszusa. 2018. Budapest, Hungary. *Katalin Éva Sikura, László Potor, Tamás Szerafin, Abolfazl Zarjou, Anupam Agarwal, Paolo Arosio, Maura Poli, Zoltán Hendrik, Gábor Méhes, Melinda Oros, Niké Posta, Lívía Beke, Ibolya Fürtös, György Balla, József Balla, HYDROGEN SULFIDE ABROGATES HEART VALVE CALCIFICATION: IMPLICATIONS FOR CALCIFIC AORTIC VALVE DISEASE.*
8. IRONHEART - GINOP 2.3.2-15-2016-00043 projekt tudományos ülés. 2018. Debrecen, Hungary. *Katalin Éva Sikura, László Potor, Tamás Szerafin, Abolfazl Zarjou, Anupam Agarwal, Paolo Arosio, Maura Poli, Zoltán Hendrik, Gábor Méhes, Melinda Oros, Niké Posta, Lívía Beke, Ibolya Fürtös, György Balla, József Balla, HYDROGEN SULFIDE ABROGATES HEART VALVE CALCIFICATION: IMPLICATIONS FOR CALCIFIC AORTIC VALVE DISEASE.*
9. Magyar Osteológiai és Osteoarthrológiai Társaság Osteológiai Kongresszusa, 2019. Balatonfüred, Hungary. *Katalin Éva Sikura, László Potor, Tamás Szerafin, Abolfazl Zarjou, Anupam Agarwal, Paolo Arosio, Maura Poli, Zoltán Hendrik, Gábor Méhes, Melinda Oros, Niké Posta, Lívía Beke, Ibolya Fürtös, György Balla, József Balla, POTENTIAL ROLE OF H-FERRITIN IN MITIGATING VALVULAR MINERALIZATION.*
10. Magyar Szabadgyök-Kutató Társaság X. Kongresszusa, 2019. Szeged, Hungary. *Katalin Éva Sikura, László Potor, Tamás Szerafin, Abolfazl Zarjou, Anupam Agarwal, Paolo Arosio, Maura Poli, Zoltán Hendrik, Gábor Méhes, Melinda Oros, Niké Posta, Lívía Beke, Ibolya Fürtös, György Balla, József Balla, HYDROGEN SULFIDE ABROGATES HEART VALVE CALCIFICATION: IMPLICATIONS FOR CALCIFIC AORTIC VALVE DISEASE.*

Membership in National and International Societies

- Hungarian Society of Cardiology (Magyar Kardiológusok Társasága (MKT))
- Hungarian Society of Cardiac Surgery (Magyar Szívsebészeti Társaság)
- Hungarian Free Radical Society (Magyar Szabadgyök - Kutató Társaság (MSZKT))
- European Society of Cardiology

10. Acknowledgement

I am forever grateful to my supervisor Professor József Balla. His support, wealth of knowledge and mentorship were invaluable during my training. He not only provided me the opportunity to enjoy science but also served as a role model to be a better scientist.

I would like to thank Professor Tamás Szerafin for his helpful co-work, advices, and to collect human heart valve samples.

I would like to thank László Potor. He is a high skilled scientist who taught me everything about being a scientist. His work ethics, skills and nature of teaching provided me the fundamentals of becoming a scientist.

My special thanks for Ibolya Fürtös and Lívia Beke for their professional, selfless and helpful work.

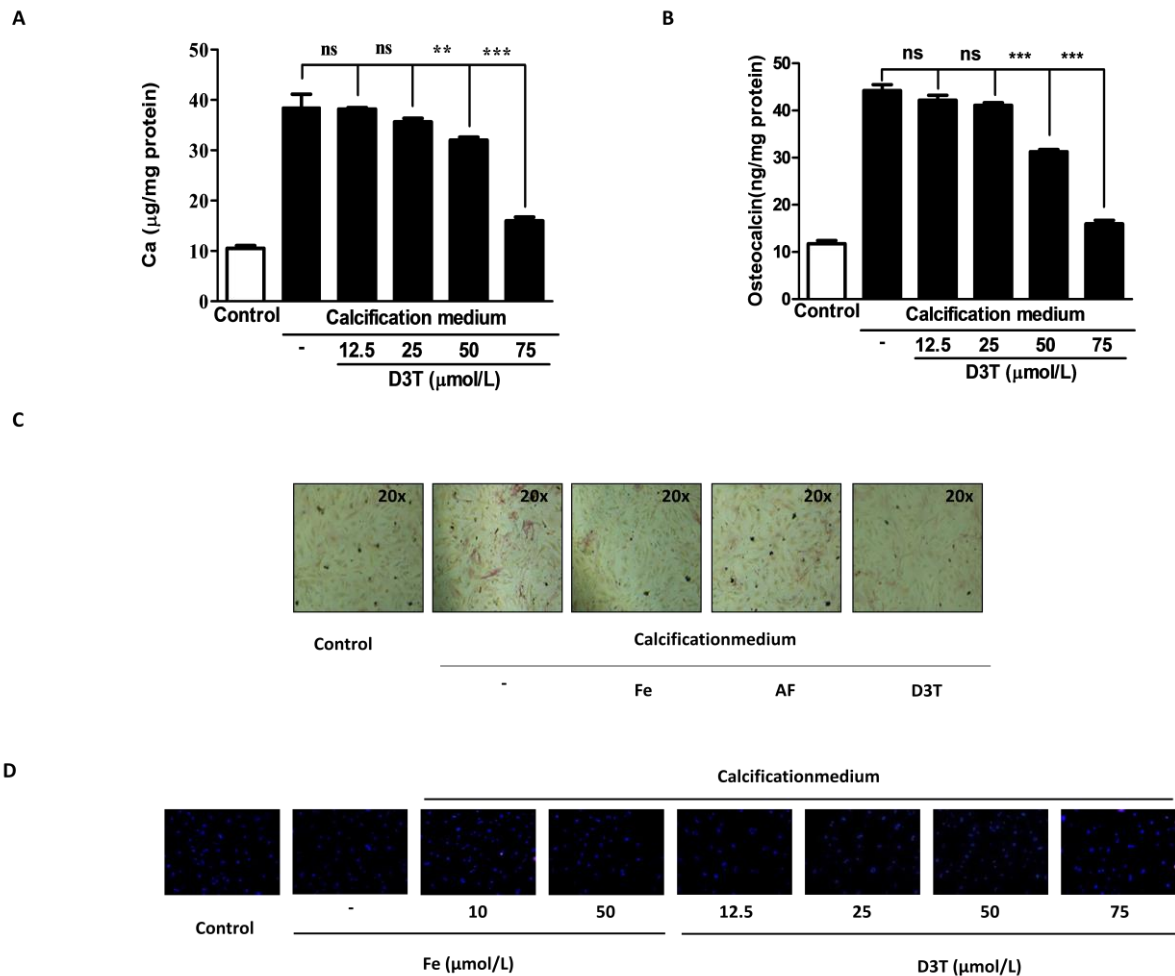
Many thanks also go to Professor György Balla for his support and mentorship.

Finally, I would like to thank every minute of my great husband, Dániel Sikura for his support during my training.

This work is supported by the Richter Gedeon Talent Scholarship award of Katalin Éva Sikura and Hungarian Academy of Sciences (11003). This research was supported by Hungarian Government grant, OTKA-K112333 (JB) and by the GINOP-2.3.2-15-2016-00043 (IRONHEART), and EFOP-3.6.2-16-2017-00006 project, 1K08HL140294-01 (to AZ). RT is also grateful to the Brian Ridge Scholarship. The project is co-financed by the European Union, the European Regional Development Fund and the Medical Research Council, UK (JB, GyB, MW and RT).

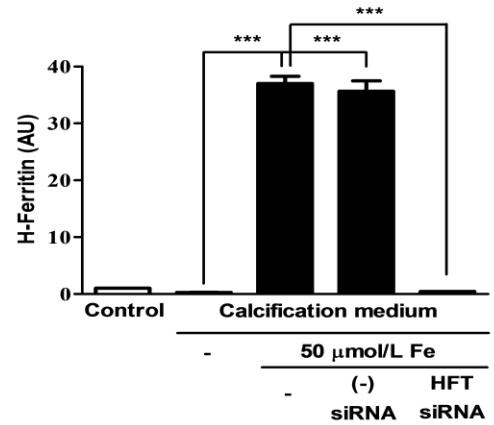
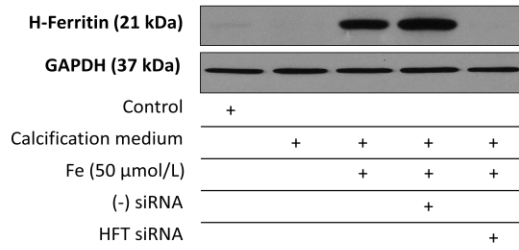
Appendix

Supplementary Figure Panels

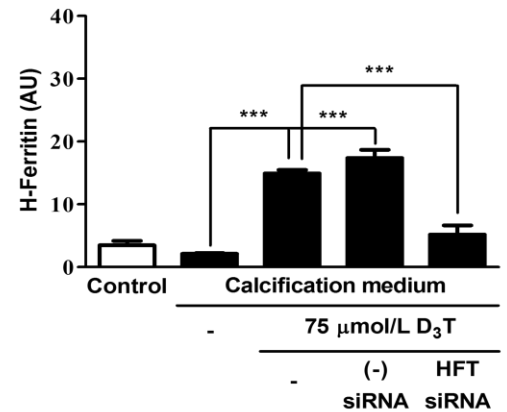
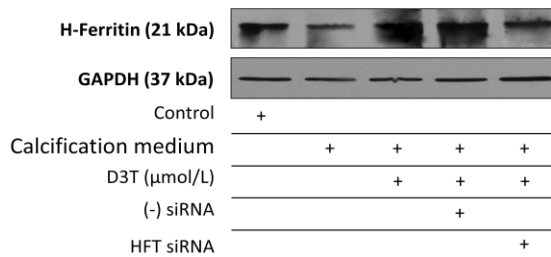


Supplementary Figure I. D3T attenuates calcification process of the valvular interstitial cell. Upregulation of ferritin levels by iron and D3T in human valvular interstitial cells decreased calcium deposition and osteocalcin levels. VIC was cultured in growth medium or calcification medium and supplemented with 10, 50 µmol/L iron (Ammonium iron (III) citrate), 2 mg/mL apo-ferritin or 12.5, 25, 50, 75 µmol/L D3T for five days and cell viability was determined using fluorescence staining assay. A) Calcium content of the cells and B) osteocalcin levels were measured and normalized by cellular protein content. C) Alkaline phosphatase staining of VIC. The samples magnifications are 20x. Scale bar: 50 µm. D) Cell viability staining of VIC was shown. Data were analyzed by One Way ANOVA, Bonferroni's Multiple Comparison Test and show average ± SEM of the three independent assays performed in triplicate. Not significant (ns), **P < 0.001, ***P < 0.0001.

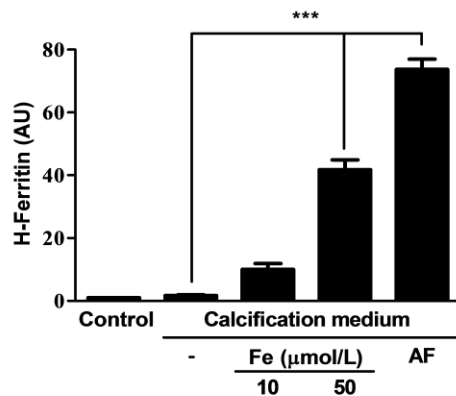
A



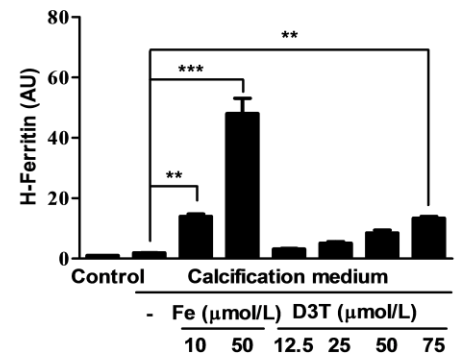
B



C

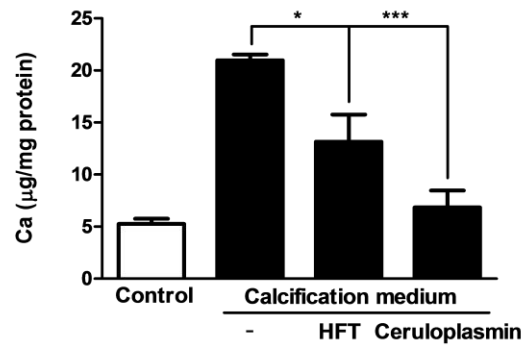


D

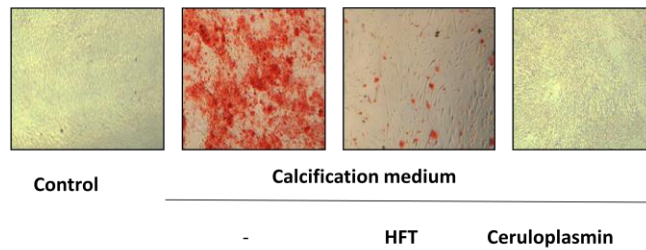


Supplementary Figure II. H-ferritin induced by iron and D3T mediates the inhibition of phosphate provoked osteoblastic transformation. VIC at 60% confluency was transfected with siRNA specific to H-ferritin or negative control siRNA 24 hours before the experiment. Cells were cultured in growth medium or calcification medium in the absence or presence of iron (Ammonium iron (III) citrate) or 75 μmol/L D3T for five days. A) and B) H-ferritin western blot shows the efficacy of H-ferritin knock-down by siRNA. Densitometry of the band intensities for H-ferritin was normalized to GAPDH. C) and D) Densitometry of H-ferritin western blot of Figure 1C. Results were analyzed by Bonferroni's Multiple Comparison test (Supplementar Figure II. A-B) and One Way ANOVA, Bonferroni's Multiple Comparison Test (Supplementary Figure II. C-D) and are presented as mean values ± SEM of at least three independent experiments each performed in triplicate. ***P < 0.0001.

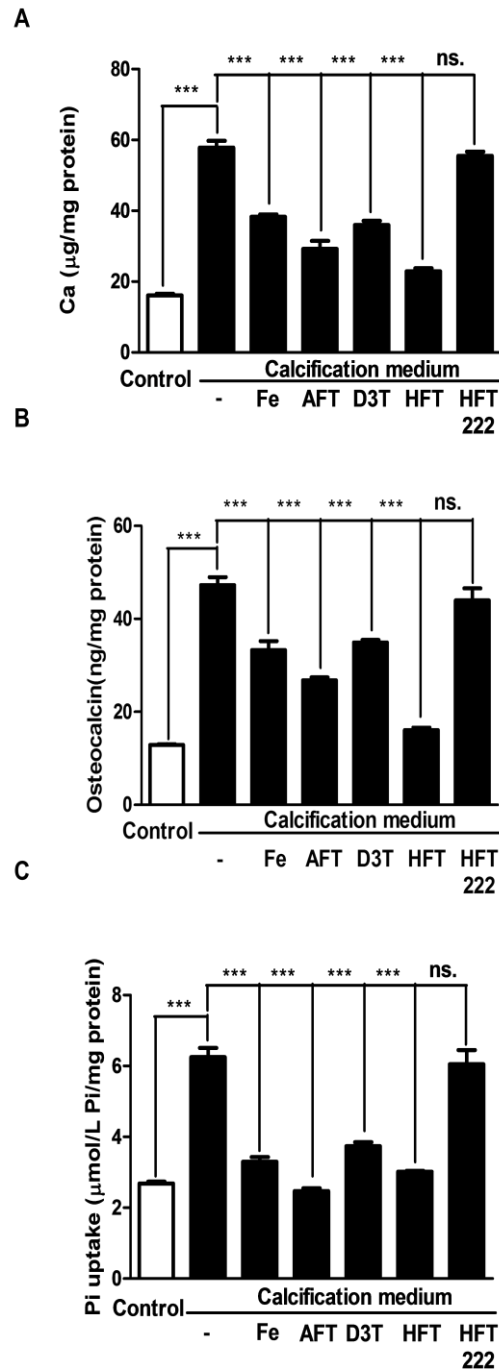
A



B

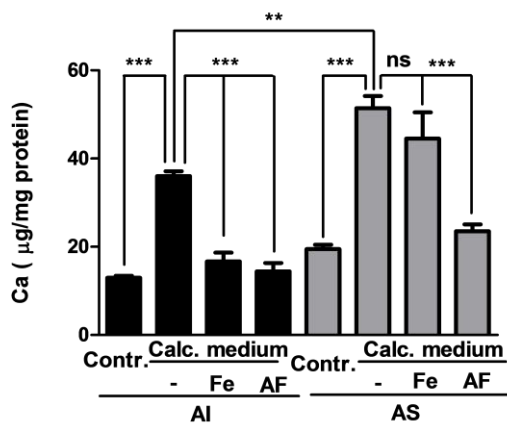


Supplementary Figure III. Ferroxidase activity of ceruloplasmin and H-ferritin is crucial in inhibiting differentiation of VIC to osteoblasts. VIC was cultured in growth medium or calcification medium in the presence or absence of 375 µmol/L ceruloplasmin and 1 mg/mL H-ferritin. A) Calcium content of the cells was measured and B) representative Alizarin Red S is shown. Data were analyzed by One Way ANOVA, Bonferroni's Multiple Comparison Test and samples were derived from four separate experiments performed in triplicates and shown as mean ± SEM ***P < 0.0001.

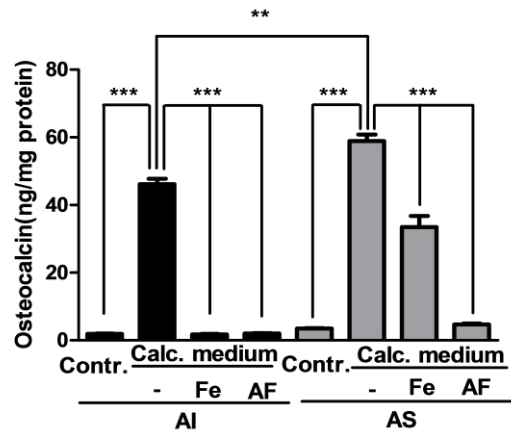


Supplementary Figure IV. Inhibition of calcification of VIC derived from healthy aortic valve by Fe, AFT,D3T, HFT and HFT222. VIC cells were cultured in growth medium alone or calcification medium in the presence or absence of 50 µmol/L iron (Ammonium iron(III) citrate), 2 mg/mL apo-ferritin, 75 µmol/L D3T, 1mg/mL H-Ferritin and 1mg/mL H-Ferritin 222 (mutant H- Ferritin without ferroxidase activity). A) Calcium deposition, B) osteocalcin level and C) phosphate uptake were measured in VIC. Graphs analyzed by One Way ANOVA, Bonferroni's Multiple Comparison Test and show mean ±SEM of three independent experiments. Not significant (ns), *** P< 0.0001.

A



B



C

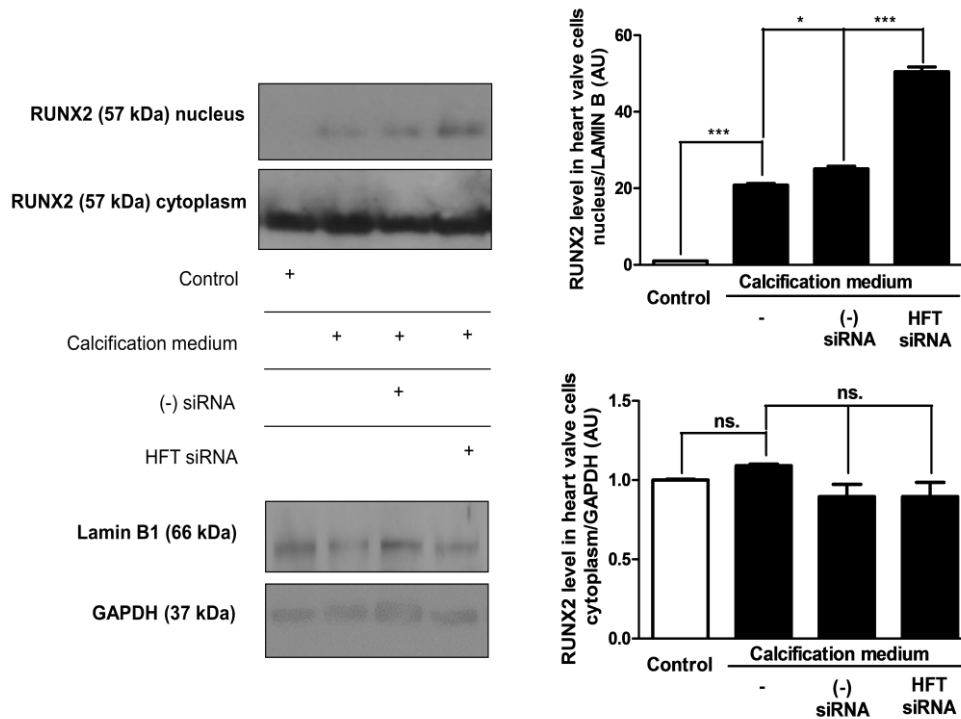


Isolated aortic valve without calcification (AI)

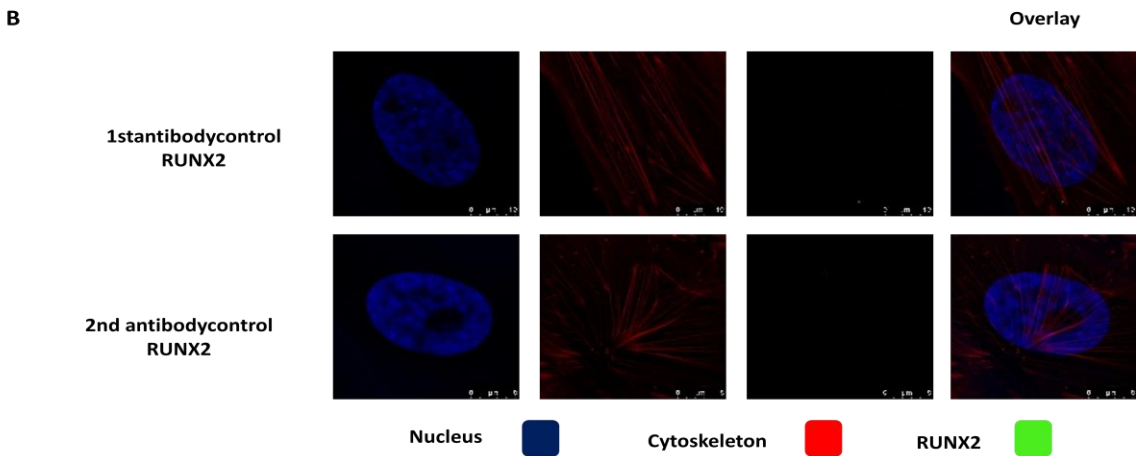
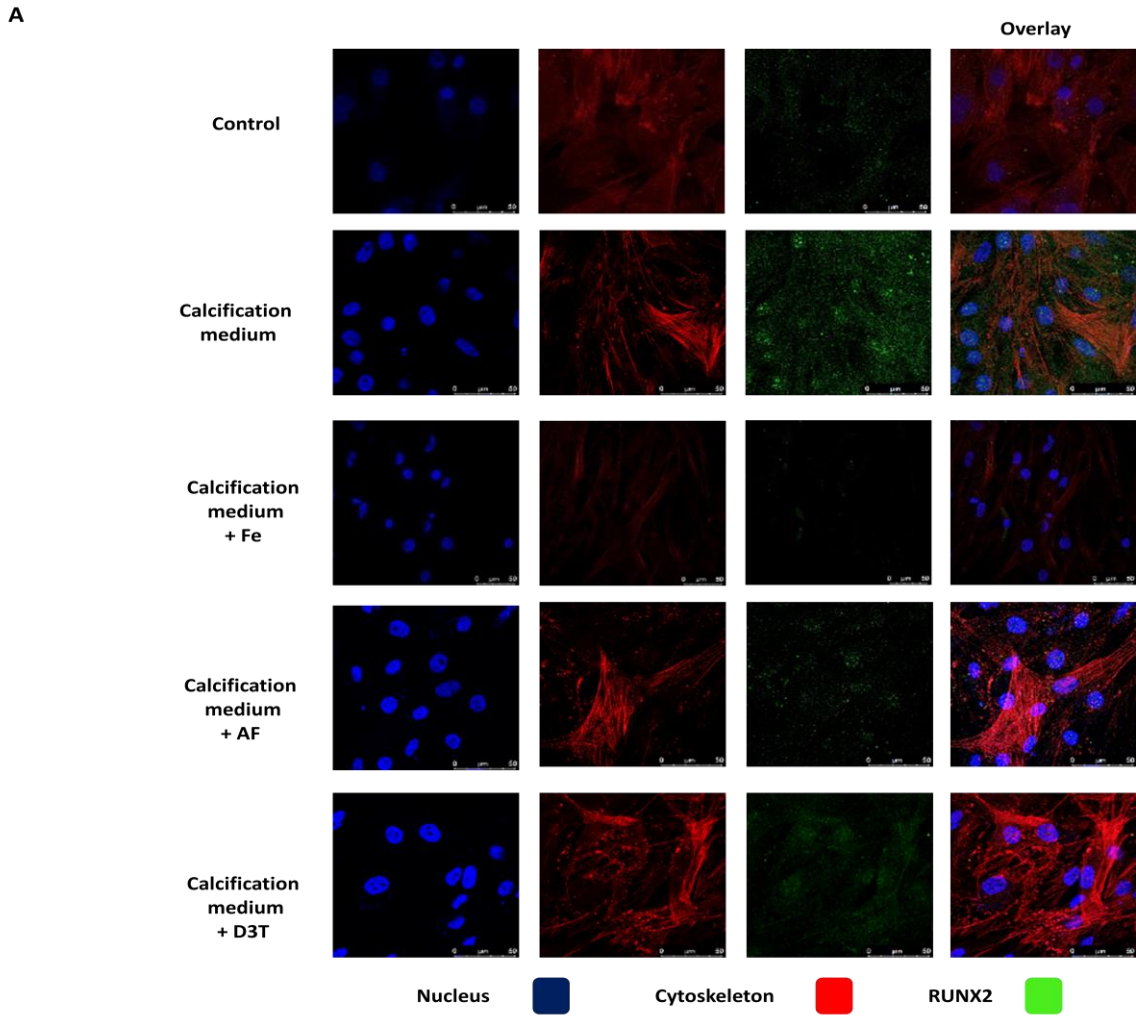


Aortic valve with stenosis and massive calcification (AS)

Supplementary Figure V. Calcification potential of AI and AS derived VIC. VIC was isolated from AI or AS tissues and cultured in growth or calcification medium and supplemented with iron (Ammonium iron (III) citrate), 2 mg/mL apo-ferritin or 75 μ mol/L D3T for five days. A) Calcium and B) osteocalcin level were measured. C) Macroscopic images of AI and AS valves are shown. Data was analyzed by One Way ANOVA, Bonferroni's Multiple Comparison Test and shown average \pm SEM of the three independent assays performed in triplicate. Not significant (ns), ** $P < 0.001$, *** $P < 0.0001$.

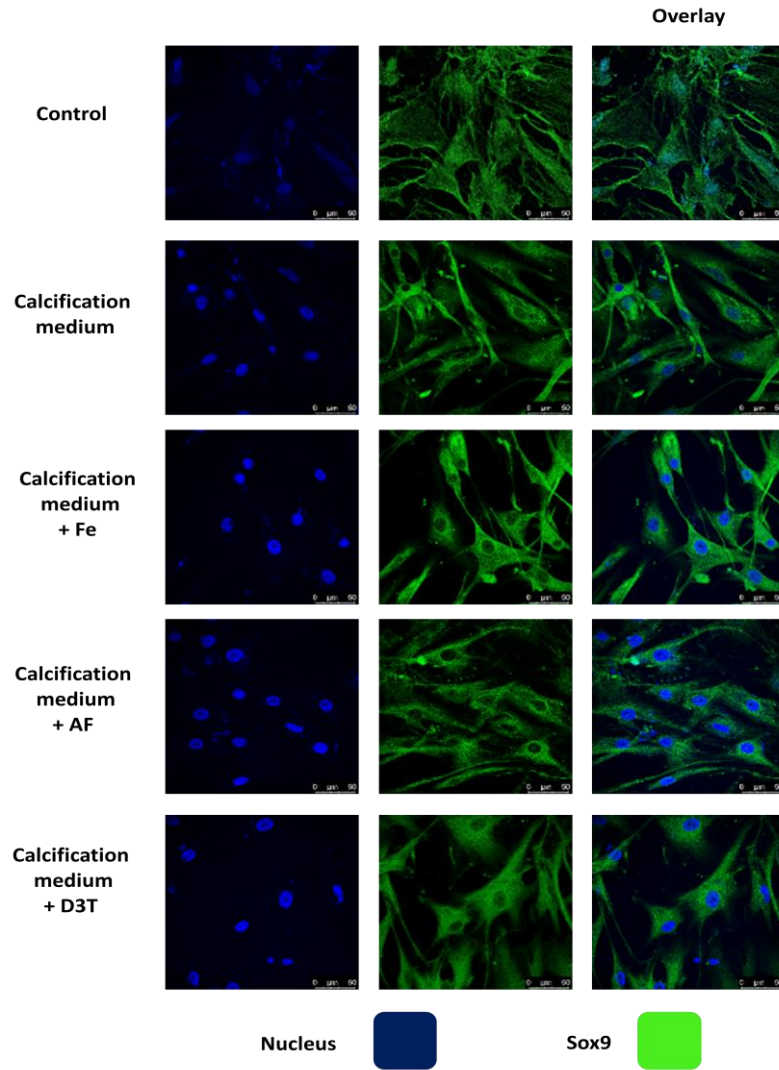


Supplementary Figure VI. Silencing of H-ferritin facilitates nuclear translocation of RUNX2 in VIC. Cells were transfected with siRNA against H-Ferritin. Next day cells were washed and maintained in calcification media supplemented with 1mg/mL of H-ferritin (for 2 days.) A) RUNX2 content in the nuclear and cytoplasmic fractions is shown. Data were analyzed by One Way ANOVA, Bonferroni's Multiple Comparison Test. Graph shows mean \pm SEM of five independent experiments. Not significant (ns); *P < 0.05; ***P < 0.001.

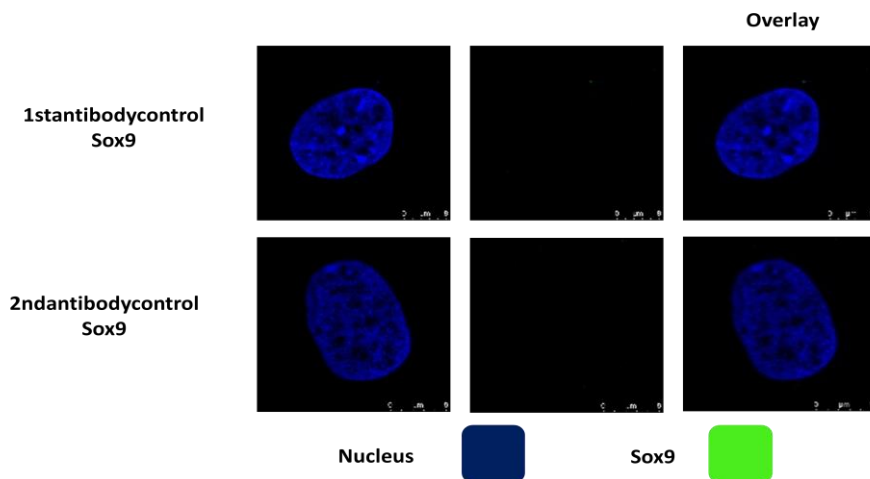


Supplementary Figure VII. RUNX2 high volume pictures. VIC was cultured in growth medium or calcification medium in the presence or absence of iron (Ammonium iron (III) citrate), 2 mg/mL apoferritin or 75 $\mu\text{mol/L}$ D3T. A) Immunofluorescence staining of VIC for RUNX2 is shown. Images were obtained employing immunofluorescence-confocal microscope. B) Antibody controls of immunofluorescence staining were shown. Representative staining is shown from at least three independent experiments.

A

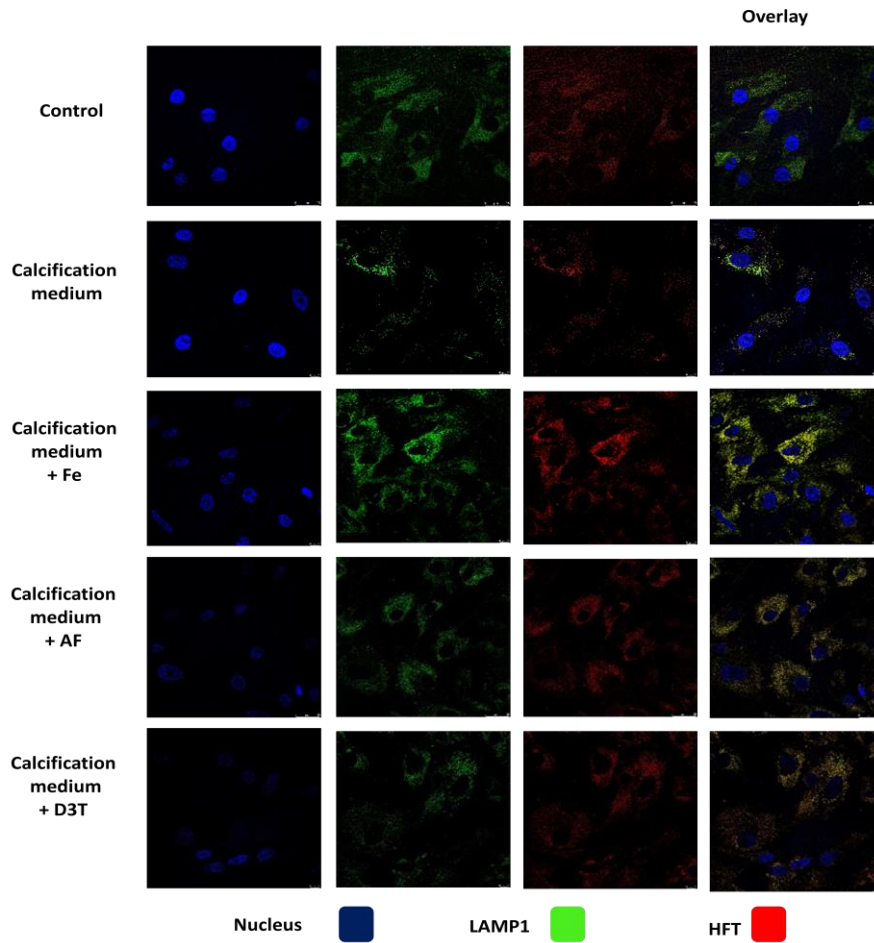


B

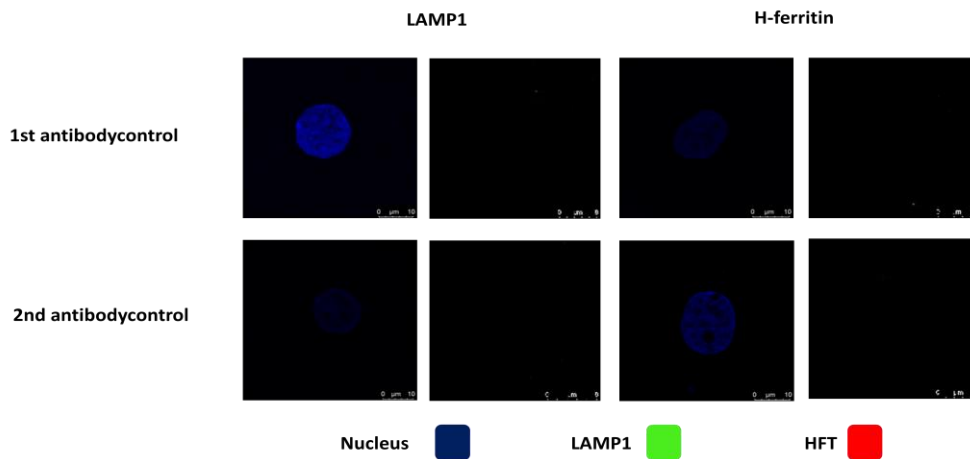


Supplementary Figure VIII. Sox9 high volume pictures. VIC was cultured in growth medium or calcification medium in the presence or absence of iron (Ammonium iron (III) citrate), 2 mg/mL apoferritin or 75 $\mu\text{mol/L}$ D3T. A) Immunofluorescence staining of VIC for Sox9 is shown. Images were obtained employing immunofluorescence-confocal microscope. B) Antibody controls of immunofluorescence staining are shown. Representative staining is shown from at least three independent experiments.

A

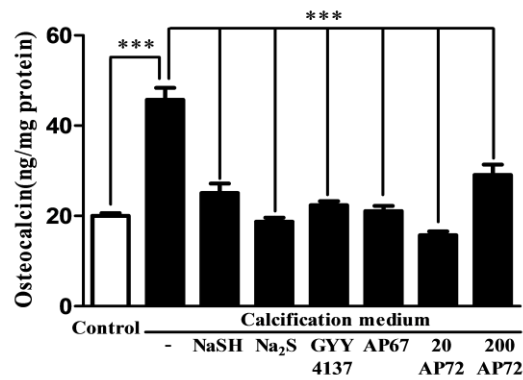


B

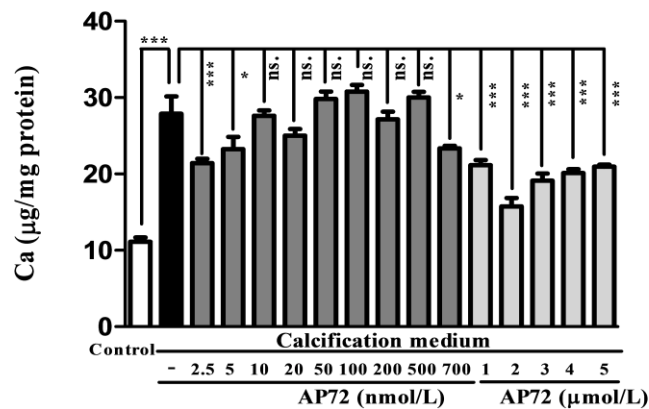


Supplementary Figure IX. LAMP1-H-ferritin double immunostaining high volume pictures. VIC was cultured in growth medium or calcification medium in the presence or absence of iron (Ammonium iron (III) citrate), 2 mg/mL apo-ferritin or 75 $\mu\text{mol/L}$ D3T. A) Double immunofluorescence staining of VIC for LAMP1 and H-ferritin are shown. Images were obtained employing immunofluorescence-confocal microscope. B) Antibody controls of immunofluorescence staining are shown. Representative staining is shown from at least three independent experiments.

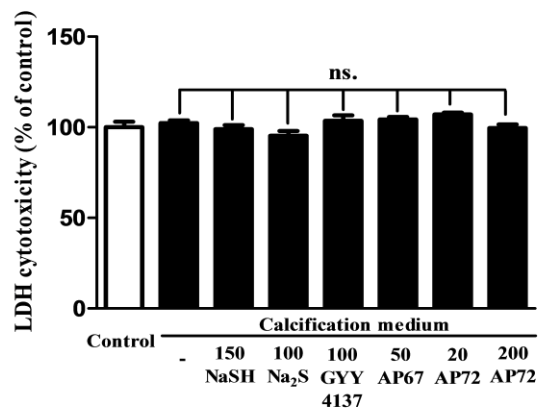
A



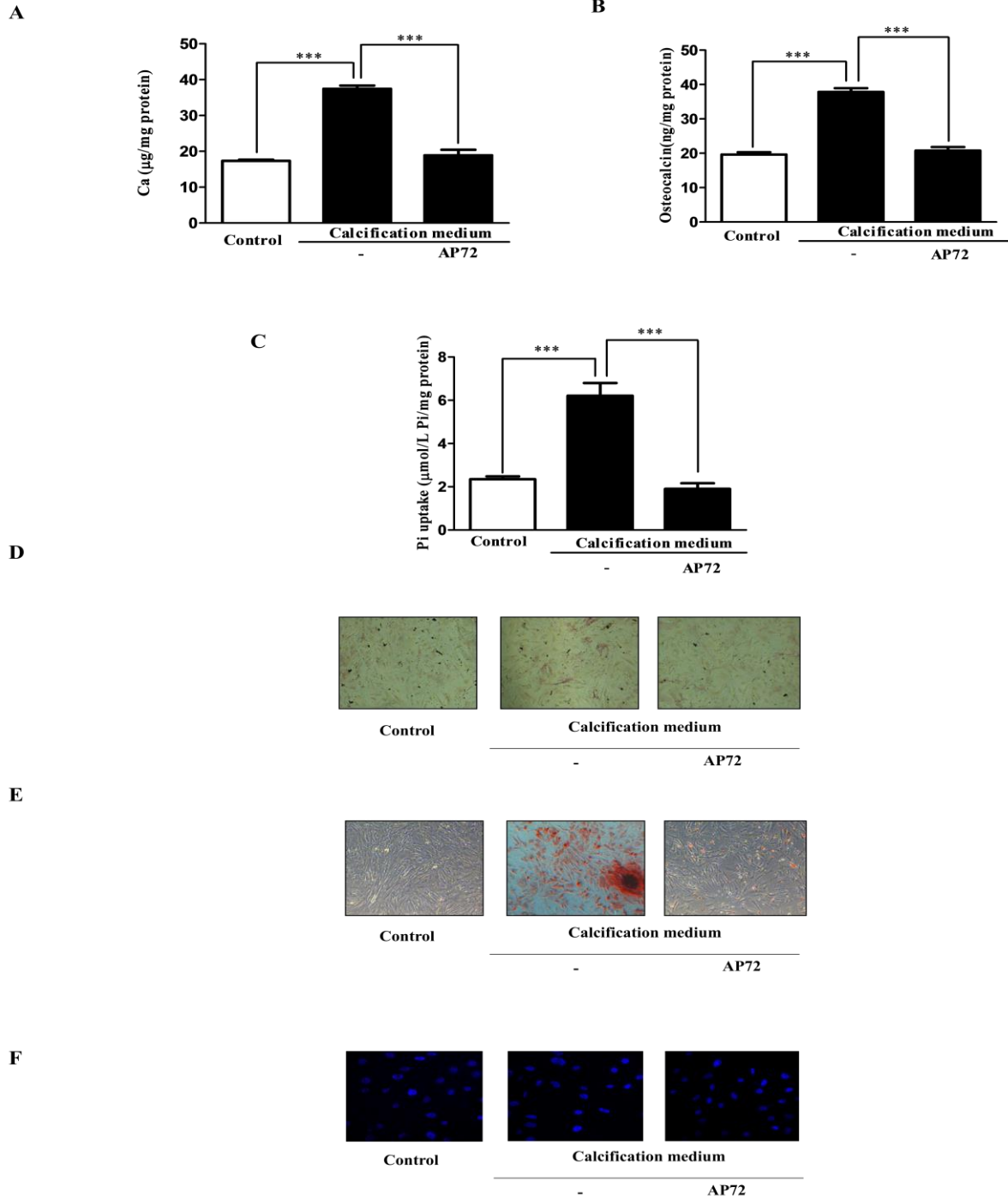
B



C

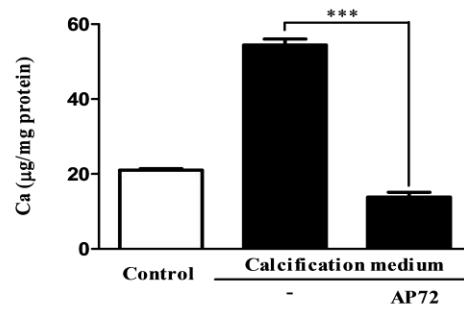


Supplementary Figure X. Osteocalcin levels, calcium deposition and cytotoxicity in VIC. Cells were cultured on 24well plates for 5 days in growth medium or calcification medium and supplemented with NaSH (150µmol/L); Na₂S (100 µmol/L); GYY4137 (50 µmol/L); AP67 (20 µmol/L); AP72 (200 µmol/L). A) Osteocalcin level of the cells were measured after 5 days and normalized to the protein content of the cells. Graph shows mean ±SEM of five separate experiments. B) VIC was cultured in phenol red-free growth or calcifying conditions or supplemented with AP72 (2.5 nmol/L to 5 µmol/L) and calcium content was measured. C) LDH cytotoxicity in VIC exposed to H₂S donors was assessed. All experiments were performed. Results were shown mean ±SEM at least of six independent experiments. Not significant (ns); *P < 0.05; ***P < 0.001.

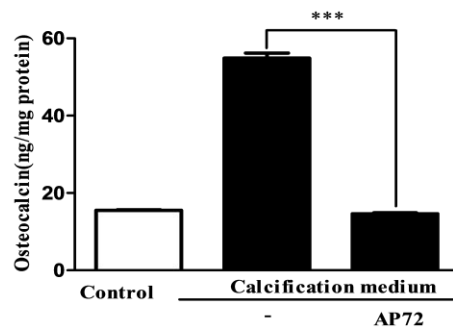


Supplementary Figure XI. In phenol red-free condition AP72 inhibits valvular calcification at 2 µmol/L. VIC were cultured in growth medium or calcification medium alone (without phenol red) or supplemented with AP72 (2 µmol/L) for 5 days. A) Calcium content and B) osteocalcin level C) Phosphate uptake of the cells were measured after 5 days and normalized to the protein content of the cells. D) Alkaline phosphatase staining, E) Alizarin Red S staining provides representative microscopic images of extracellular calcium depositions. F) Fluorescence staining assay for cytotoxicity was assessed. Scale bar: 50 µm. Graph shows mean ±SEM of five separate experiments. ***P < 0.001.

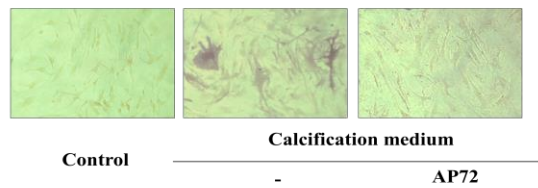
A



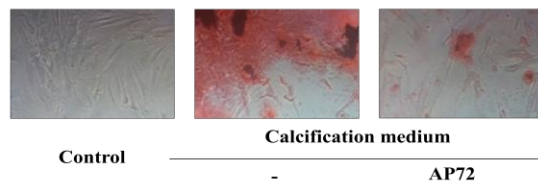
B



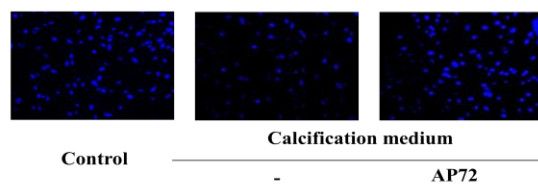
C



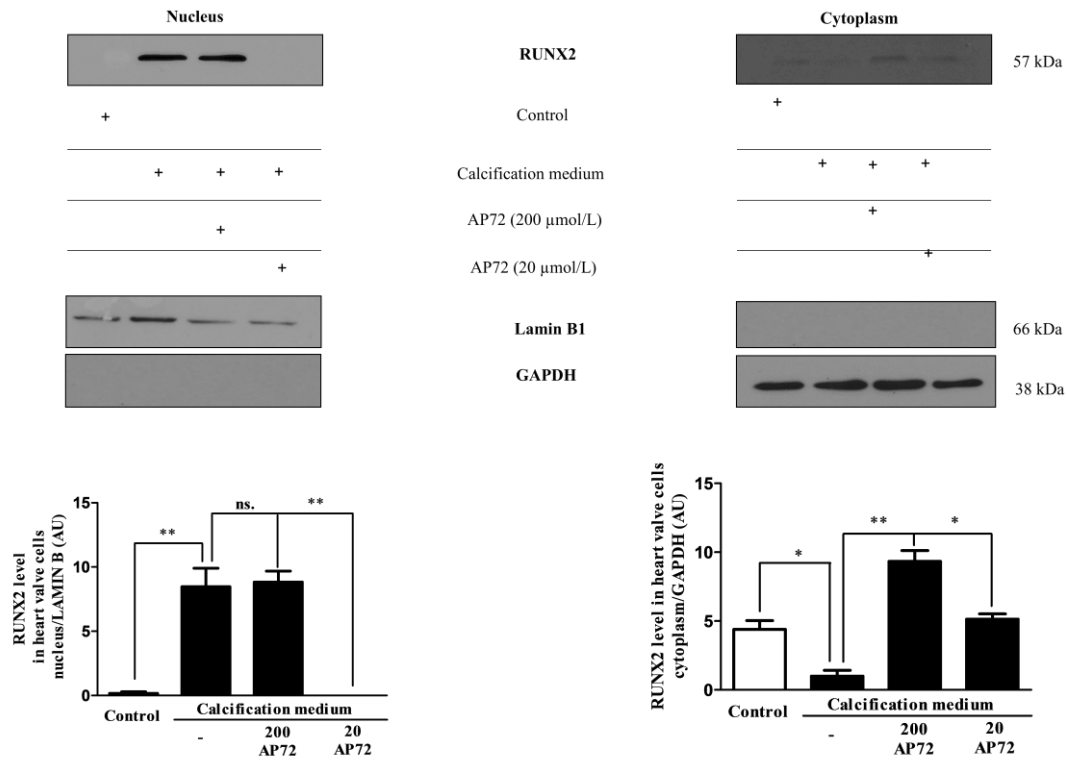
D



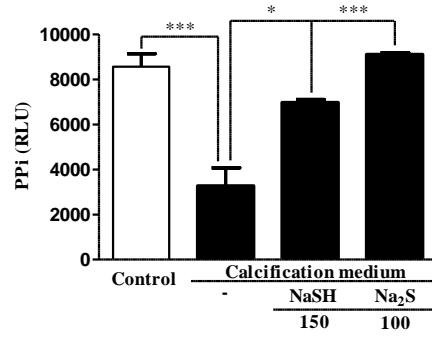
E



Supplementary Figure XII. Inhibition of valvular calcification by AP72. VIC was cultured in growth medium or calcification medium alone or supplemented with AP72 (20 µmol/L) for 5 days. A) Calcium content and B) osteocalcin level of the cells were measured after 5 days and normalized with the protein content of the cells. C) Alkaline phosphatase staining and D) Alizarin Red S staining provide representative microscopic images of extracellular calcium depositions. E) Differences in cellular cytotoxicity is visualized using a fluorescence staining assay (see Methods). Scale bar: 50 µm. Graph shows mean ±SEM of five separate experiments. ***P < 0.001.

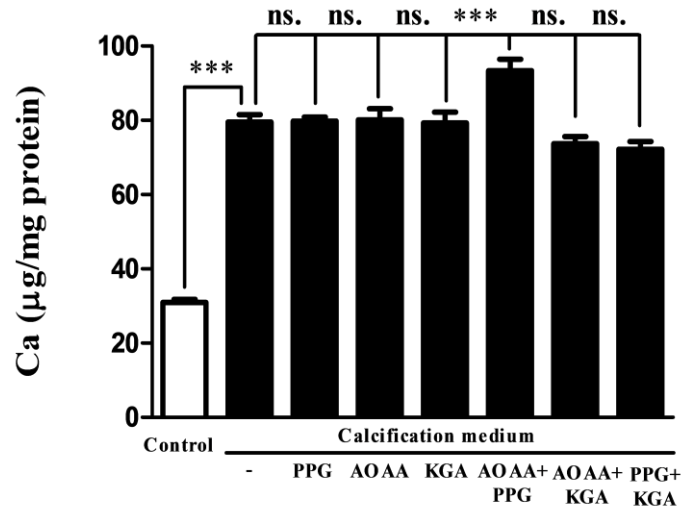


Supplementary Figure XIII. RUNX2 nuclear translocation in calcifying condition in the presence of 20 and 200 μmol/L of AP72. VIC grown on coverslips were exposed to growth medium or calcification medium alone or supplemented with AP72 (20 and 200 μmol/L) for 24hours. A) RUNX2 levels of cytoplasm and nucleus were determined by Western blot analyses. The band intensities are normalized to LaminB1 in case of nuclear extracts and for GAPDH in case of cytoplasm extracts. Representative staining of five independent experiments was shown. Not significant (ns); **P < 0.01; ***P < 0.001.

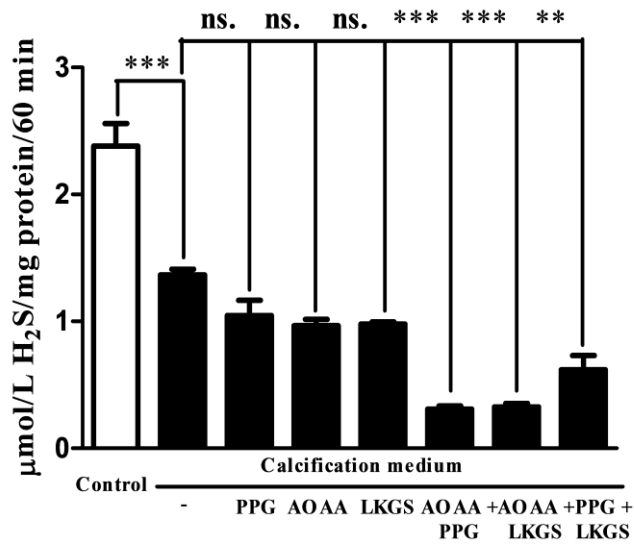


Supplementary Figure XIV. Changes of PPi levels by fast sulfide donor treatment on VIC. VIC were cultured in growth medium or calcification medium in the presence or absence of NaSH or Na₂S for 5 days. PPi levels of VIC were measured and normalized to protein content of the cells. Graph shows mean ±SEM of five separate experiments. *P < 0.05; ***P < 0.001.

A

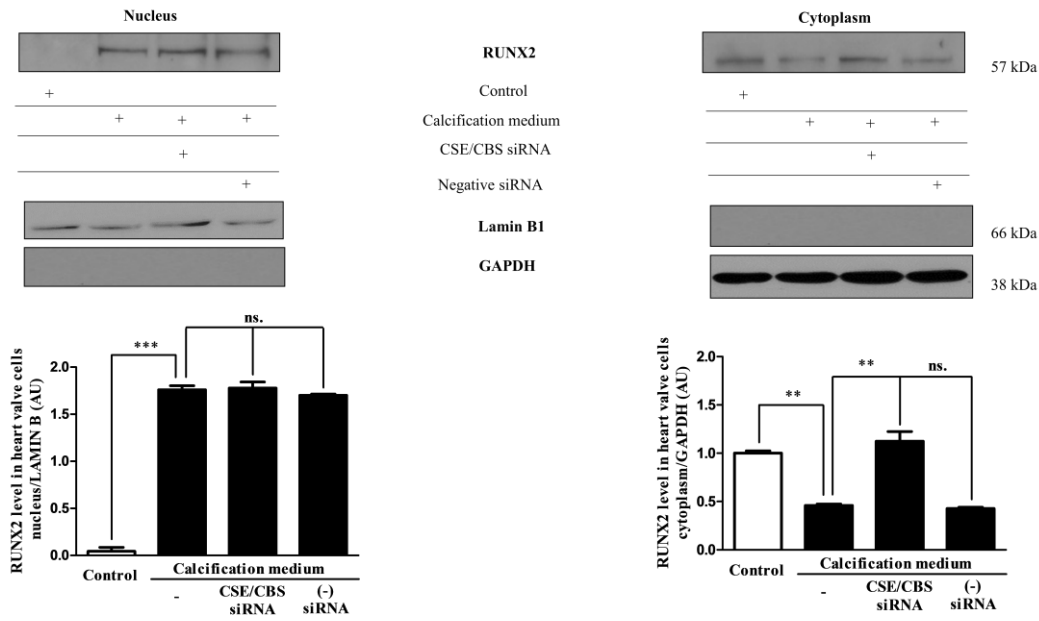


B

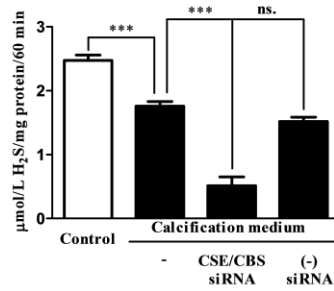


Supplementary Figure XV. Inhibition of H₂S production by pharmacological inhibitors in VIC. A) Calcium accumulation of extracellular matrix of VIC maintained in growth medium or calcification medium after 5 days treatment with PPG; AOAA; KGA; AOAA+PPG; AOAA+KGA; PPG+KGA (20 µmol/L each inhibitor). Calcium levels of VIC were normalized to protein content of the cells. B) H₂S production of VIC treated with pharmacological inhibitors alone or in combination was detected. Generation of H₂S was normalized to the protein content of cells. Graph shows mean ± SEM of five separate experiments. Not significant (ns); ***P < 0.001.

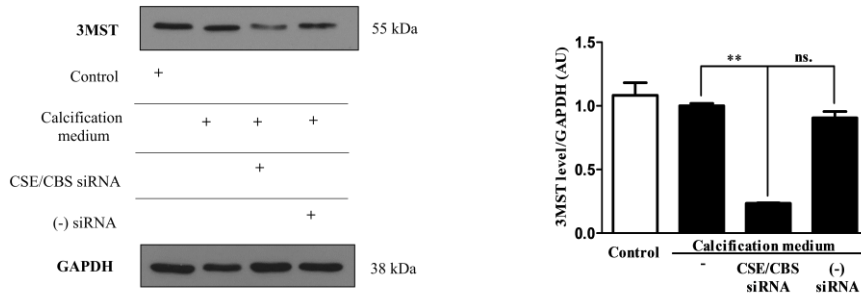
A



B

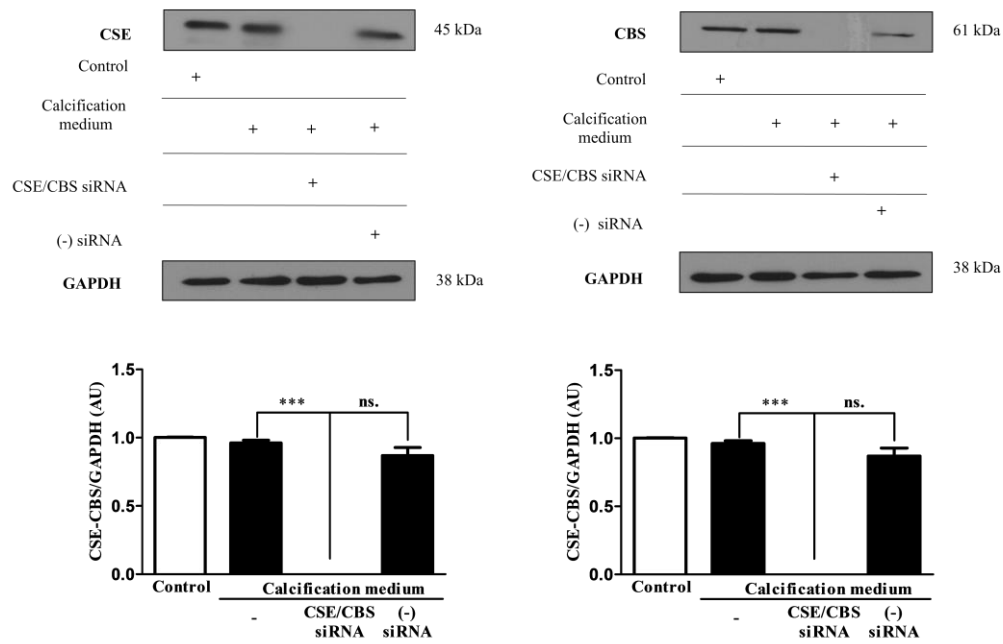


C

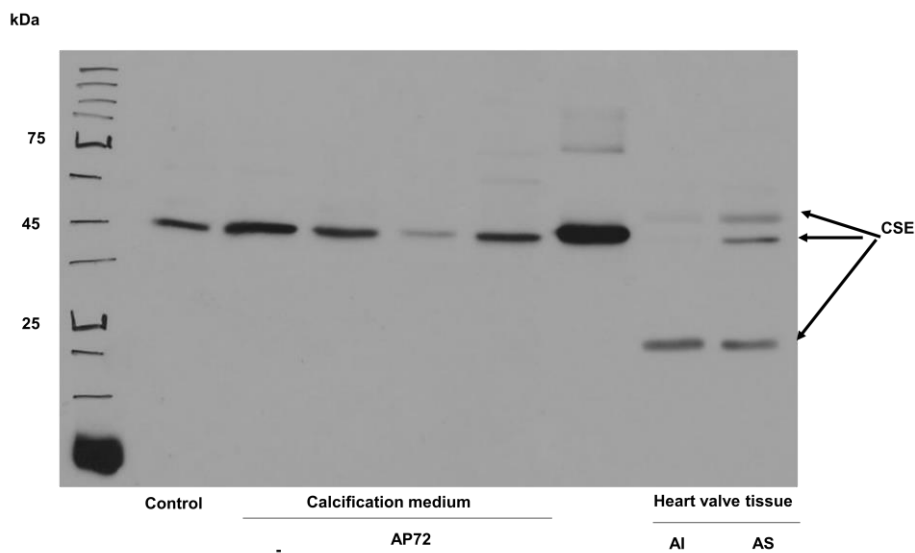


Supplementary Figure XVI. CSE/CBS silencing enhanced the progression of calcification and decreased the expression of 3-MST. CSE and CBS double gene silencing using siRNAs were performed. Cells were transfected with siRNA against CSE/CBS. Next day cells were washed and treated with high inorganic phosphate and calcium for 3 days. A) RUNX2 expression in a nuclear and cytoplasmic fraction were shown. B) H₂S production of CSE/CBS silenced samples was measured. C) Western blot demonstrated expression of 3-MST in CSE/CBS silenced VIC. Graph shows mean \pm SEM of five independent experiments. Not significant (ns); **P < 0.01; ***P < 0.001.

A



B



Supplementary Figure XVII. CSE and CBS expression of the double silenced VIC. A) VIC were cultured in growth or calcification medium and transfected with siRNA for CSE/CBS. Next day VIC were treated with calcification medium for 3 days. CSE (left panel) and CBS (right panel) protein level were measured. Samples were normalized to GAPDH. B) Western blot of the CSE protein of VIC lysate and AI/AS were shown. Human recombinant CSE protein (5 and 10 ng) was used as a positive control. Not significant (ns); *** $P < 0.001$.